

BEHAVIOUR OF RESIN VOIDS IN OUT-OF-AUTOCLAVE PREPREG PROCESSING

by

Jeremy Wells

B.A.Sc., The University of British Columbia, 2014

A THESIS SUBMITTED IN PARTIAL FULFILLMENT OF THE REQUIREMENTS
FOR THE DEGREE OF

MASTER OF APPLIED SCIENCE

in

THE FACULTY OF GRADUATE AND POSTDOCTORAL STUDIES
(Materials Engineering)

THE UNIVERSITY OF BRITISH COLUMBIA
(Vancouver)

October 2015

© Jeremy Wells, 2015

ABSTRACT

Resin in prepreg contains small bubbles called resin voids. These voids are isolated from the laminate inter-connected breathing network and cannot be removed by vacuum debulk. Initially these voids contribute negligibly to porosity; however, they may grow and contribute significantly to porosity by vapourization of dissolved volatile species and/or ideal gas expansion particularly in low pressure out-of-autoclave (OOA) processes. Modern advanced prepregs have low volatile content except for moisture due to the hygroscopic property of epoxy. The goal of this study is to investigate the behaviour of resin voids and determine the mechanisms and processing conditions that cause resin void growth. The first part of this study investigates the growth of resin voids in neat resin specimens under controlled temperature, resin pressure and moisture content. Neat resin was vacuum bagged on a glass tool and visually observed in-situ by use of a digital microscope. A criterion that predicts the critical resin pressure below which resin voids can grow due to moisture vapourization was tested for two separate moisture contents and accurately predicts the onset of resin void growth. Additionally, resin voids were observed to contribute significantly to porosity in the very low resin pressure regime due to ideal gas expansion. The results indicate that resin pressure is a critical parameter for mitigating resin void porosity.

The second part of this study investigates resin void growth in laminates by stimulating moisture vapourization and/or ideal gas expansion and comparing them to a porosity free baseline. In order to isolate the effect of resin voids, laminates were fully evacuated before cure. Reduced resin pressure, increased moisture content and increased cure temperature were tested parameters. Laminates were laid up on a glass tool and observed and recorded in-situ. Both surface and bulk porosity were measured for each laminate. In-situ observations and resin pressure correlate well with porosity results based on the resin void growth mechanisms investigated for all test conditions except increased cure temperature. Possible explanations for the discrepancy are discussed. Resin pressure was seen as a critical parameter in porosity management and the concept of a minimum resin pressure is proposed and discussed.

PREFACE

The research work presented in this thesis was performed and analyzed by Jeremy Wells (author). This research received valuable input and supervision by Dr. Göran Fernlund, input by Malcolm Lane of Convergent Manufacturing Technologies and helpful discussions with Leyla Farhang, James Kay and Martin Roy.

A manuscript based on a version of chapters 3 and 4 has been published. [Jeremy Wells]. Wells, J., Kay, J., Lane, M., Poursartip, A. and Fernlund, G. (2015) Surface and Bulk Porosity in Out of Autoclave Prepregs. *Proceedings of the 17th International Conference on Composite Materials (ICCM), Copenhagen, Denmark*. All work presented in the manuscript was performed and analyzed by Jeremy Wells and written by Jeremy Wells in conjunction with James Kay.

A manuscript based on chapter 3 is in the process of submission for publication. [Jeremy Wells]. Wells, J., Lane, M., Poursartip, A. and Fernlund, G. (2015) Porosity Management in Composites Manufacturing: Behaviour of Resin Voids in Neat Resin. All work presented in this manuscript was performed, analyzed and written by Jeremy Wells and supervised by Dr. Göran Fernlund.

A manuscript based on chapter 4 is in the process of submission for publication. [Jeremy Wells]. Wells, J., Lane, M., Poursartip, A. and Fernlund, G. (2015) Porosity Management in Composites Manufacturing: Behaviour of Resin Voids in Laminates. All work presented in this manuscript was performed, analyzed and written by Jeremy Wells and supervised by Dr. Göran Fernlund.

TABLE OF CONTENTS

ABSTRACT.....	ii
PREFACE.....	iii
TABLE OF CONTENTS.....	iv
LIST OF TABLES.....	vi
LIST OF FIGURES.....	vii
LIST OF SYMBOLS.....	x
1 INTRODUCTION.....	1
1.1 Scope & Objectives.....	2
2 BACKGROUND & LITERATURE REVIEW.....	4
2.1 Composite Prepreg Processing.....	4
2.1.1 Prepreg.....	4
2.1.2 Lay-up and Cure.....	5
2.2 Porosity in Out-of-Autoclave Prepreg Processing.....	7
2.2.1 Resin Voids.....	10
2.2.1.1 Resin Void Growth by Volatile Vapourization.....	12
2.2.1.2 Resin Void Growth by Ideal Gas Expansion.....	15
2.3 Hydrostatic Resin Pressure.....	17
3 NEAT RESIN EXPERIMENTS.....	18
3.1 Neat Resin Test Methods.....	18
3.1.1 Kardos Criterion Test Method.....	21
3.1.2 Ideal Gas Expansion Test Method.....	22
3.2 Neat Resin Results & Observations.....	23
3.2.1 Kardos Criterion Results & Observations.....	23
3.2.2 Ideal Gas Expansion Results & Observations.....	28
3.3 Neat Resin Results Discussion.....	32
4 LAMINATE EXPERIMENTS.....	34
4.1 Laminate Test Methods.....	34
4.1.1 Baseline Laminates.....	37
4.1.2 Reduced Consolidation Pressure Laminates.....	37
4.1.3 Resin Bleed Laminates.....	39
4.1.4 Increased Moisture Content Laminates.....	40

4.1.5	Increased Cure Temperature Laminates.....	40
4.1.6	In-situ Resin Pressure.....	41
4.2	Laminate Tests Results & Observations	42
4.2.1	In-Situ Resin Pressure Results & Observations	42
4.2.2	Baseline Laminates Results & Observations	43
4.2.3	Reduced Consolidation Pressure Laminates Results & Observations	45
4.2.4	Increased Moisture Content Laminates Results & Observations.....	48
4.2.5	Resin Bleed Laminates Results & Observations.....	50
4.2.6	Increased Cure Temperature Laminates Results & Observations.....	53
4.3	Laminate Tests Results Discussion.....	54
4.3.1	MRP Applied to Laminates.....	54
4.3.2	MRP as Part of a Comprehensive Porosity Mitigation Tool.....	57
4.3.3	Uninfiltrated Fiber Tows.....	59
4.3.4	Bubble Mobility and Evacuation	61
4.3.5	Environmental Considerations	64
5	CONCLUSION.....	66
5.1	Conclusions of the Study	66
5.2	Future Work	68
5.3	Contributions.....	69
	REFERENCES	70
	APPENDICES	75
	Appendix A: Laminate Air Evacuation	75
	Appendix B: Resin Void Generation by an Uninfiltrated Fiber Tow	77
	Appendix C: 75% RH Kardos Criterion Result with Incorrect Boundary Pressures	78
	Appendix D: Measuring Bulk Porosity by Density and Thickness	79

LIST OF TABLES

Table 2.1: List and description of consumables used in composites manufacturing	6
Table 2.2: Local RVE variables of interest.....	12
Table 2.3: Moisture values used for the Clausius-Clapeyron relation.....	15
Table 3.1: High, low and critical resin pressure values.....	22
Table 3.2: Initial resin void porosity, ϕ_0	32
Table 4.1: Baseline laminate test parameters.....	37
Table 4.2: Reduced consolidation pressure laminate test parameters.....	39
Table 4.3: Bleed laminate test parameters.....	40
Table 4.4: Increased moisture content laminate test parameters.....	40
Table 4.5: Increased cure temperature laminate test parameters.....	41
Table 4.6: Laminate resin pressure for varying consolidation pressure.....	43
Table 4.7: Time constant calculation parameters.....	56
Table A.1: Values used for the parameters in Equation 31.....	75

LIST OF FIGURES

Figure 2.1: MTM45-1/CF2426A prepreg resin poor side (left) and resin rich side (right).	5
Figure 2.2: Standard vacuum bag assembly used to manufacture composite materials.	5
Figure 2.3: Types of voids in an OOA prepreg (Reproduced with permission [9]).	8
Figure 2.4: Surface porosity (black) on a small, flat prepreg laminate.	8
Figure 2.5: Void sources and void sinks on the global scale (Adapted with permission [25]).	10
Figure 2.6: Representative volume element (RVE) of a composite.	11
Figure 2.7: Schematic of resin void growth by moisture.	14
Figure 3.1: Experimental test setup.	18
Figure 3.2: Experimental test setup in-situ observation vantage.	19
Figure 3.3: Neat resin vacuum bag assembly.	19
Figure 3.4: In-situ neat resin image used for measuring bubble diameter.	18
Figure 3.5: Kardos criterion evaluation test plan for neat resin conditioned at 75% RH.	21
Figure 3.6: In-situ image of 75% RH neat resin at 0.49 atm; 50X magnification, image size 6901 x 4927 μm^2	23
Figure 3.7: Average normalized void diameters for the 75% RH neat resin tests.	24
Figure 3.8: Average normalized void diameters for the 33% RH neat resin tests.	25
Figure 3.9: Desiccated resin subjected to the 75% RH pressure cycle.	26
Figure 3.10: Desiccated resin subjected to the 33% RH pressure cycle.	27
Figure 3.11: Reducing resin pressure in a desiccated resin; $T = 100^\circ\text{C}$, Mag. = 50X, Image size = 2608 x 2608 μm^2	29
Figure 3.12: Neat resin sample at $P_{\text{Resin}} = 0.19$ atm used for void density quantification.	31
Figure 3.13: Minimum resin pressure for $\phi_0 = 0.15\%$ and $RH_0 = 33\%$	33
Figure 4.1: Schematic test plan for the laminate experiments.	35
Figure 4.2: Left) Method for capturing high contrast surface images, Right) Surface porosity image taken by light reflecting off of the surface.	36
Figure 4.3: Baseline laminate vacuum bag assembly.	37

Figure 4.4: Reduced consolidation pressure laminate vacuum bag assembly.	38
Figure 4.5: a) Primary vacuum bag b) Primary and secondary vacuum bags.....	38
Figure 4.6: Resin bleed laminate vacuum bag assembly.	39
Figure 4.7: In-situ resin pressure vacuum bag assembly used to measure resin pressure under varying consolidation pressures.	41
Figure 4.8: Resin pressure under varying consolidation pressure.....	42
Figure 4.9: In-situ laminate surface with inter- and intra-tow voids.....	43
Figure 4.10: In-situ surface evolution of a baseline laminate.	44
Figure 4.11: Baseline resin pressure compared to the minimum resin pressure: $RH_0 = 33\%$, $\phi_0 = 0.15\%$	44
Figure 4.12: Top: Reduced consolidation pressure quantified porosity, bottom: in-situ images at 66 minutes a) 2/3 atm b) 1/3 atm c) 0/3 atm.	45
Figure 4.13: Surface porosity on a 2/3 atm consolidation laminate.....	46
Figure 4.14: Reduced consolidation resin pressures compared to the minimum resin pressure: $RH_0 = 33\%$, $\phi_0 = 0.15\%$	46
Figure 4.15: Resin void arriving at a pinhole and evacuating through an EVaC.....	47
Figure 4.16: Bubble stagnation and growth in a 1/3 atm consolidation laminate.....	48
Figure 4.17: Left: Quantified bulk and surface porosity for increased moisture content tests, right: 75% RH laminate at 66 min.	49
Figure 4.18: Increased moisture content resin pressure compared to the minimum resin pressure: $RH_0 = 75\%$, $\phi_0 = 0.15\%$	49
Figure 4.19: Left: Quantified bulk and surface porosity for bleed tests, right: 5 peel ply bleed laminate at 66 min.	51
Figure 4.20: Top: Series of images showing resin void growth, Bottom: 5 peel ply resin bleed resin pressure profile and MRP: $RH_0 = 33\%$, $\phi_0 = 0.15\%$	52
Figure 4.21: Resin void generation due to uninfiltreated surface fiber tows.....	53
Figure 4.22: Increased cure temperature resin pressure compared to the minimum resin pressure: $RH_0 = 33\%$, $\phi_0 = 0.15\%$	54
Figure 4.23: Evacuation of a moisture molecule in an air evacuated laminate.....	53

Figure 4.24: Time constants for Darcy flow and diffusion of moisture in an evacuated laminate (to reach 90% equilibrium diffusion requires one time constant, Darcy flow requires six time constants).	57
Figure 4.25: Schematic representation of fiber tow void pressure during debulk and heat up.	60
Figure 4.26: Stringy look due to capillary infiltration in a 5 peel ply bleed laminate.	60
Figure 4.27: Resin void immersed in resin under a pressure gradient.	62
Figure 4.28: Resin void immersed in resin under constant pressure.	63
Figure 4.29: Observed bubble mobility (note that 1 = on and 0 = off) in a 1/3 atm consolidation pressure laminate compared to fiber tow infiltration and Kardos criterion satisfaction.	63
Figure 4.30: Atmospheric pressure decrease with elevation.	64
Figure A.1: Relative mass of air in the laminate during debulk.	76
Figure B.1: Resin void generation due to uninfiltreated surface fiber tows.	77
Figure C.1: Average normalized void diameters for 75% RH neat resin tests with high and low pressure values chosen due to a calculation error for $P_{R,Critical}$	78

LIST OF SYMBOLS

v	Fluid velocity
K	Fluid permeability of a porous medium
μ	Fluid viscosity
dP/dx	Pressure gradient within the fluid
P_{Resin}	Hydrostatic resin pressure
$P_{G,Bulk}$	Bulk void gas pressure
$P_{G,Bubble}$	Resin void (bubble) gas pressure
$[X]_{i,\infty}$	Concentration of dissolved specie i away from any void interface
$[X]_{i,Bulk}$	Concentration of dissolved specie i at a bulk void interface
$[X]_{i,Bubble}$	Concentration of dissolved specie i at a resin void interface
S	Solubility of moisture in the resin
k_1	Solubility empirical proportionality constant
p_{H_2O}	Partial pressure of moisture vapour
$p_{H_2O}^*$	Equilibrium partial pressure of moisture vapour
RH	Relative humidity
RH_0	Initial relative humidity
C	Concentration of moisture in the resin
$C_{H_2O,Bubble}$	Concentration of moisture in the resin at a resin void interface
$C_{H_2O,\infty}$	Concentration of moisture in the resin away from a resin void interface
ρ_{Resin}	Resin density
V	Volume
P_0	Clausius-Clapeyron reference pressure
T_0	Clausius-Clapeyron reference temperature
R	Ideal gas constant
ΔH_{vap}	Enthalpy of vapourization
$P_{R,Critical}$	Critical resin pressure for moisture vapourization based resin void growth

γ_{LV}	Resin void interfacial tension
$P_{Applied}$	Applied pressure
$\sigma_{Fiberbed}$	Fiberbed effective stress
P_H	High pressure value used to validate the Kardos criterion
P_L	Low pressure value used to validate the Kardos criterion
d	Resin void diameter
d_0	Initial resin void diameter
d/d_0	Normalized resin void diameter
ϕ	Porosity
ϕ_0	Initial porosity
$\phi_{Critical}$	Critical porosity for part acceptance
ρ	Resin void number density
f_{Small}	Number fraction of small resin voids
f_{Large}	Number fraction of large resin voids
$d_{0,Small}$	Initial diameter of small resin voids
$d_{0,Large}$	Initial diameter of large resin voids
α	Incident angle of light reflection
t_{Darcy}	Time constant for Darcy flow
L	Part length
ΔP	Pressure difference
K_{eff}	Effective permeability due to Klinkenberg effect
t_{Diff}	Time constant for diffusion
Δx	Diffusion length
D	Diffusivity of moisture in resin
ΔC	Concentration difference
ρ_{H2O}	Density of moisture vapour
$P_{Capillary}$	Capillary pressure for resin infiltration of the fiber mat

1 INTRODUCTION

Composite materials incorporate two or more physically and chemically distinct materials resulting in improved properties over the component materials alone. The most commonly used composite materials are comprised of a reinforcing or dispersed phase and a matrix or continuous phase. Of particular interest to industry are fiber reinforced polymer (FRP) composites. The chief advantage of this material combination is the high strength and stiffness of fibers with the low density of polymers. Commonly used fibers include carbon, aramid, glass, boron and flax. Polymers can either be thermoplastic (able to be melted) or thermoset (cannot be melted once solid) and commonly used polymers include epoxy, polyester, polypropylene and polyether ether ketone. For aerospace application carbon fiber reinforced epoxy is used since it provides excellent mechanical, fatigue and corrosion properties [1]. Carbon fiber reinforced epoxy is the material system of choice for this research and all further references to composites or prepregs refer to this material system.

Composite materials have been used in the aerospace industry for decades but traditionally in non-critical structure applications. In the past decade however, aerospace manufacturers have begun using composite materials in primary structural components of planes such as the wings and fuselage. Examples include Boeing's 787 Dreamliner (50% by weight composite) [2], Airbus' A350XWB (53% by weight composite) [3] and Bombardier's C Series aircraft [4]. The use of composites allows manufacturers to make large one-piece parts minimizing the amount of part joining required. For example, the Boeing 787 fuselage is comprised of 6 barrel pieces as opposed to an aluminum fuselage which is made of numerous splice plates riveted together. Composites also offer significant weight reduction over conventional aluminum structures increasing the fuel efficiency of the airplane (Boeing 787 is 20% more fuel efficient). Currently, industry manufactures composite parts using an autoclave. Autoclave manufacturing is a reliable and robust process that produces high quality parts; however it is slow and expensive. To meet the forecasted market demands manufacturers are looking at out-of-autoclave (OOA) manufacture of composite parts, whereby an oven is used instead of an autoclave [5]. OOA manufacturing has the potential to increase process throughput and reduce manufacturing costs, however, it is a less robust process and composite parts are more susceptible to part quality issues. One notorious part quality issue, which is the subject of this study, is the presence of voids within the material. Voids are regions within the laminate devoid of both resin and fiber and the volume fraction of voids is called porosity. Porosity reduces the mechanical performance of composite parts and as a result the aerospace industry imposes a 2% by volume limit on porosity in structural members. Therefore, in order to successfully implement

OOA manufacturing in the advanced composites industry, a detailed understanding of the drivers and mitigation strategies of porosity is required.

1.1 Scope and Objectives

Initially the scope of this study was to investigate porosity development on the mould side surface of composite prepreg laminates. However due to interesting results from some preliminary tests the scope of this study evolved and was modified as discoveries were made. The modified scope of this study is investigating resin voids and how they manifest into porosity in carbon fiber reinforced epoxy composites. Since the initial scope of the project was investigating surface porosity, resin voids were studied on the surface of prepreg laminates. The first portion of this study investigates two hypothesized growth mechanisms (detailed in section 2.2) of resin voids in samples of neat MTM45-1 resin (i.e. only resin, no fibers). The results and conclusions from the neat resin experiments are used for the second portion of this study which investigates the behaviour and growth of resin voids in laminates. Relevant process parameters are changed with the intent of stimulating one or both of the resin void growth mechanisms. Process parameters, resin pressure and in-situ visual observations are correlated with final bulk and surface porosity based on the two growth mechanisms of interest.

The original scope of the study was justified by an absolute lack of understanding of the mechanisms and drivers of surface porosity. A literature search on surface porosity (at the start of the project) yielded only one article from Boeing which details a trouble shooting operation rather than an investigation into underlying physics [23]. Surface porosity causes the exterior of the composite part to be rough and aesthetically displeasing. Industry, especially OOA manufacturing, is plagued by surface porosity which, due to a lack of fundamental understanding, is dealt with by post processing reparations. The initial project motivation was due to these reparations being both laborious and costly. The scope of the study was modified because the significance of resin voids as a source of significant bulk and surface porosity was serendipitously discovered. Traditionally resin voids were considered a very minor, even negligible, contributor to porosity and thus hardly any literature can be found on the subject of resin void porosity. No new test methods or physics were developed in this study, however the novelty of this study is applying previously developed test methods and physics to resin voids and linking them to porosity development in OOA manufactured composite laminates.

The objectives of this study were to:

- Qualitatively and quantitatively observe resin voids in neat resin and investigate resin void growth mechanisms
- Qualitatively and quantitatively observe resin void growth in-situ in laminates
- Correlate resin void growth to final surface and bulk porosity in laminates
- Develop a resin void growth porosity prediction tool

2 BACKGROUND & LITERATURE REVIEW

2.1 Composite Prepreg Processing

Fiber reinforced polymer composites consist of fibers surrounded by a polymer matrix. The fibers and resin can be separate and combined during processing, such as in an infusion process, or come in the form of a resin impregnated fiber mat called prepreg. Prepreg is commonly used in advanced applications, such as aerospace, due to the precise control of resin content, high degree of fiber alignment and a sticky surface (tack) which helps in the stacking process.

2.1.1 Prepreg

Prepreg consists of a fiber mat pre-impregnated with a catalyzed and partially cured resin and comes in the form of rolled sheets. The fiber mat can be unidirectional or woven. Traditional prepreps are fully impregnated with resin while modern OOA prepreps are partially impregnated with resin leaving dry fibers for gas evacuation pathways [6].

The material used in this study is an OOA prepreg consisting of Cytec MTM45-1 epoxy resin partially impregnating a 5-harness satin woven fiber mat. MTM45-1 is a toughened epoxy based resin system designed for high performance application and flexible curing temperatures [7]. It can be cured at temperatures as low as 80°C to allow use of inexpensive tooling with a 180°C post cure heat treatment to maximize mechanical properties. The fiber mat consists of 6K IM7 carbon fiber tows measuring 2 mm in width woven in a 5-harness satin pattern (5 tows per crimp). The fiber mat is partially impregnated by a film of MTM45-1 on one side resulting in a resin poor and resin rich side. Figure 2.1 shows both sides of the prepreg in its uncured form. This prepreg is 36% resin by weight which translates to the laminates since OOA prepreps are net resin systems (i.e. no resin bleeds out of the laminate during cure).

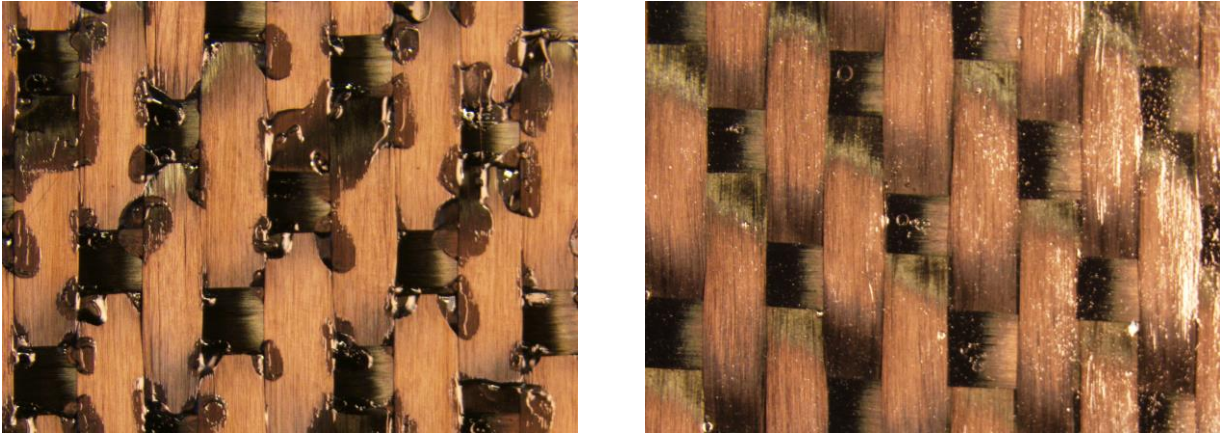


Figure 2.1: MTM45-1/CF2426A prepreg resin poor side (left) and resin rich side (right).

2.1.2 Lay-up and Cure

Composite parts are made by stacking layers of prepreg (lamina) onto a tool or mould. Sequential stacking of lamina to form a laminate (called lay-up) builds the part to the required thickness and allows for tailoring of properties in certain directions. Once the laminate is assembled, it along with several consumables are vacuum bag sealed. Figure 2.2 shows a schematic vacuum bag assembly. Each consumable performs a specific role summarized in Table 2.1.

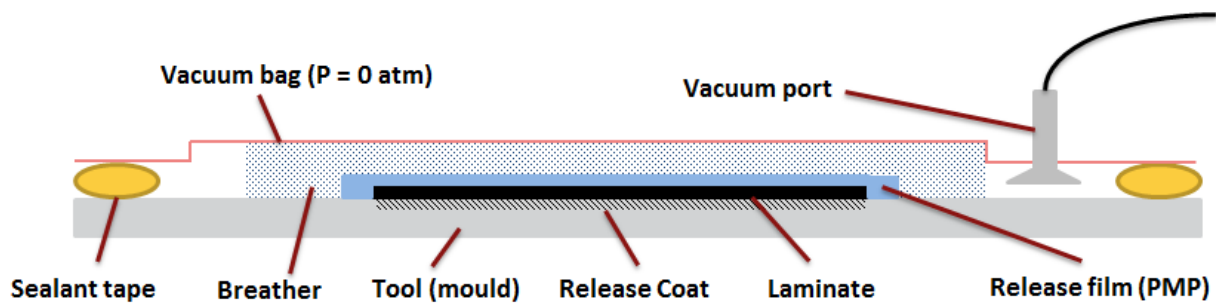


Figure 2.2: Standard vacuum bag assembly used to manufacture composite materials.

Table 2.1: List and description of consumables used in composites manufacturing.

Consumable	Description/Purpose
Vacuum bag	Air impermeable polymer sheet that covers the laminate and applies consolidation pressure to the laminate
Sealant tape	Air impermeable rubber tape that seals the edges of the vacuum bag to the mould
Release coat	Prevents adhesion of the laminate to the mould
Release film	Resin impermeable polymer sheet that prevents resin bleed from the system and adhesion of the laminate to the breather
Breather	Air permeable cloth that facilitates gas transport within the bag to the vacuum port

After vacuum bagging the laminate and ensuring a good vacuum seal the entire assembly is placed in an autoclave. An autoclave is a pressurized oven that applies positive external pressure onto the laminate (upwards of 5-10 atm) and provides heat for the curing chemical reaction. The atmosphere within the vacuum bag is evacuated imposing a higher consolidation pressure on the laminate. Gas remaining within the laminate is compressed and forced into solution by the high applied pressure. Initially resin viscosity is very high but drops rapidly with temperature such that it flows within the laminate compressing and all void space. Voids are defined as any region not occupied by resin or fibers [8]. High temperature accelerates the resin curing reaction and polymerization and cross linking of the thermoset polymer begins. The goal with the curing reaction is to maximize the resin glass transition temperature [1]; this gives the highest possible operating temperature and best mechanical properties for a given resin system. Autoclave processing is a robust and reliable method for processing composite materials; however it is expensive (both capital and operating cost), imposes limitations on part dimensions and restricts process throughput [10]. An alternative to using an autoclave is out-of-autoclave processing using ovens. Ovens have several advantages over autoclaves in that they are not as limited in use and lower processing costs, however, the main disadvantage is the external applied pressure is at maximum atmospheric pressure. The low applied pressure inherent in OOA processing is insufficient to compress gas bubbles in the laminate and force them into solution. Due to this porosity is a significant part quality issue in OOA processing. Porosity in a composite part greatly reduces its mechanical performance since the voids act as points of weakness (stress concentrators) [13, 14].

Since OOA processing cannot force gas within the laminate into solution, the gas must be removed by a vacuum otherwise it will end up in the final laminate rendering it porous [11, 12]. Therefore in OOA processing gas within the laminate is extracted via vacuum prior to curing the part unlike

autoclave processing where the gas is dissolved into the resin. Early work on OOA processing discovered that a higher degree of impregnation (DI) of resin within the fiber mat results in higher porosity since entrapped air cannot be removed [15]. Recent advances in epoxy resin chemistry and partial impregnation of fiber mats have led to a new generation of OOA prepreg materials that allow the laminate to “breathe” and trapped gas and volatiles to be removed prior to cure [6]. Autoclave quality composite parts can be made using these new generation OOA prepreps however part quality, in-particular porosity, is very sensitive to process parameters. High humidity [16, 17], deficient vacuum [17, 18] and insufficient debulk (gas removal) [17] have all been shown to manifest porosity in OOA processing.

2.2 Porosity in Out-of-Autoclave Prepreg Processing

OOA prepreg laminates, prior to processing, contain numerous types of porosity in varying quantities. Figure 2.3 shows a micrograph highlighting the different types of porosity that exist within the laminate termed bulk porosity. The vast majority of porosity studies have investigated bulk porosity due to its negative impact on mechanical properties. Fiber tow voids exist in-between fibers within the fiber tow and act as the inter-connected in-plane breathing network for gas extraction [9, 19, 20, 21, 22]. In other contexts fiber tow voids are referred to as engineered vacuum channels (EVCs) or micro-voids [22]. Interlaminar voids, also called macro-voids, exist between neighbouring prepreg laminae and are formed by air entrapment between the laminae during the lay-up process. In-situ observations confirm that they are in contact with the in-plane breathing network [9, 22]. Fiber tow and interlaminar voids are labelled as bulk voids since they are connected to the breathing network and can be evacuated by debulking. Resin voids are another form of void, however, they differ from interlaminar and fiber tow voids in that they exist within the resin disconnected from the in-plane breathing network. Their existence is attributed to the resin and/or prepreg manufacturing process. Resin voids are the focus of this research and will be discussed in more detail in section 2.2.1. Initial porosity in laid up OOA laminates (prior to cure) was measured to be 33% and comprised mostly of fiber tow voids and interlaminar voids at approximately 20% and 12.5% respectively. Resin voids comprised less than 0.2% of the overall initial porosity [9].

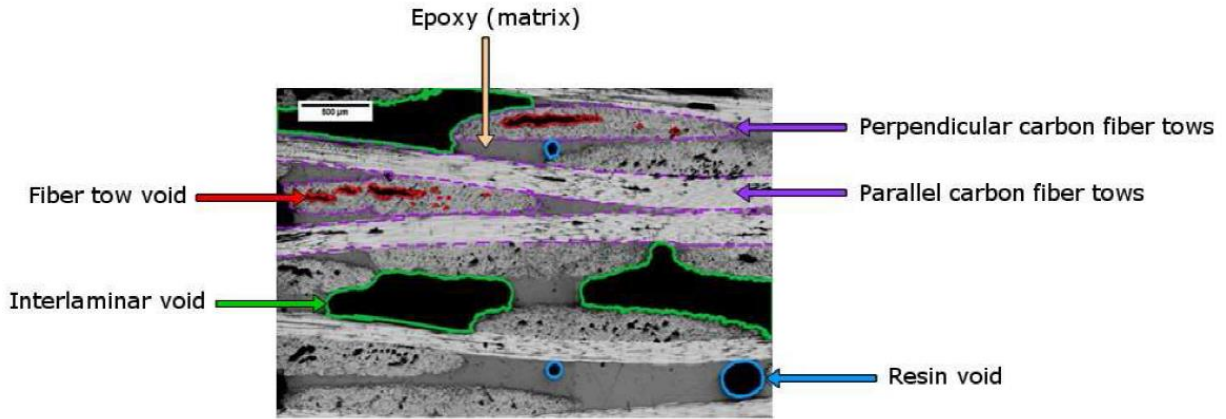


Figure 2.3: Types of voids in an OOA prepreg (Reproduced with permission [9]).

Porosity can also exist on the laminate surface, termed surface porosity, shown in Figure 2.4. Surface porosity does not impact mechanical properties significantly but rather causes the surface to be aesthetically displeasing and, in the aerospace industry, parts fail to meet aerodynamic requirements [23]. As discussed in section 1.1, the original scope of this study was to investigate the causes of surface porosity since little information on surface porosity can be found in the literature. Since surface porosity was the original focus, this study investigates the behaviour of resin voids using surface visualization methods and how they manifest into surface porosity. Due to the change in scope of the study, bulk porosity was measured after the fact using density and thickness methods (discussed in detail in section 4.1 and Appendix D) but was not the primary focus.



Figure 2.4: Surface porosity (black) on a small, flat prepreg laminate.

Porosity management in composites manufacturing is a balance between void sources and void sinks. A void source is any mechanism that contributes to the generation or growth of voids. Conversely a void sink is any mechanism that contributes to the removal or shrinkage of voids [24, 25]. Figure 2.5 schematically shows a laminate cross section and the relevant void sources and void sinks on the global

scale. The major global system parameters manufacturers have control of are vacuum pressure, applied pressure and temperature. In order to produce a void free part the three global parameters must be manipulated such that the void sinks sufficiently mitigate the void sources. This requires several processes to occur in a particular sequence [26]:

1. Gas initially present in the laminate must be removed. This is achieved by applying vacuum to the laminate and allowing adequate time for the air to flow out of the part and to be removed by the vacuum system. Resin viscosity needs to be high during this process so the vacuum channels remain open.
2. The ideal gas expansion of resin voids and vapourization of dissolved volatiles during heat up and softening of the resin must be suppressed. This can be achieved by applying pressure and ensuring the resin pressure exceeds a minimum required resin pressure defined by the initial system conditions.
3. The resin must flow into the spaces previously occupied by gas. This occurs after sufficient debulking and at elevated temperature when the resin viscosity is low, when void pressure is low and resin pressure is high.

Numerous studies have been reported on gas flow and evacuation of OOA laminates [24, 27, 28, 29, 30]. In order to remove the entrapped air, the laminate must be held under vacuum (debulking) for a prolonged period of time. Gas flow within OOA laminates has been shown to be well approximated by Darcy's Law, Equation 1, for fluid flow within porous media [24].

$$v = -\frac{K}{\mu} \frac{dP}{dx} \quad (1)$$

Where v is the fluid velocity, K is the permeability of the porous media, μ is the fluid viscosity and dP/dx is the pressure gradient within the fluid. Darcy's Law is applied to both air evacuation and resin infiltration of the partially infiltrated fiber mat. In the case of debulking the porous media are the partially impregnated fiber tows which form the interconnected breathing network and the fluid flowing is air. During this phase of cure the resin viscosity is very high and thus will not flow and close off the interconnected breathing network. The permeability of MTM45-1/CF2426A 5HS prepreg during debulk was measured to be $\sim 10^{-14}$ m² in-plane and $\sim 10^{-18}$ m² through thickness [27, 28]. During the temperature ramp resin viscosity begins to decrease and resin begins to flow into the void spaces. In the case of resin

infiltrating the fiber mat the porous media are the locally uninfiltrated fiber tows and the fluid flowing is resin. As resin flows into the void spaces in-plane breathing permeability has been shown to steadily decrease to zero as the fiber tows become infiltrated [9] therefore gas extraction must occur while the resin viscosity is high. Once the permeability reaches zero, any gas remaining in the laminate will equilibrate with the hydrostatic resin pressure according to the ideal gas law. Resin pressure is an important process parameter and is discussed in detail in section 2.3. Resin flow and infiltration has been studied and reported in the literature [22, 31, 32, 33].

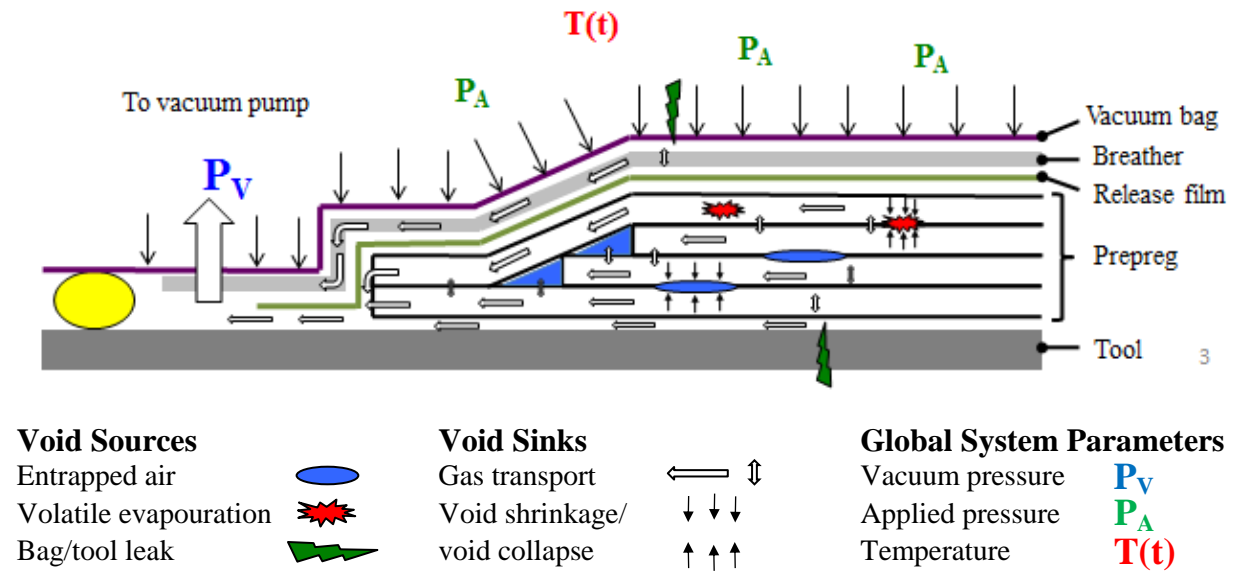


Figure 2.5: Void sources and void sinks on the global scale (Adapted with permission [25]).

The focus of this study is step 2: ideal gas expansion and dissolved volatile vapourization and how these mechanisms interact with resin voids. Many authors discuss these mechanisms in relation to porosity in autoclave processing [34, 35], however, there is little evidence directly linking these mechanisms to porosity especially in OOA processing.

2.2.1 Resin Voids

Resin voids are gas bubbles located within the resin disconnected from the laminate breathing network. Figure 2.6 shows a representative volume element (RVE) of a composite laminate on the local scale highlighting the main difference between bulk voids (fiber tow and interlaminar voids) and resin voids. The RVE contains fibers, resin and voids. The fibers are taken as inert and have negligible solute

solubility. The resin has a hydrostatic pressure, P_R , and contains dissolved species at some concentration away from a void interface, $[X]_{i,\infty}$ (i represents the specie, ∞ represents a location away from a void interface). Bulk voids are connected to the laminate breathing network and have a gas pressure, $P_{G,Bulk}$, and interfacial solute concentration $[X]_{i,Bulk}$. Resin voids (being isolated from the prepreg breathing network) have a gas pressure, $P_{G,Bubble}$, and interfacial solute concentration $[X]_{i,Bubble}$ different from that of the bulk voids. Table 2.2 lists the local variables of interest. Prior to beginning the manufacturing process (i.e. no global parameters have been changed) each void-resin interface will have established force equilibrium (determined by gas pressure, resin pressure and surface tension) and thermodynamic solution equilibrium (determined by specie partial pressure and dissolved concentration). Changing the global parameters changes some of the local variables by disrupting the equilibria in the laminate which manifests various mass transport phenomena. For example, during debulk bulk voids will evacuate (i.e. $P_{G,Bulk} \rightarrow 0$) while resin voids remain unaffected (i.e. $P_{G,Bubble} = \text{Const.}$) and P_{Resin} will change since the external applied pressure is now imposing on the vacuum bag. Resin voids, in the past, have been mostly ignored since they contribute only $\sim 0.2\%$ to overall porosity; however, these voids have the capacity to grow and manifest significant porosity both by dissolved volatile vapourization and ideal gas expansion.

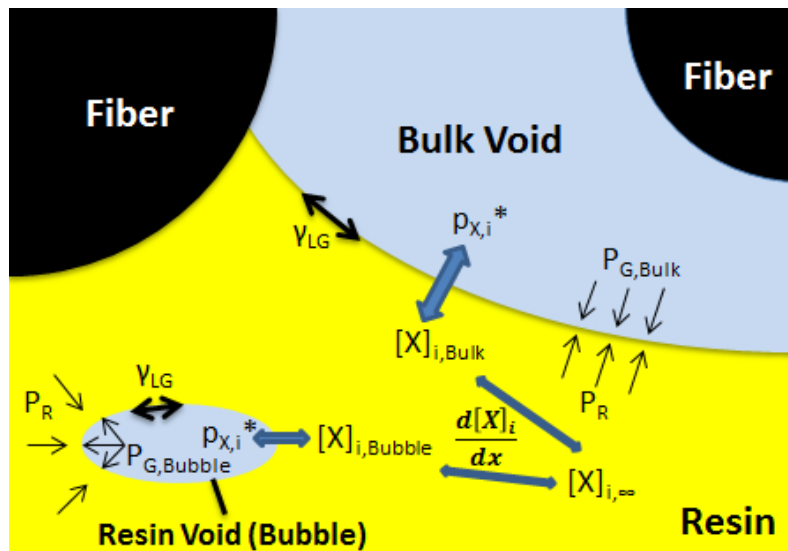


Figure 2.6: Representative volume element (RVE) of a composite.

Table 2.2: Local RVE variables of interest.

Location	Variable
Resin	P_R $[X]_{i,\infty}$
Bulk voids	$P_{G,Bulk}$ $[X]_{i,Bulk}$
Resin voids	$P_{G,Bubble}$ $[X]_{i,Bubble}$

2.2.1.1 Resin Void Growth by Volatile Vapourization

Previous investigations into bubble growth behaviour were primarily focused on dissolution of gases within the resin under autoclave pressure. Based on Scriven’s formulation [36] and a quasi-stationary boundary assumption, bubble growth/shrinkage was modeled based on moisture vapourization/dissolution under autoclave processing [34, 35]. Gas bubbles suspended within a nitrogen saturated resin were observed to grow both by diffusion and ideal gas expansion when subjected to vacuum pressure and shrink under autoclave pressure [37]. A recent study builds on previously developed models by coupling diffusion with visco-mechanical theory [38]. Due to the low pressure inherent in OOA processing, removing resin voids by dissolution of gas into the resin is not possible. Therefore an understanding of other mechanisms of removal and/or mitigation of resin void growth is needed. The phenomenon of resin void removal through “bubble mobility” has been reported in the literature. Resin voids are transported by the resin to an EVaC and subsequently evacuated [39, 40]. With respect to mitigating resin void growth, there is a distinct knowledge gap of how and under what conditions resin voids grow and manifest into significant porosity under OOA processing conditions.

Older generations of prepreg were solvent impregnated and thus contained dissolved volatile species in the resin. Modern OOA prepreps are manufactured using either the hot melt or resin filming process both of which do not require the use of solvents and therefore the content of dissolved volatile species in the resin is significantly reduced [1]. Despite this epoxy resin is hygroscopic and will absorb moisture from the environment. This moisture can vapourize from the resin causing voids to stabilize resulting in porosity in the final part. Prepreg exposed to relative humidity (RH) above ~70% RH has been shown to develop porosity in OOA processing but not in autoclave processing [16]. This result was explained using a moisture diffusion based void growth criterion developed by Kardos [35]. The authors claim that the lower pressure in OOA processing allowed moisture to vapourize and stabilize as porosity.

Kardos developed the model for moisture as the only vapourizing specie but it can be extended to any volatile component.

Moisture concentration in the resin is a function of the solubility of moisture in the epoxy resin. The solubility of moisture in epoxy resin is dependent on the activity of moisture, which is normally expressed as relative humidity, RH , and follows an empirical parabolic relationship, Equation 2 [34].

$$S = k_1 RH^2 = k_1 \cdot 10^4 \left(\frac{p_{H_2O}}{p_{H_2O}^*} \right)^2 \quad (2)$$

Where S is solubility in wt% (moisture per unit weight of resin), k_1 is a curve fitting constant in wt% (moisture per unit weight of resin), RH is percent relative humidity, p_{H_2O} is the partial pressure of moisture vapour in atm and $p_{H_2O}^*$ is the equilibrium partial pressure of moisture vapour in atm. The epoxy resin used in this study (MTM45-1) was found to behave according to this empirical solubility relation [41]. Solubility corresponds to concentration, C , by Equation 3.

$$C = \frac{S}{100} \rho_{Resin} = \frac{\rho_{Resin}}{100} k_1 \cdot 10^4 \left(\frac{p_{H_2O}}{p_{H_2O}^*} \right)^2 \quad (3)$$

Moisture content away from a void interface, $C_{H_2O,\infty}$, will equilibrate with the initial RH the resin is exposed to while the resin void interfacial concentration, $C_{H_2O,Bubble}$, will equilibrate with the current RH in the void. Before processing these concentrations are equal since the RH in the resin void will equal the ambient RH . Figure 2.7 shows a schematic of the mechanism. Initially resin voids will contain an air-water vapour mixture, however, it has been shown that neglecting the air component results in minimal loss of accuracy [35].

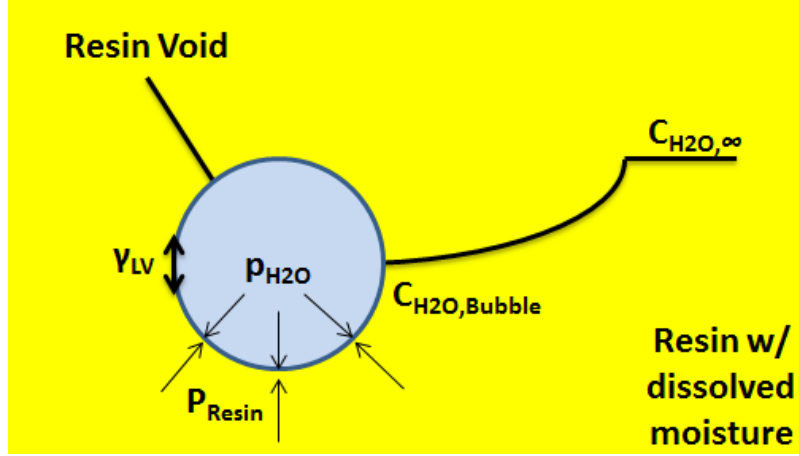


Figure 2.7: Schematic of resin void growth by moisture.

Growth of the resin void can only occur if bulk moisture diffuses to the resin void interface which requires $C_{H_2O, \infty} > C_{H_2O, Bubble}$.

$$C_{H_2O, \infty} > C_{H_2O, Bubble} \quad (4)$$

$$\frac{k_1 RH_0^2 \rho_{Resin}}{100} > \frac{k_1 \rho_{Resin}}{100} \left(\frac{p_{H_2O}}{p_{H_2O}^*} \right)^2 \quad (5)$$

Rearranging and isolating for p_{H_2O} yields the criterion for diffusion.

$$RH_0 p_{H_2O}^* > p_{H_2O} \quad (6)$$

Of more practical use is the criterion for resin void growth which will occur when $P_{Resin} < p_{H_2O}$ because $P_{Resin} = p_{H_2O}$ at equilibrium.

$$P_{Resin} < p_{H_2O} \quad (7)$$

$$P_{Resin} < p_{H_2O}^* RH_0 \quad (8)$$

Inequality 8 is the criterion for which resin voids can grow by moisture diffusion. Equilibrium vapour pressure of a specie is described by the Clausius-Clapeyron relation.

$$P_{Resin} < P_0 \exp\left(\frac{\Delta H_{vap}}{RT_0}\right) \exp\left(\frac{-\Delta H_{vap}}{RT}\right) (RH_0) \quad (9)$$

Where ΔH_{vap} is the enthalpy of vapourization, P_0 and T_0 are the Clausius-Clapeyron reference pressure and temperature respectively. The base Clausius-Clapeyron equation is in differential form and a reference pressure and temperature are required to determine the constant of integration when solving for pressure. The variables in Equation 9 are P_{Resin} , T and RH_0 ; all other terms are constants. Inserting moisture values for the constants (shown in Table 2.3) and equating the sides yields the critical resin pressure below which moisture can cause resin voids to grow by diffusion and vapourization.

$$P_{R,Critical} = 4962 \exp\left(\frac{-4892}{T}\right) (RH_0) \quad (10)$$

This Equation, developed by Kardos [35], predicts resin pressure, temperature and moisture content (proxied by RH_0) to be variables influencing this type of porosity mechanism. Resin pressure is predicted to be the most critical of the three parameters because of the square relation between moisture vapour pressure and resin void concentration ($C_{H2O,Bubble}$, Equation 3) which influences diffusion driving force and because of the indirect control (see section 2.3 for more details) of resin pressure and inherently low pressures in OOA processing.

Table 2.3: Moisture values used for the Clausius-Clapeyron relation.

Variable	Value
$\Delta H_{vap}/R$	4892 K
P_0	1 atm
T_0	373 K

2.2.1.2 Resin Void Growth by Ideal Gas Expansion

Ideal gas expansion of gas bubbles is by no stretch of the imagination a novel concept, however, it has never been considered in regards to resin void growth in OOA composites processing. Autoclave processing mitigates porosity by shrinking gas bubbles and dissolving the gaseous species into the resin with large positive pressure [42], however, due to the low applied pressure in OOA processing resin voids cannot be shrunk or forced into solution.

The force equilibrium of a bubble immersed in a fluid is given by the Laplace pressure, Equation 11 [43].

$$P_{Internal} - P_{External} = \frac{3\gamma_{LV}}{r} \quad (11)$$

Where $P_{Internal}$ is the pressure within the bubble, $P_{External}$ is the pressure outside of the bubble, γ_{LV} is the interfacial surface tension between the bubble constituents and surrounding fluid and r is the bubble radius. The pressure difference across the bubble interface is balanced by the interfacial tension. For increasingly larger bubbles the interfacial tension acts solely in the tangential direction and the term becomes increasingly negligible. For example, using an interfacial tension of 0.05 N/m the last term in Equation 11 equals 0.148 atm for $r = 10 \mu\text{m}$, 0.049 atm for $r = 30 \mu\text{m}$ and 0.03 atm for $r = 50 \mu\text{m}$. This term quickly falls off for bubble radii $> 30 \mu\text{m}$ ($< 5\%$ of an atm) and since resin voids are typically larger than this, the interfacial tension term can be neglected and therefore internal pressure equals external pressure. For a resin void immersed in epoxy resin, assuming viscosity is low enough for the forces to equilibrate, the internal pressure is the resin void pressure and the external pressure is the hydrostatic resin pressure.

$$P_{Resin Void} = P_{Resin} \quad (12)$$

Resin void volume can be approximated by the ideal gas law, Equation 13. Resin void pressure can be directly replaced with resin pressure.

$$V_{Resin Void} = \frac{nRT}{P_{Resin Void}} = \frac{nRT}{P_{Resin}} \quad (13)$$

This Equation predicts, rather intuitively, that increasing mole content, increasing temperature and decreasing resin pressure contributes to resin void growth. Increasing mole content is described by volatile evaporation in section 2.2.1.1. Resin pressure is, again, hypothesized to be a critical variable in mitigating resin void growth due to ideal gas expansion since volume goes to infinity as resin pressure goes to zero.

2.3 Hydrostatic Resin Pressure

Resin pressure is an important processing parameter that has been rather extensively studied [10, 44, 45]. It is not a directly controlled parameter; the external pressure applied to the laminate is shared between the resin and the fiber bed according to Equation 14.

$$P_{Applied} = P_{Resin} + \sigma_{Fiberbed}(V_f) \quad (14)$$

The fiber bed is assumed to be a deformable, non-linear elastic network that supports load by fiber bending between sites of fiber-fiber contact [46]. The fiber bed effective stress, $\sigma_{Fiberbed}$, is dependent on fiber volume fraction due to the increased density of fiber contact sites at higher volume fractions. The load the fiber bed can support asymptotically approaches infinity for fiber volume fractions in the range of 60-70% depending on the fiber architecture. Older generation prepreg systems used resin bleed as a form of porosity management and it has been shown that resin bleeding out of the laminate decreases the resin pressure [10, 44]. Too much resin bleed can reduce the resin pressure to zero [10]. In both cases the fiber volume fraction increases and is able to support more load, and potentially the entire load. Modern prepreps are net resin systems and thus the fiber volume fraction remains constant. However, configured structures introduce gaps and pockets within the laminate which resin can bleed into and locally reduce the resin pressure [47].

3 NEAT RESIN EXPERIMENTS

3.1 Neat Resin Test Methods

Samples of Cytec MTM45-1 neat resin were used to observe the in-situ behaviour of resin voids. It is a toughened epoxy designed for cure cycle flexibility [7]. Small samples of resin (approximately circular samples measuring $\sim 5\text{-}7\text{ cm}^2$ and 0.19 mm thick) were placed and vacuum bagged on a 6 mm thick boro-silicate glass tool. The resin was visually observed and recorded in-situ using a Keyence VHX-1000 digital microscope. Figure 3.1 shows the experimental lab setup, Figure 3.2 shows the in-situ observation vantage and Figure 3.3 schematically shows the vacuum bag assembly. A heater was placed on the resin inside the vacuum bag to facilitate temperature control. The heating pad is sufficiently light that squeeze flow of the resin did not occur. The resin pressure was controlled by shielding the resin from external atmospheric pressure by placing it under an aluminum bridge and controlling the pressure inside the vacuum bag using a vacuum pressure regulator. The regulator allowed for manual control of the internal bag pressure during the test. Moisture content was controlled by humidity conditioning the neat resin in environmental chambers containing a saturated salt solution. Saturated salt solutions depress the water activity enabling accurate control of the relative humidity inside the chamber [49].

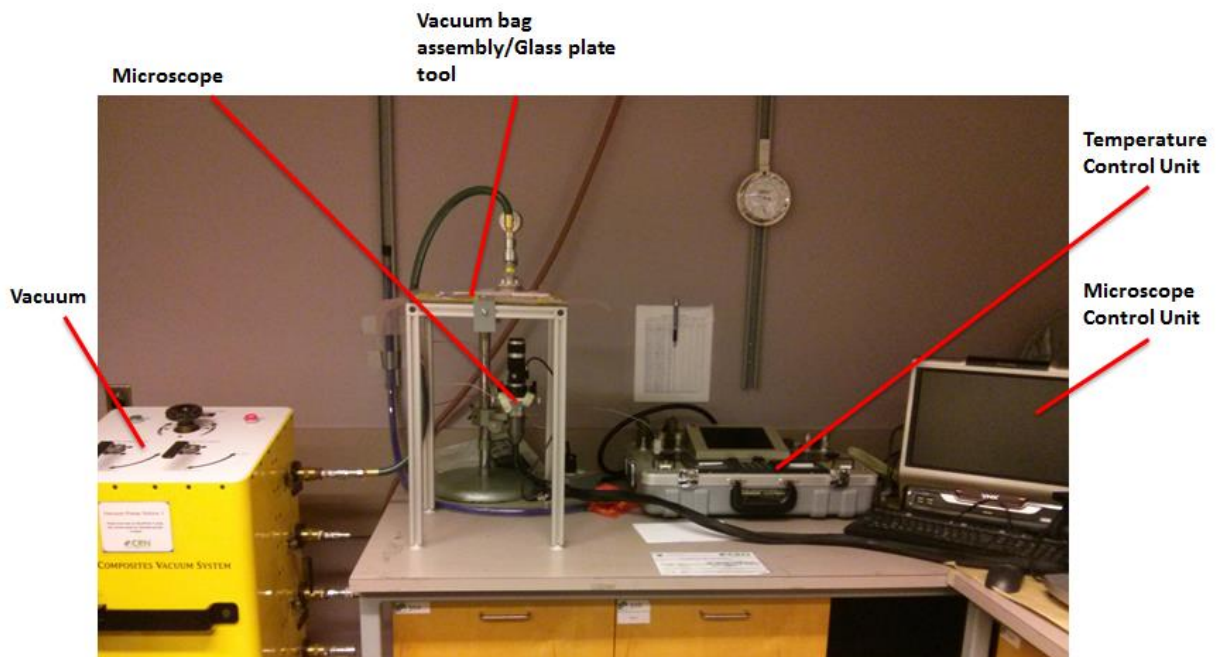


Figure 3.1: Experimental test setup.

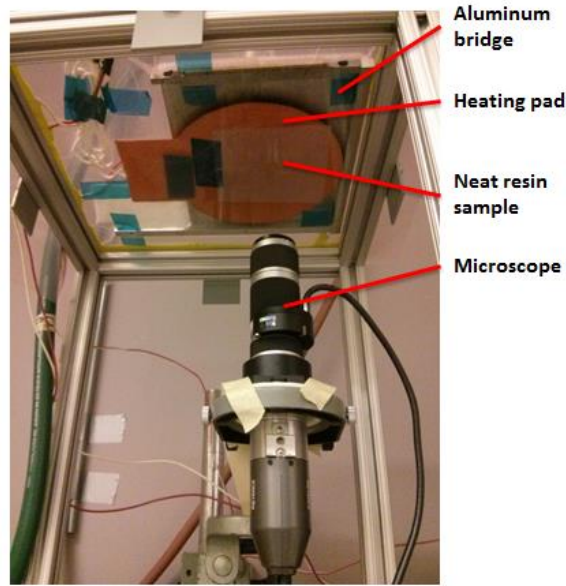


Figure 3.2: Experimental test setup in-situ observation vantage.

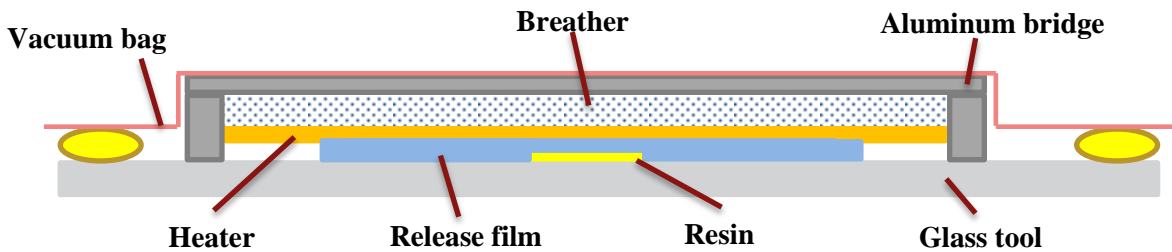


Figure 3.3: Neat resin vacuum bag assembly.

Quantitative analysis was performed using ImageJ image analysis software to measure resin void diameter. In-situ videos and images were recorded at 50X magnification with a field of view of $6901 \times 4927 \mu\text{m}^2$. Figure 3.4 shows an in-situ image of 75% RH conditioned neat resin used to measure resin void diameters. Resin voids were selected for measurement based on apparent sphericity, isolation from neighbouring voids (both for ease of visually distinguishing bubble size and to mitigate overlapping moisture diffusion paths) and diameters less than the thickness of the resin film to avoid surface effects. Resin film thickness was measured to be $190 \mu\text{m}$ and only resin voids with diameters less than $190 \mu\text{m}$ were measured in order to mitigate surface effects (such as oval shaped bubbles) from either the glass tool or resin surface. An example of a diameter measurement is shown in Figure 3.4 indicated by the red line. Resin void diameter was measured five times in each image and average diameter values were reported.

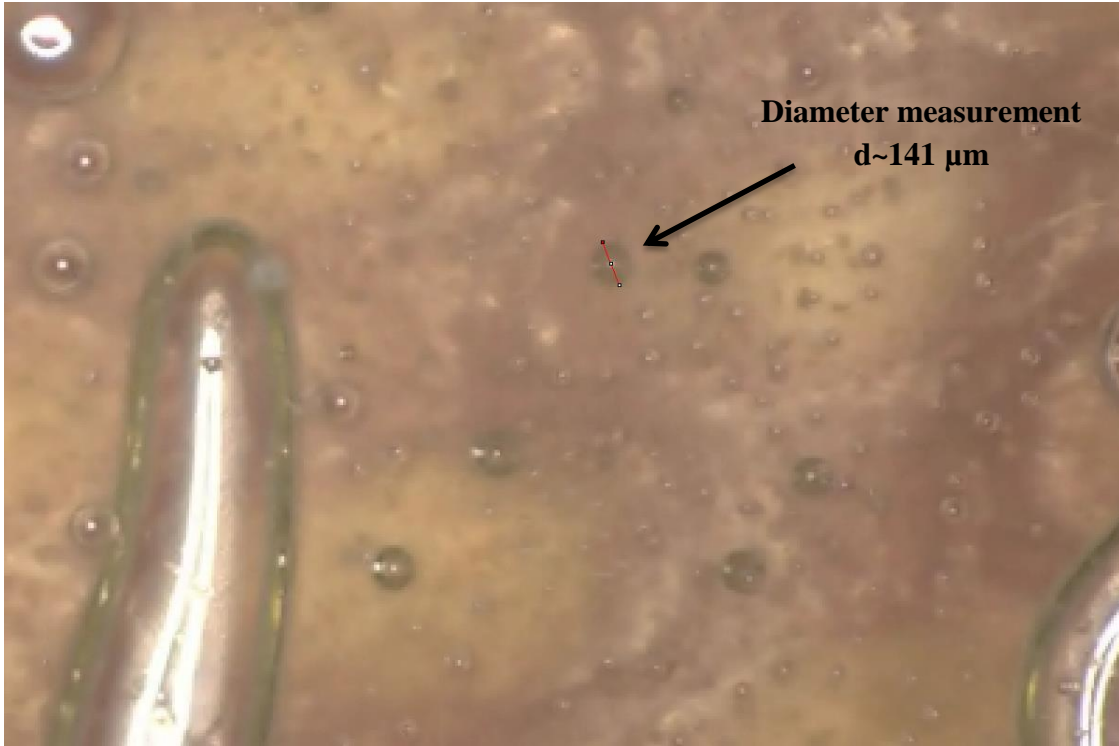


Figure 3.4: In-situ neat resin image used for measuring bubble diameter.

3.1.1 Kardos Criterion Test Method

The Kardos criterion predicts the critical resin pressure below which resin voids can grow due to dissolved volatile vapourization (see section 2.2.1.1 for details). Equation 15 below is the Kardos criterion for moisture.

$$P_{R,Critical} = 4962 \exp\left(\frac{-4892}{T}\right) (RH_0) \quad (15)$$

To evaluate the Kardos criterion humidity conditioned neat resin samples were subjected to resin pressure just above and just below the predicted critical resin pressure and the diameter of the resin voids was measured as a function of time. No time dependent growth should be seen for $P_R > P_{R,Critical}$ and time dependent growth should be seen for $P_R < P_{R,Critical}$. Resin samples were humidity conditioned at 75%, 33% and 0% RH. Figure 3.5 shows the test plan used to evaluate the Kardos criterion on resin conditioned at 75% RH. The test plan consists of four time segments:

1. Ramp at 50°C/min to 100°C
2. Reduce pressure to $P_H > P_{R,Critical}$, hold for ~60 seconds
3. Reduce pressure to $P_L < P_{R,Critical}$, hold for ~60 seconds
4. Increase pressure to $P_H > P_{R,Critical}$, hold for ~60 seconds

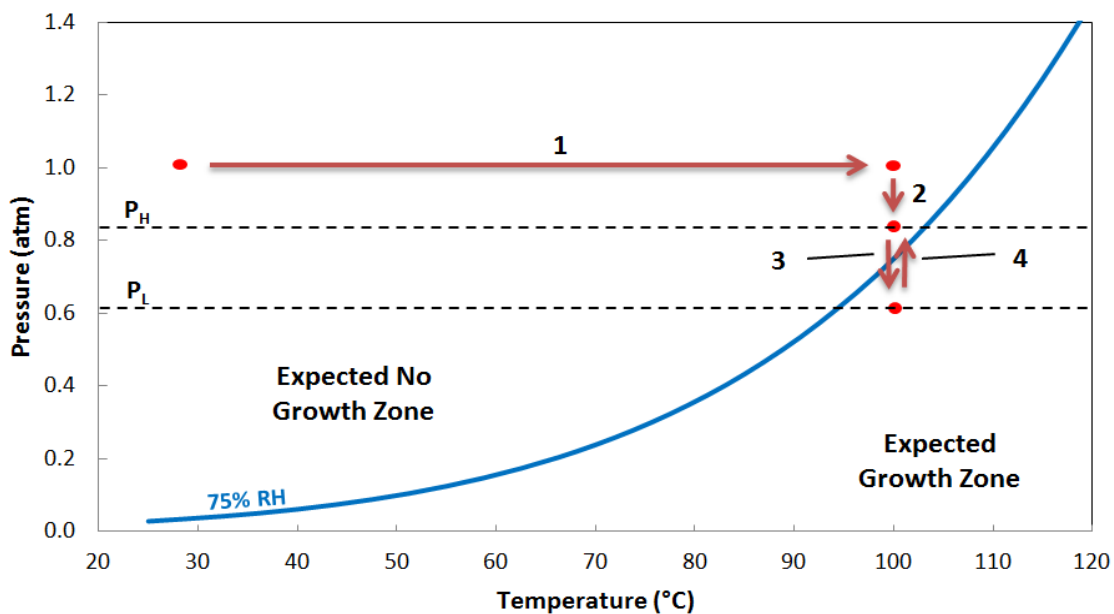


Figure 3.5: Kardos criterion evaluation test plan for neat resin conditioned at 75% RH.

Short hold times were used to minimize moisture loss due to vapourization out of the resin during the tests. Samples of desiccated resin (RH = 0%) were subjected to the same test procedure as the 75% RH and 33% RH samples in order to confirm the observed behaviour is due to moisture. Table 3.1 shows the high, low and critical resin pressure values for each test.

Table 3.1: High, low and critical resin pressure values.

RH	P_H (atm)	P_L (atm)	Predicted P_{R,Critical} (atm) (Equation 15)
75%	0.82	0.61	0.75
33%	0.40	0.19	0.33
0%	0.82 & 0.40	0.61 & 0.19	N/A

3.1.2 Ideal Gas Expansion Test Method

The resin void internal pressure will equal the surrounding resin pressure when ignoring the interfacial tension term in the Laplace pressure, Equation 11, (see section 2.2 for details) and therefore the volume of a resin void is described by Equation 16.

$$V_{Resin\ Void} = \frac{nRT}{P_{Resin}} \quad (16)$$

Mathematically, as the resin pressure approaches zero the resin void volume will tend to infinity, however, for a real system the resin voids will rupture as the resin surrounding the bubbles thins out and the internal pressure escapes and evacuates.

To qualitatively evaluate the ideal gas expansion behaviour of resin voids, neat resin samples were desiccated in an environmental chamber and subjected to stepwise resin pressure reduction from one to zero atmospheres. To determine if resin voids behave according to the ideal gas law, desiccated resin was subjected to the 75% and 33% Kardos criterion evaluation tests and *PV* (pressure x volume) was checked for constancy (these tests were designed with dual purpose). The neat resin was heated to 100°C and kept isothermal throughout each test.

3.2 Neat Resin Results & Observations

Figure 3.6 is an in-situ image of 75% RH conditioned neat resin at 0.49 atm ($P_R < P_{R,Critical}$). Inspecting the image one can see that the neat resin contains a significant amount of voids of varying size. The void sizes span orders of magnitude: the void in section 1 is on the order of 1 mm, voids in section 2 are on the order of 100 μm and voids in section 3 are on the order of 10 μm . The very large voids (section 1) are due to air entrapment from placing the resin on the glass tool while the smaller voids in sections 2 & 3 are due to the resin manufacturing process. The diameter of resin voids in sections 2 & 3 forms a bimodal distribution with mode peaks around 15 μm for the small resin voids and 120 μm for the large resin voids.



Figure 3.6: In-situ image of 75% RH neat resin at 0.49 atm; 50X magnification, image size 6901 x 4927 μm^2 .

3.2.1 Kardos Criterion Results & Observations

Figures 3.7 and 3.8 show normalized diameter averaged over 5 voids (i.e. each data point represents 25 measurements) for 75% RH and 33% RH conditioned neat resin respectively. Time zero represents the beginning of segment 2. Throughout segment 2 ($P_H > P_{R,Critical}$) no void growth is observed or measured in agreement with the Kardos criterion. Upon reducing the pressure to P_L ($P_L < P_{R,Critical}$) the

resin voids grow quickly due ideal gas expansion followed by a time dependent growth response. The time dependent response is due to moisture vapourization and diffusion. Increasing the pressure back to P_H ($P_H > P_{R,Critical}$) results in an instantaneous contraction, however, no time dependent behaviour is observed. Tests at both relative humidity levels show time dependent growth in the $P_R < P_{R,Critical}$ regime providing strong evidence for Kardos criterion validity. Time dependent shrinkage was expected in segment 4 since this growth mechanism should theoretically operate in reverse for $P_R > P_{R,Critical}$, however each test showed no time dependent behaviour in segment 4. The exact mechanism is uncertain, however, a possible explanation is that bubble shrinkage occurs at a slower rate than bubble growth and is not observable in the short time windows used for these tests. Srinivasan et al [53] modeled nitrogen gas bubble growth and shrinkage in blood and show bubble shrinkage being significantly slower than bubble growth. They claim this occurs due to decreased gas diffusivity within the boundary layer and increased boundary layer thickness for bubbles that are shrinking. Another observation is that the resin voids in the 33% RH test grew to substantially larger normalized diameters than resin voids in the 75% RH test. The lower resin pressure in the 33% RH test will induce a greater driving force for diffusion since solubility at the resin void interface is proportional to $p_{H_2O}^2$.

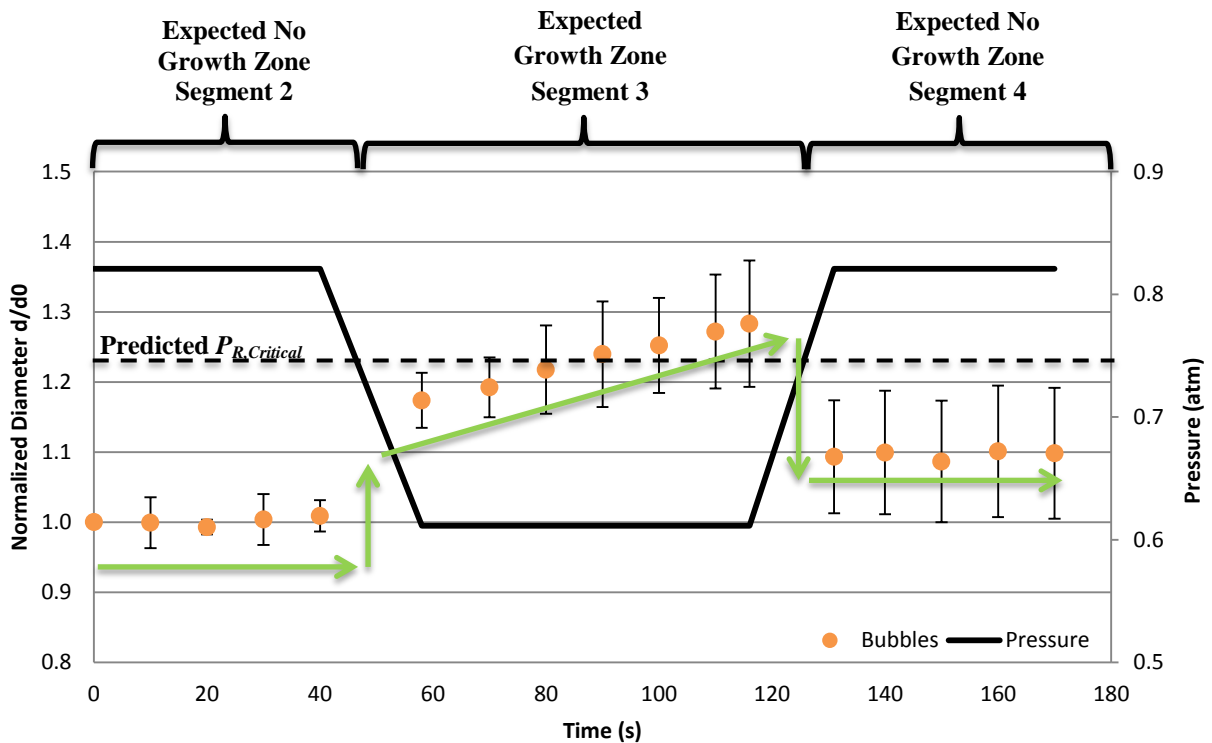


Figure 3.7: Average normalized void diameters for the 75% RH neat resin tests.

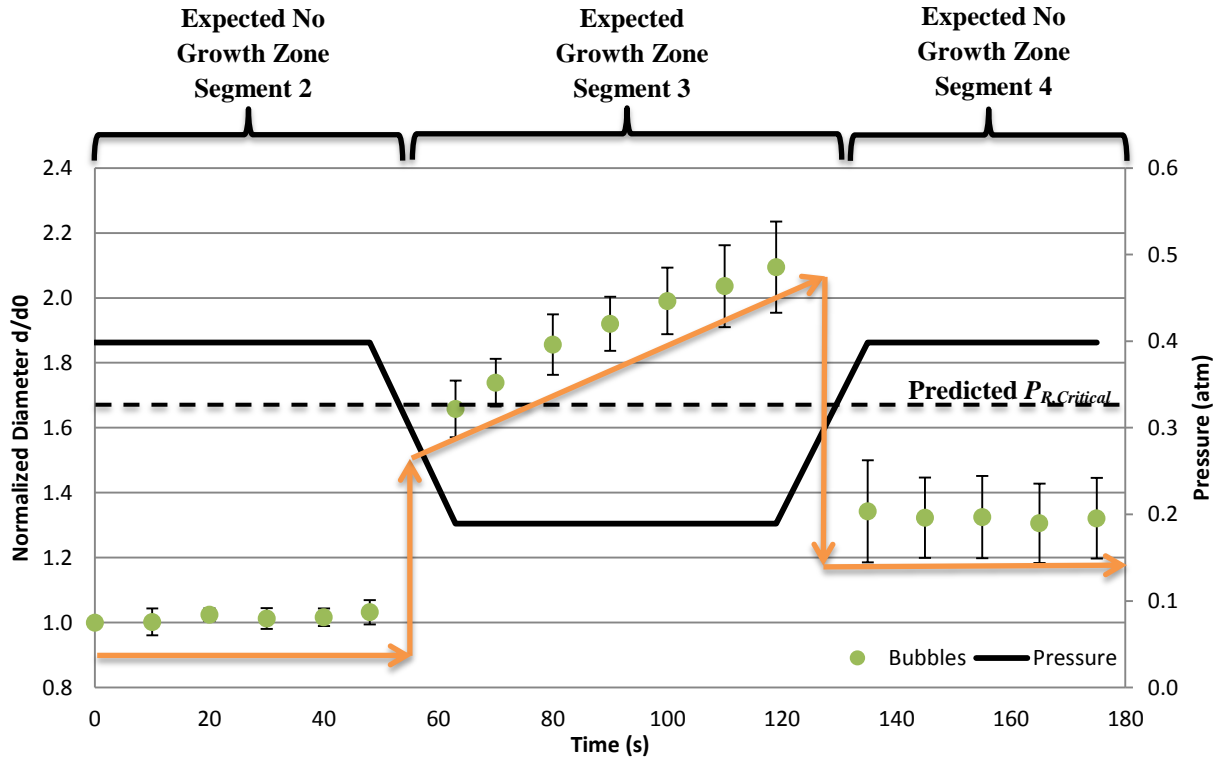


Figure 3.8: Average normalized void diameters for the 33% RH neat resin tests.

To confirm the observed behaviour in Figures 4.6 and 4.7 is due to moisture, desiccated resin was subjected to the same respective resin pressure cycles. In the absence of dissolved moisture voids subjected to the same pressure cycle should not show any time dependent growth and therefore PV (pressure x volume), assuming the bubbles are spheres, should be constant at all times. Figure 3.9 plots normalized PV averaged over 6 voids versus time for a desiccated resin subjected to the 75% RH test procedure. Also plotted is the PV behaviour for the 75% RH conditioned resin. Voids in desiccated resin were found to behave with constant PV ; in other words moles of gas in the voids were constant and no dissolved species were vapourizing into them. This confirms that moisture is indeed the cause of the time dependent growth behaviour observed in the 75% RH conditioned resin test. PV for the 75% RH resin was not constant (as expected from the results in Figure 3.7) indicating that moles of gas, n , is not constant but increasing. An interesting observation is that the voids show near instantaneous growth due to moles, n , as soon as the resin pressure is reduced. The reverse is also seen, increasing the resin pressure results in near instantaneous (mole based) shrinkage of the resin voids likely due to dissolution of moisture into the immediate vicinity of the resin void.

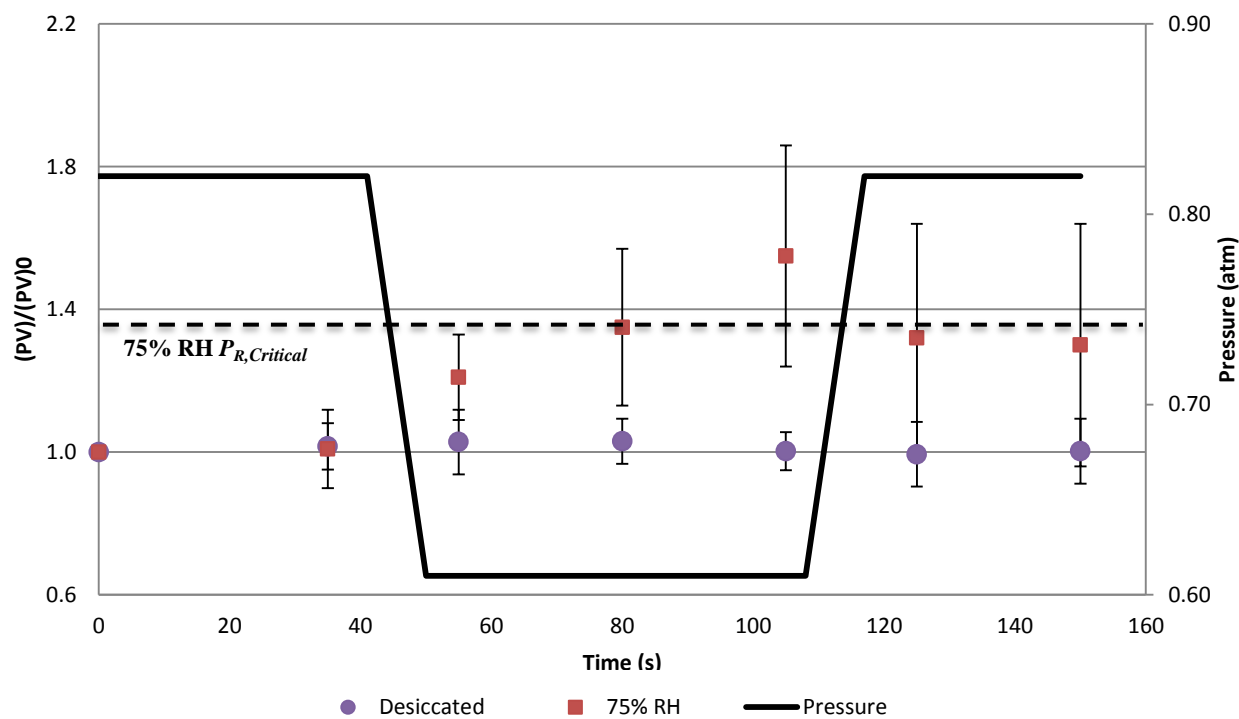


Figure 3.9: Desiccated resin subjected to the 75% RH pressure cycle.

Desiccated resin subjected to the 33% RH pressure cycle did not exhibit constant PV behaviour. Figure 3.10 shows the normalized PV behaviour of desiccated resin subjected to the 33% RH pressure cycle compared to the PV behaviour for the 33% RH conditioned resin. The resin voids in the desiccated resin grew less than the resin voids in the 33% RH resin due to the lack of moisture vapourization, however, growth of resin voids in desiccated resin suggests that MTM45-1 neat resin contains another volatile specie (or species), other than moisture, that is vapourizing into the resin voids. The presence of other volatile species contributing to void growth also helps explain why larger resin void growth was observed in the 33% RH test ($d/d_0 \sim 2.1$) relative to the 75% RH test ($d/d_0 \sim 1.3$). Resin voids again show non constant PV behaviour during pressure changes likely indicating rapid vapourization/dissolution of the volatile specie in the immediate vicinity of the resin voids. This specie did not contribute to void growth in the desiccated resin subjected to the 75% RH pressure cycle likely because its critical resin pressure is lower than the resin pressures experienced in that test. The 33% RH test experiences lower resin pressures and thus the critical resin pressure for the other specie must have been crossed. As stated previously the Kardos criterion can be used for any dissolved specie and characterization of the specie in the resin would yield the critical resin pressure curve for it.

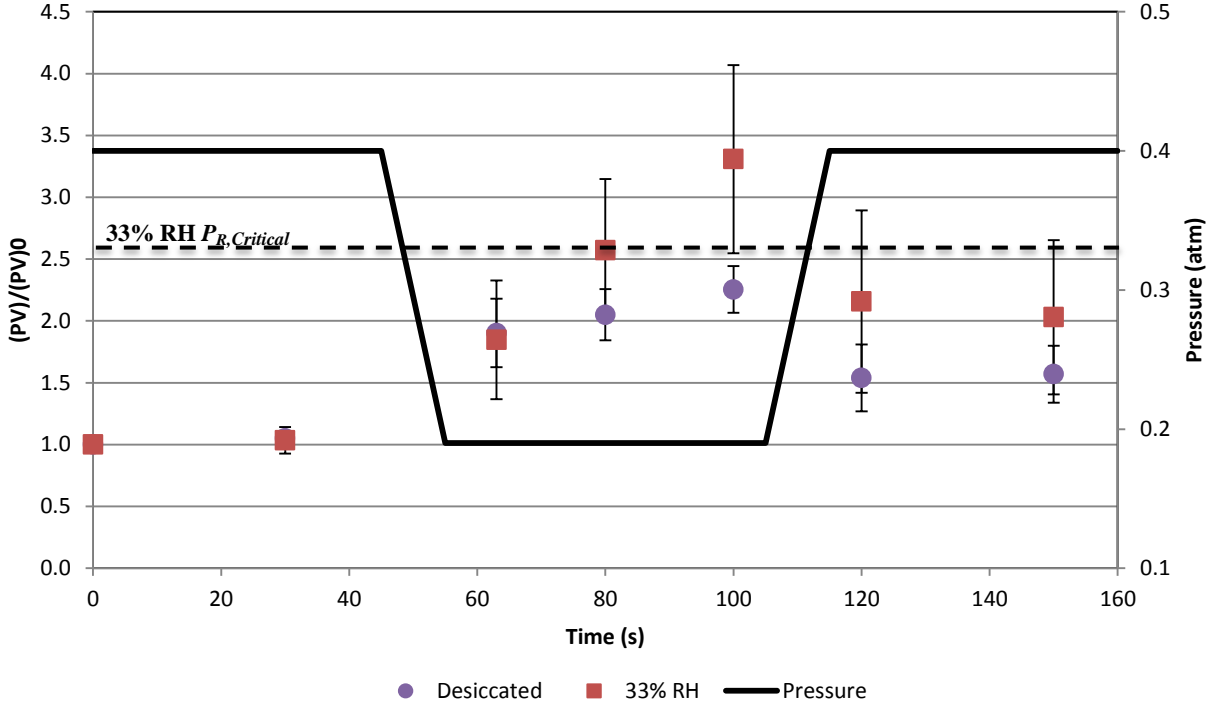


Figure 3.10: Desiccated resin subjected to the 33% RH pressure cycle.

It was found that the ideal gas equation consistently under-predicted resin void expansion/contraction when subjected to a pressure change for both the 75% and 33% RH conditioned neat resin tests (i.e. expected resin void volume based solely on pressure change did not equal measured resin void volume). This result implies that during the pressure change moles of gas, n , is not constant and that moisture is very rapidly vapourizing or dissolving during the pressure change. This can be rationalized by considering the variables present and how they are affected by resin pressure. Prior to the pressure drop below the critical resin pressure the resin voids contain moisture vapour in equilibrium with the dissolved moisture in the near vicinity of the resin-void interface. The sudden decrease in pressure acts as a shock to the system and all resin voids instantaneously grow due to PV . The decrease in pressure within resin voids will decrease the moisture vapour partial pressure decreasing the relative humidity (i.e. activity). Moisture solubility, Equation 17, is a direct function of $(RH)^2$ and the dissolved moisture at the resin-void interface is suddenly super-saturated.

$$S_0 = k_1(RH)^2 = k_1 \left(\frac{p_{H_2O}}{p_{H_2O}^*} \right)^2 \quad (17)$$

Where S_0 is moisture solubility, k_f is the proportionality constant, $p_{H_2O}^*$ is the equilibrium moisture partial pressure. The super-saturated moisture will vapourize into the void in order to increase the void RH and re-establish equilibrium. This explains the near instantaneous non PV related void growth observed during pressure changes. After the initial pressure shock to the system, the resin pressure is below the critical resin pressure and thus moisture equilibrium can never be attained. Moisture from the bulk resin will diffuse down the concentration gradient to the resin void. Kardos, Scriven and Wood [35, 36, 37] all predict this growth mechanism to be proportional to \sqrt{time} . A square root function does fit the growth data however with the short time frames where growth was measured it is impossible to draw conclusions.

3.2.2 Ideal Gas Expansion Results & Observations

MTM45-1 neat resin was found to contain a significant amount of small resin voids ranging in initial size from 10 – 500 μm . At modest resin pressures these voids remain quite small and contribute a negligible amount to porosity. However as resin pressure reduces and approaches zero these voids can grow very large according to the ideal gas equation (Equation 16) and contribute significantly to porosity. Figure 3.11 shows a sequence of desiccated neat resin images with reducing resin pressure; no moisture is contributing to the void growth shown (i.e. RH = 0%) however the unknown volatile (refer to section 3.2.1, Figure 3.10) will contribute in the lower pressure regime. Initially only the large voids can be seen and with reducing pressure these voids increase in size. At 0.26 atm the initially invisible small resin voids have expanded sufficiently to be seen. Further reduction in pressure increases their size and at 0.05 atm all voids expand uncontrollably filling the entire field of view. This porosity mechanism is only relevant in situations of low resin pressure regime.

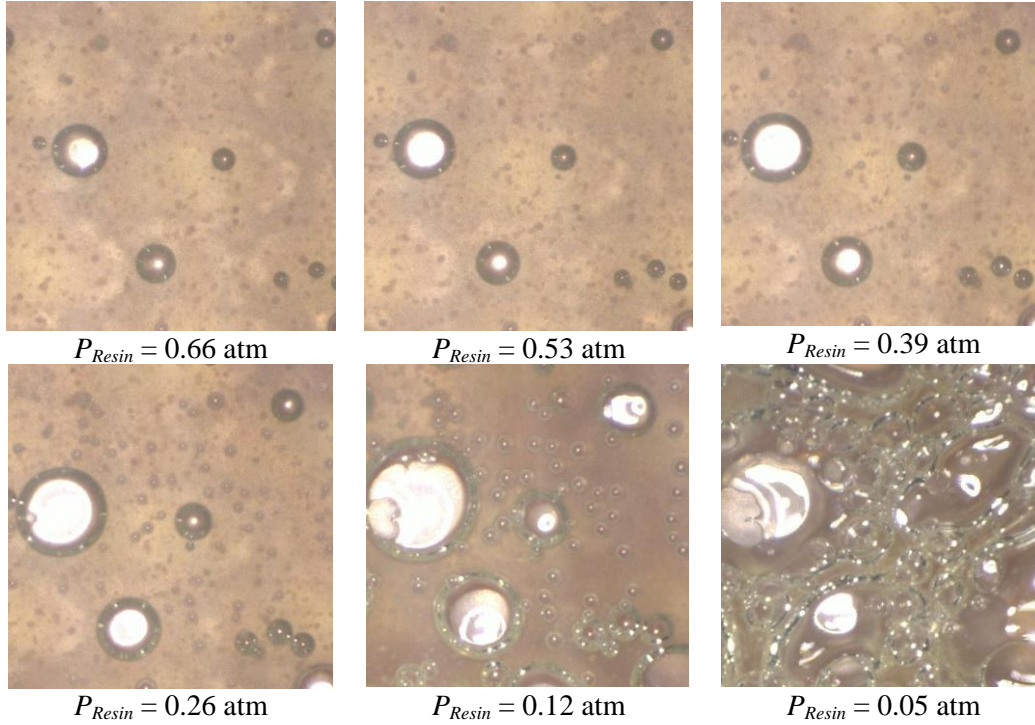


Figure 3.11: Reducing resin pressure in a desiccated resin; $T = 100^{\circ}\text{C}$, $\text{Mag.} = 50\text{X}$, $\text{Image size} = 2608 \times 2608 \mu\text{m}^2$.

A simple equation can be derived to predict ideal gas expansion porosity. As shown in Figure 3.9, without contributions from volatile species PV is constant; however real processes are not isothermal and thus PV/T is constant. Bulk voids are not present and thus we only consider resin voids in this derivation. Resin viscosity is not considered but assumed to be sufficiently low for ideal gas expansion to occur.

$$\frac{PV}{T} = \frac{P_0V_0}{T_0} \quad (18)$$

Dividing both sides of Equation 18 by resin volume, V_{Resin} , substituting in porosity, ϕ , and isolating pressure yields the ideal gas expansion porosity equation, Equation 20.

$$\frac{PV}{TV_{Resin}} = \frac{P_0V_0}{T_0V_{Resin}} \quad (19)$$

$$P = \frac{P_0\phi_0T}{T_0\phi} \quad (20)$$

It is most convenient to take initial porosity, ϕ_0 , at atmospheric pressure ($P_0 = 1 \text{ atm}$) and ambient temperature ($T_0 = \text{ambient}$). Changing porosity, ϕ , to the critical porosity (porosity above which the part is not acceptable) yields the critical resin pressure (in atm) for ideal gas expansion of resin voids, Equation 21.

$$P_{R,Critical} = \frac{T\phi_0(1 \text{ atm})}{\phi_{Critical}T_0} \quad (21)$$

Critical resin pressure is a function of the initial porosity of resin voids, the critical porosity and temperature. Critical porosity is an assumed value that depends on the manufacturer's requirements; in aerospace the critical porosity is commonly taken as 2% which yields Equation 22 for the critical resin pressure. A less stringent requirement on critical porosity will decrease the critical resin pressure.

$$P_{R,Critical} = \frac{T\phi_0(1 \text{ atm})}{0.02T_0} \quad (22)$$

Attempts at quantifying resin void initial porosity, ϕ_0 , using Equation 23 were made on neat resin samples assuming the voids are spherical in shape. The very large voids will likely have an oval shape due to contact with the mould or resin film surface however they represent the minority of resin voids present in the system and the error induced is acceptable.

$$\phi_0 = (\rho V_0)_{voids} = \frac{\pi}{6} \rho_{voids} d_0^3 \quad (23)$$

Where ρ_{voids} is void density in voids/mm³ and d_0 is the average void diameter at 1 atm of pressure and room temperature. Void density is defined as the number of bubbles per unit volume of resin. Void density was found to vary considerably from sample to sample and spatially within samples. Figure 3.12 shows a 50X magnification image of a neat resin sample at $P_{Resin} = 0.19 \text{ atm}$ used to determine resin void density, ρ_{voids} . Void density was measured at low pressure so the very small resin voids were visible; growth of these voids will displace their neighbours reducing the local density, however, the average density over the image will not be significantly affected. Neat resin images were partitioned into a grid and the number of voids within each grid space was counted. Some voids lie in multiple grid spaces, in these cases the void was counted only once in the space containing majority of the void. Void density was calculated by dividing the number of counted voids by the grid space volume (neat resin thickness was measured to be ~0.19 mm). Shown in Figure 3.12 are the calculated resin void densities in each grid

space (yellow numbers, in units of voids/mm³). Average resin void density over multiple samples was calculated to be approximately 100 voids/mm³.

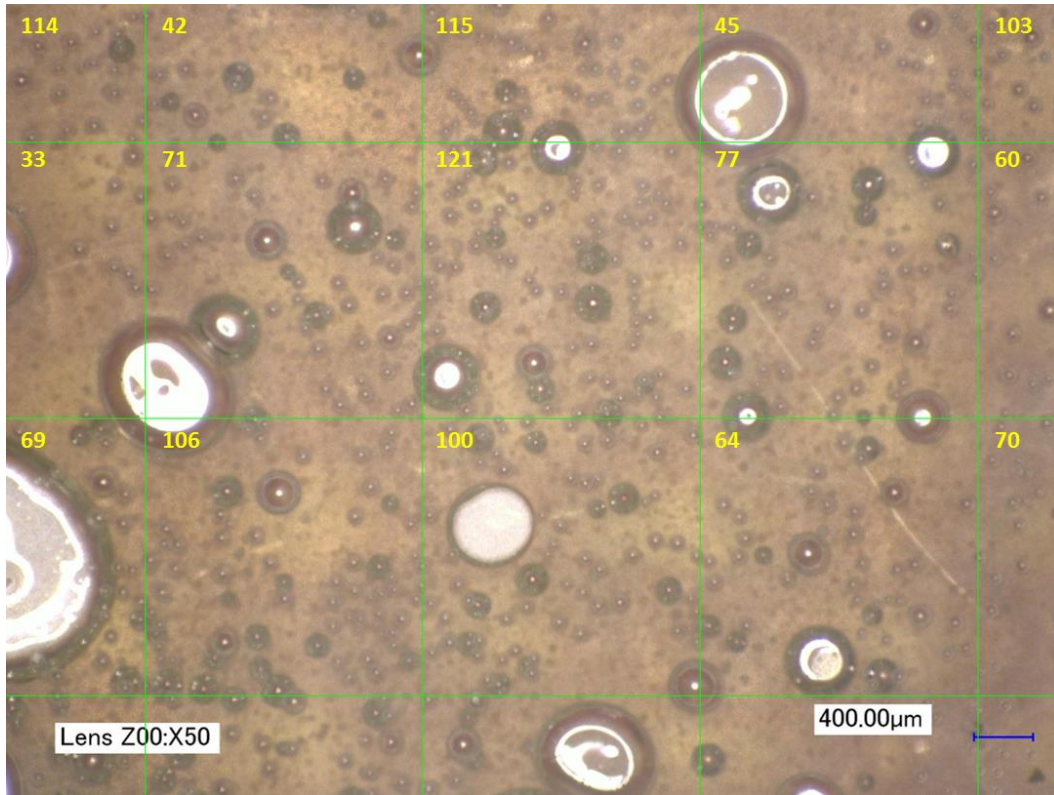


Figure 3.12: Neat resin sample at $P_{Resin} = 0.19$ atm used for void density quantification.

Resin voids were observed to be either small ($d_0 = 10 - 50 \mu\text{m}$) or large ($d_0 = 100 - 500 \mu\text{m}$). For a first order approximation of ϕ_0 , a weighted average between small and large resin voids was used, Equation 24.

$$\phi_0 = \frac{\pi}{6} \rho_{Voids} (d_{0,small}^3 f_{small} + d_{0,large}^3 f_{large}) \quad (24)$$

Where ρ is void density, $d_{0,small}$ is the initial diameter of small resin voids, $d_{0,large}$ is the initial diameter of large resin voids, f_{small} is the fraction of small voids and f_{Large} is the fraction of large voids. The small resin voids were found to comprise approximately 98% of the void population while the large resin voids comprise only 2%. Average initial diameter of small resin voids at 1 atm pressure and room temperature was measured to be approximately 15 μm and for large resin voids was measured to be approximately 120 μm . Using these average initial diameters and the fraction of small voids, f_{small} , as 0.98 yields a ϕ_0 of 0.2%. For a 2% porosity cut-off (as used in the aerospace industry), resin voids alone comprise 10% of the total allowable porosity prior to processing. Since OOA manufacturing can only experience resin

pressures equal to or less than atmospheric pressure the calculated ϕ_0 represents the minimum porosity contributed by resin voids (i.e. they cannot shrink because pressure greater than atmospheric is not applied). Let us suppose that the neat resin contains bigger resin voids with average initial diameter for the small resin voids is 35 μm and for the large resin voids is 160 μm . Using these new average initial diameters and the fraction of small voids, f_{small} , as 0.98 yields a ϕ_0 of 0.65%. These larger resin voids now comprise 32.5% (0.65/2) of the total allowable porosity prior to processing. Based on this it is important to know the initial state of resin voids in the prepreg resin before processing. Table 3.2 shows values of ϕ_0 for various combinations of $d_{0,small}$ and $d_{0,large}$ for $f_{small} = 0.98$. Observations and measurements of neat resin samples indicate ϕ_0 is approximately 0.20% (consistent with Farhang [9]) however the larger values of ϕ_0 have been included for illustrative purposes since manufacturing a composite part using a resin with large resin voids can be detrimental to OOA prepreg composite manufacturing.

Table 3.2: Initial resin void porosity, ϕ_0 , for different combinations of $d_{0,small}$ and $d_{0,large}$.

		Large Void Diameter, $d_{0,large}$ (μm)			
		120	140	160	180
Small Void Diameter, $d_{0,small}$ (μm)	15	0.20%	0.30%	0.45%	0.63%
	25	0.26%	0.37%	0.51%	0.69%
	35	0.40%	0.51%	0.65%	0.83%
	45	0.65%	0.75%	0.90%	1.08%

3.3 Neat Resin Results Discussion

The results presented in sections 3.1 and 3.2 clearly show that resin voids in neat resin can grow to significant sizes and thus cannot be ignored in manufacturing. In processes that utilize low pressures and/or have geometries with caul plates or gaps that locally reduce resin pressure, resin pressure may become compromised enabling the growth of resin voids. However both mechanisms are easily kept in check with adequate resin pressure. It follows then that a ‘minimum required resin pressure’ (MRP) would be a useful manufacturing guideline in industry. Using the Kardos criterion and ideal gas expansion porosity equation, Equations 15 and 21 respectively, a first order approximation of the minimum required resin pressure is introduced. The minimum required resin pressure is defined as the greater of:

- $P_{R,Critical}$ predicted by the Kardos criterion
- $P_{R,Critical}$ predicted by ideal gas expansion for $\phi_{Critical} = 2\%$

For simplicity and illustration purposes, resin flow, resin void evacuation and timing of events are not considered.

With knowledge of the initial conditions of a prepreg system the MRP required to prevent excessive resin void growth is known. Figure 3.13 shows the MRP as a function of temperature for a given initial condition state. The Kardos criterion sets the MRP for the processing temperatures of interest ($> 80^{\circ}\text{C}$) and is the more relevant porosity mechanism to design against. At low temperature the MRP is very low and arguably negligible, however, resin pressure can reduce to zero in certain circumstances due to part design and therefore the low temperature portion is retained. The MRP can be used in situations where part design is flexible; careful design can ensure caul sheets, ply drops, gaps, etc. do not reduce the resin pressure below the MRP.

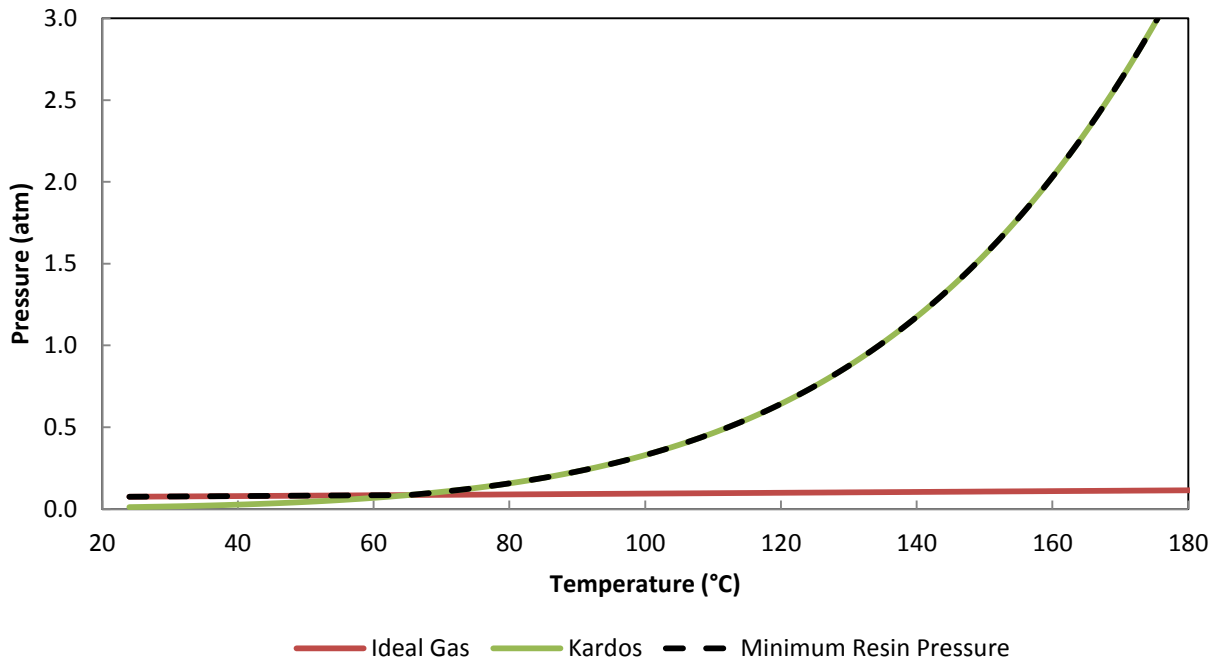


Figure 3.13: Minimum resin pressure for $\phi_0 = 0.15\%$ and $RH_0 = 33\%$.

4 LAMINATE EXPERIMENTS

Experiments on laminates were performed in order to evaluate the growth of resin voids due to the growth mechanisms observed from the neat resin experiments.

4.1 Laminate Test Methods

The material used for the laminate tests was Cytac MTM45-1 5HS OOA prepreg. The prepreg consists of a resin film (MTM45-1) on one side that has partially impregnated the carbon fabric (see section 2.1.1 for details). The resin is the same as that used in the neat resin experiments. All tests were performed with the resin poor side on the tool. The 5HS fiber mat is made from 6K IM7 carbon fiber tows that measure approximately 2 mm in width and 8 mm in length between crimps.

To evaluate the resin void growth mechanisms in laminates, porosity was promoted in evacuated laminates by changing a test parameter and comparing the final porosity to a porosity free baseline. Figure 4.1 shows a schematic test plan for the laminate experiments. Small, flat laminates were made in order to allow for quick air evacuation during debulk while minimizing the amount of dissolved moisture lost to evaporation. Laminates measured 10cm x 10cm x 4 plies. A gas evacuation model developed by Arafath et al [24] predicts 99% air evacuation in 1 min for a laminate of this size (see Appendix A). Test parameters were selected based on the Kardos and ideal gas expansion resin void growth mechanisms, Equations 25 & 26 below. The selected parameters were resin pressure, temperature and moisture content (proxied as RH_0).

$$P_{R,Critical} = 4962 \exp\left(\frac{-4892}{T}\right) (RH_0) \quad (25)$$

$$P_{R,Critical} = \frac{T\phi_0(1 \text{ atm})}{\phi_{Critical}T_0} \quad (26)$$

Results from the neat resin experiments have shown resin pressure to be a critical parameter for resin void growth mitigation. In laminates resin pressure cannot be directly controlled since it manifests as the difference between applied pressure, $P_{Applied}$, and the fiberbed effective stress, $\sigma_{Fiberbed}$, Equation 27 [46].

$$P_{Resin} = P_{Applied} - \sigma_{Fiberbed} \quad (27)$$

In the following laminate experiments resin pressure was manipulated by reducing the applied consolidation pressure and by allowing resin to bleed out of the laminate. In order to evaluate resin pressure as the cause of resin void growth laminate resin pressure was measured in-situ by using a tool plate with embedded pressure sensors. Moisture content of the laminate was controlled by conditioning the laminates in environment chambers containing a saturated salt solution (same method as the neat resin experiments, see section 3.1). Temperature of the system was controlled by a heat pad vacuum bagged on top of the laminate.

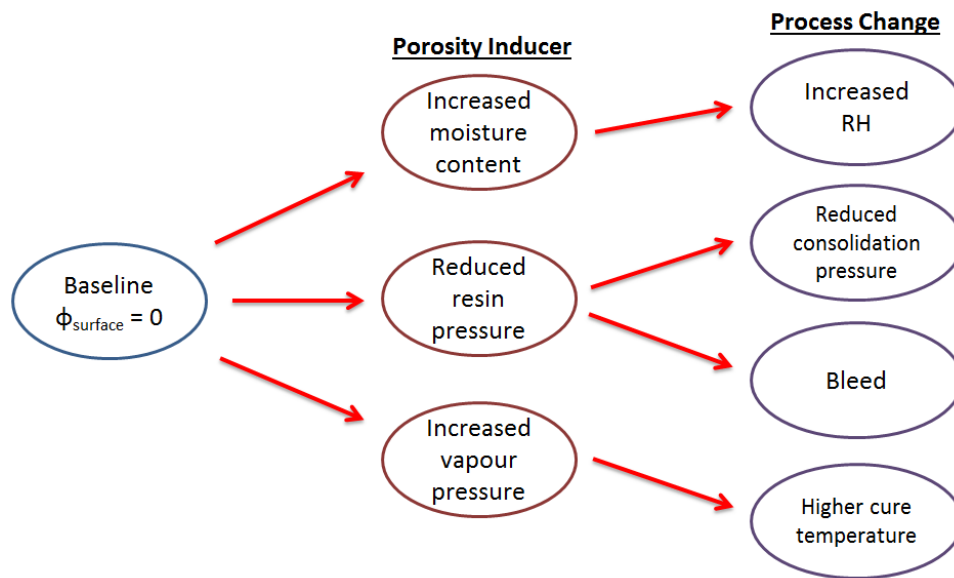


Figure 4.1: Schematic test plan for the laminate experiments.

Evolution of the laminate surface was observed in-situ; each laminate was laid up and cured on a 6 mm thick borosilicate glass tool and video micrographs were recorded using a Keyence VHX-1000 digital microscope. The experimental setup was the same as the neat resin experiments (see section 3.1 for figures). After cure, bulk and surface porosity were measured for each laminate. Surface porosity on laminates was quantified using black and white binary image analysis since the surface voids are highly non-spherical. Surface voids tend to be rough and so reflect light diffusely whereas other regions of the

part's surface are smooth and produce a specular reflection. Figure 4.2 shows the method used to capture highly reflective surface images of laminates and an example image of surface porosity captured using this method. An incident angle, α , of approximately 30 - 40° relative to the laminate surface was found to result in the best images. Voids in the image are on the order 1-2 mm in size. Images taken of light reflecting off of the laminate surface have very high contrast between the voids and the resin which allows for easy quantification of surface porosity. Reflective surface porosity images were analyzed using ImageJ image analysis software by converting the high contrast images to binary images and counting the black pixels. In this case surface porosity is the number of black pixels divided by the total number of pixels.

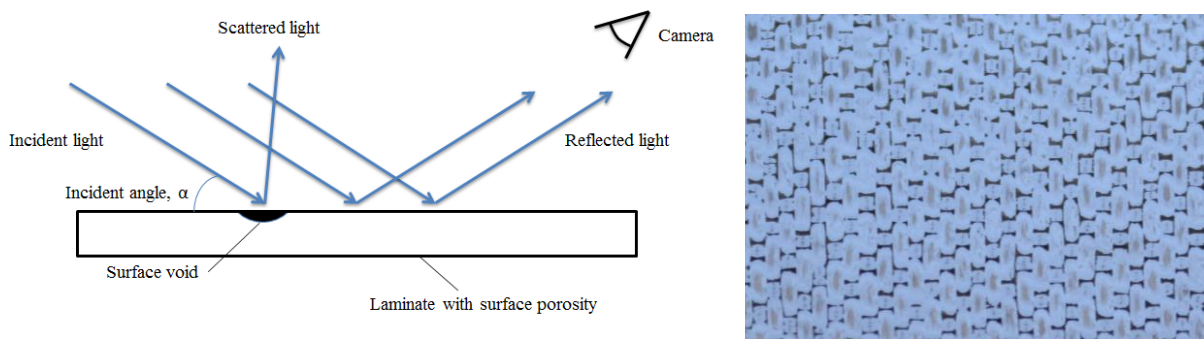


Figure 4.2: Left) Method for capturing high contrast surface images, Right) Surface porosity image taken by light reflecting off of the surface.

After surface porosity quantification, laminates were cut into 6 x 6 cm² pieces and bulk porosity was quantified using both density and thickness measurements. Measuring porosity by density was performed according to a modified version of ASTM B962 - 15 [54] (described in appendix D) using an electronic balance. Measuring bulk porosity by thickness was performed using digital calipers; an average thickness was obtained over 5 measurements and porosity was calculated according to methodology described by Farhang [9]. Density provides an accurate, volume average value of bulk porosity since it measures buoyancy of the part. Thickness via calipers provides an above average measurement of bulk porosity since the part thickness is measured by the peaks of the surface roughness [9]. Both methods were performed for comparative purposes, however, bulk porosity values reported were from the density method.

4.1.1 Baseline Laminates

Baseline laminates were cured under the conditions listed in Table 4.1. Porosity was measured and, as required for a baseline (shown in section 4.2.2, Figure 4.10), these laminates have no surface or bulk porosity. Figure 4.3 shows a schematic of the vacuum bag assembly.

Table 4.1: Baseline laminate test parameters.

Parameter	Baseline Value
Temperature ramp rate	1.5°C/min
Hold temperature	120°C
Consolidation pressure	1 atm
RH ₀	33%
Plies of bleed cloth	0

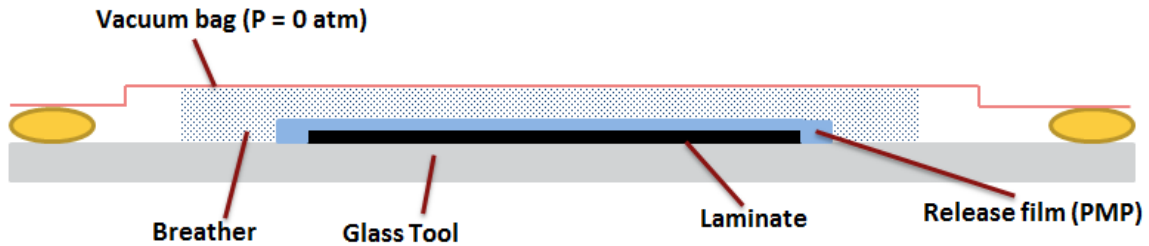


Figure 4.3: Baseline laminate vacuum bag assembly.

4.1.2 Reduced Consolidation Pressure Laminates

Reduced consolidation pressure (RCP) is used to simulate situations where shielding of consolidation pressure may occur, for example in configured structures a caul plate may reduce the consolidation pressure locally by failing to conform to the laminate geometry [47]. The porosity inducing mechanism for these tests is the reduction in resin pressure due to lower applied pressure. These tests are different from reduced vacuum pressure studies in which the vacuum pressure the laminate experiences is reduced [17, 18]. Under reduced vacuum pressure the air in the laminate does not fully evacuate and the laminate experiences 1 atm of pressure. For the reduced consolidation pressure tests the laminate experiences full vacuum and reduced applied consolidation pressure by using a double vacuum bag assembly and an aluminum bridge. Figure 4.4 shows a schematic of the vacuum bag assembly. The primary vacuum bag contains the laminate and is identical to the baseline vacuum bag assembly, shown

in Figure 4.5a. The aluminum bridge is placed over the laminate outside of the primary vacuum bag and sealed inside the secondary vacuum bag, shown in Figure 4.5b. Full vacuum is drawn on the primary vacuum bag (and therefore the laminate) while the secondary vacuum bag is set to the desired consolidation pressure by use of a pressure regulator. Atmospheric pressure is supported by the aluminum bridge and therefore the laminate experiences consolidation pressure equal to the gas pressure in the secondary vacuum bag.

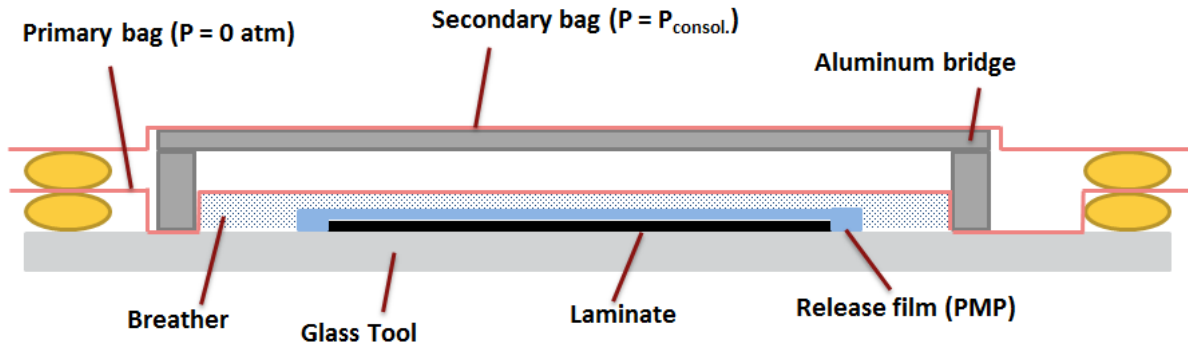


Figure 4.4: Reduced consolidation pressure laminate vacuum bag assembly.

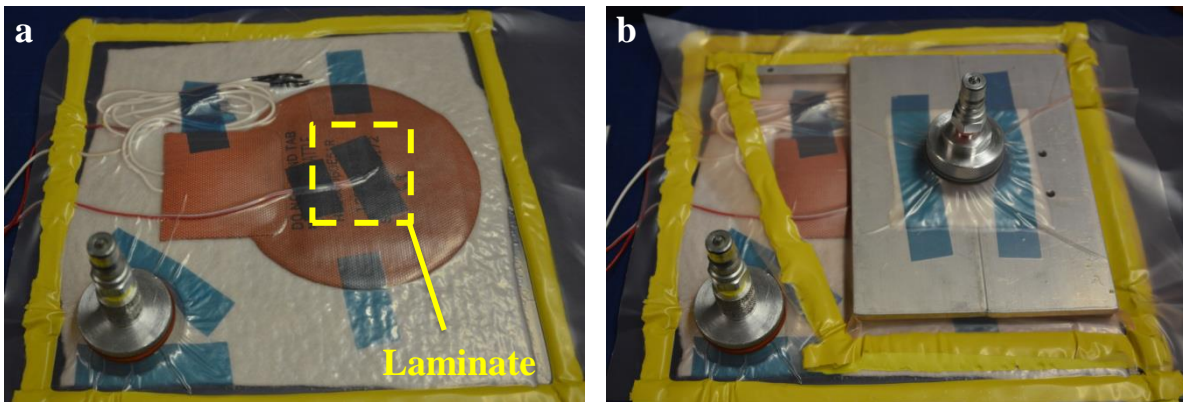


Figure 4.5: a) Primary vacuum bag b) Primary and secondary vacuum bags.

Laminates were cured under 2/3, 1/3 or 0/3 atm of consolidation pressure. Table 4.2 lists the test parameters for the reduced consolidation pressure laminates and compares them to the baseline values.

Table 4.2: Reduced consolidation pressure laminate test parameters.

Parameter	Baseline Value	RCP Value
Temperature ramp rate	1.5°C/min	1.5°C/min
Hold temperature	120°C	120°C
Consolidation pressure	1 atm	2/3, 1/3 or 0/3 atm
RH ₀	33%	33%
Plies of bleed cloth	0	0

4.1.3 Resin Bleed Laminates

Modern prepregs are net resin systems (i.e. resin does not bleed out of the system). Resin bleed is used to simulate situations where significant change in fiber volume fraction due to redistribution of resin may occur, for example in configured structures a caul plate over a ply drop region may create a pocket for resin to flow into by failing to conform to the laminate geometry [47]. The porosity inducing mechanism for these tests is the reduction in resin pressure by transferring load to the fiberbed due to increased fiber volume fraction. Figure 4.6 shows a schematic of the vacuum bag assembly. To facilitate controlled bleed, peel ply cloth was placed between the laminate and the release film. The peel ply cloth is perforated allowing low viscosity resin to flow into it. Laminates were cured with either 2 or 5 layers of peel ply cloth. Mass was measured before and after cure to determine the percent resin loss. Table 4.3 lists the test parameters for the bleed laminates and compares them to the baseline values.

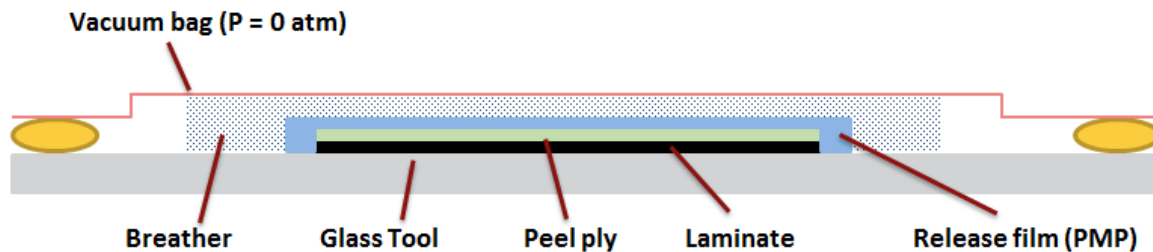


Figure 4.6: Resin bleed laminate vacuum bag assembly.

Table 4.3: Bleed laminate test parameters.

Parameter	Baseline Value	Bleed Value
Temperature ramp rate	1.5°C/min	1.5°C/min
Hold temperature	120°C	120°C
Consolidation pressure	1 atm	1 atm
RH ₀	33%	33%
Plies of bleed cloth	0	2 or 5

4.1.4 Increased Moisture Content Laminates

Increasing the moisture content of a laminate will only impact the moisture vapourization resin void growth mechanism (Kardos criterion). The porosity inducing mechanism for these tests is increased moisture activity. Increased moisture content laminates were conditioned at 75% RH for 5 days using an environment chamber containing a saturated solution of NaCl. These laminates were cured using the same vacuum bag assembly as the baseline (see Figure 4.3). Table 4.4 lists the test parameters for the increased moisture content laminates and compares them to the baseline values.

Table 4.4: Increased moisture content laminate test parameters.

Parameter	Baseline Value	Increased Moisture Content Value
Temperature ramp rate	1.5°C/min	1.5°C/min
Hold temperature	120°C	120°C
Consolidation pressure	1 atm	1 atm
RH ₀	33%	75%
Plies of bleed cloth	0	0

4.1.5 Increased Cure Temperature Laminates

Increased cure temperature laminates were ramped to a hold temperature of 180°C. The porosity inducing mechanisms for these tests are increased equilibrium vapour pressure of moisture and increased resin void gas pressure. These laminates were cured using the same vacuum bag assembly as the baseline (see Figure 4.3). Table 4.5 lists the test parameters for the increased cure temperature laminates and compares them to the baseline values.

Table 4.5: Increased cure temperature laminate test parameters.

Parameter	Baseline Value	Increased Cure Temperature Value
Temperature ramp rate	1.5°C/min	1.5°C/min
Hold temperature	120°C	180°C
Consolidation pressure	1 atm	1 atm
RH ₀	33%	33%
Plies of bleed cloth	0	0

4.1.6 In-situ Resin Pressure

Resin pressure measurements were performed using an aluminum tool plate with pressure sensors embedded in the plate at the laminate-tool interface. A DAQ tool and LabView software were used to measure resin pressure in-situ. The pressure sensors are accurate to within 0.1 atm. Resin pressure was assumed to be path independent and therefore consolidation pressure was varied during the test to determine the resin pressure for each consolidation pressure used in this study (i.e. 1 atm, 2/3 atm and 1/3 atm). Figure 4.7 shows the vacuum bag assembly for this test. Resin pressure evolution was also measured for resin bleed laminates with 5 peel ply cloths.

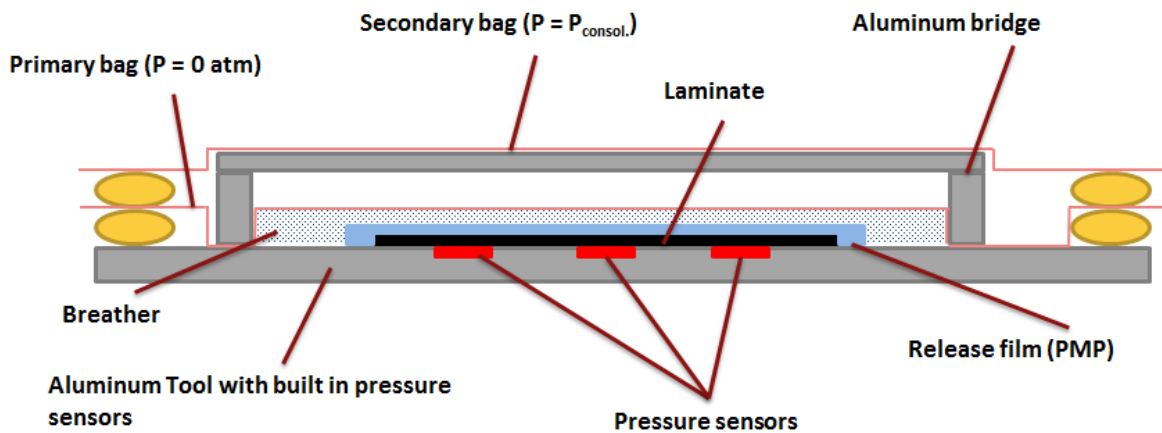


Figure 4.7: In-situ resin pressure vacuum bag assembly used to measure resin pressure under varying consolidation pressures.

4.2 Laminate Tests Results & Observations

4.2.1 In-Situ Resin Pressure Results & Observations

Figure 4.8 shows in-situ resin pressure in a laminate subjected to 1, 2/3 and 1/3 atm consolidation pressure. The test was kept isothermal at 120°C. Table 4.6 summarizes the resin pressure results and the test types pertinent to each. Decreasing the consolidation pressure results in an instantaneous resin pressure response while increasing consolidation pressure results in a time dependent resin pressure response. The mechanism responsible for this behaviour is unknown. Another interesting observation in Figure 4.8 is fiberbed effective stress appears to be a function of consolidation pressure in the low pressure regime. At 1/3 atm consolidation pressure the resin pressure is also ~1/3 atm and the fiberbed does not support any load. At 1atm consolidation pressure the resin pressure is ~0.85 atm and the fiberbed is supporting the remaining ~0.15 atm. Gu et al have shown that fiberbed effective stress is independent of consolidation pressure under high autoclave pressure [45] suggesting this phenomenon is only relevant to low pressure processes.

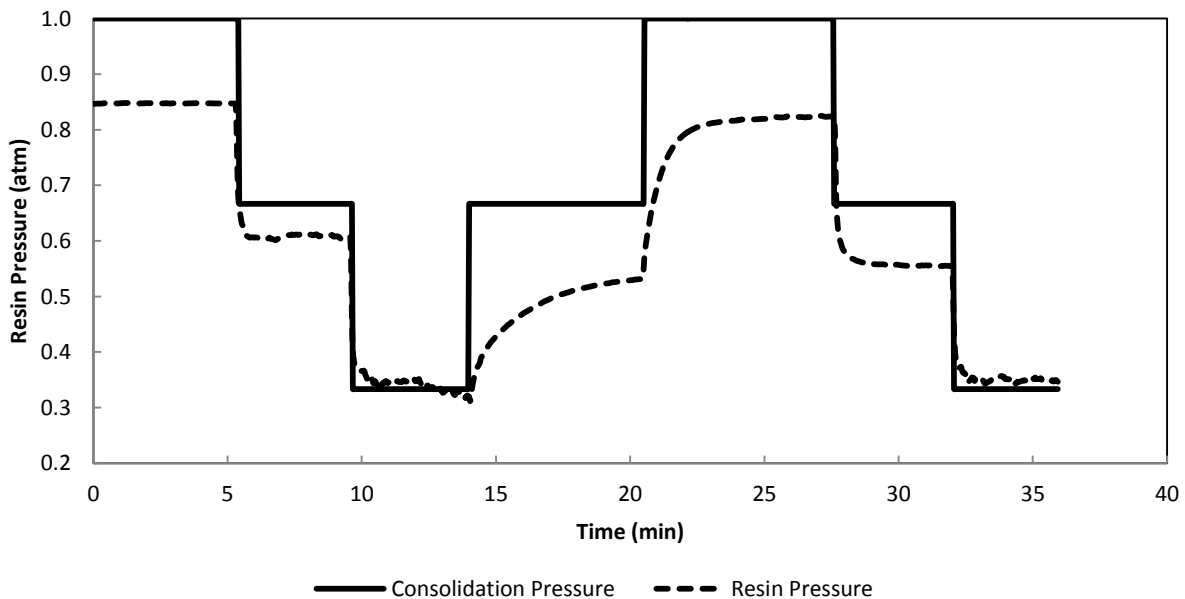


Figure 4.8: Resin pressure under varying consolidation pressure.

Table 4.6: Laminate resin pressure for varying consolidation pressure.

Consolidation Pressure (atm)	Resin Pressure (atm)	Test Type
3/3	0.80 – 0.85	Baseline, 75% RH, 180°C cure
2/3	0.55 – 0.61	2/3 atm consolidation pressure
1/3	0.32 – 0.33	1/3 atm consolidation pressure
0/3	0	0/3 atm consolidation pressure

4.2.2 Baseline Laminates Results & Observations

Figure 4.9 shows a representative image of a laminate surface in-situ with surface porosity. Two types of surface porosity have been identified: voids residing in the inter-tow channels and dry fiber tows (intra-tow voids).

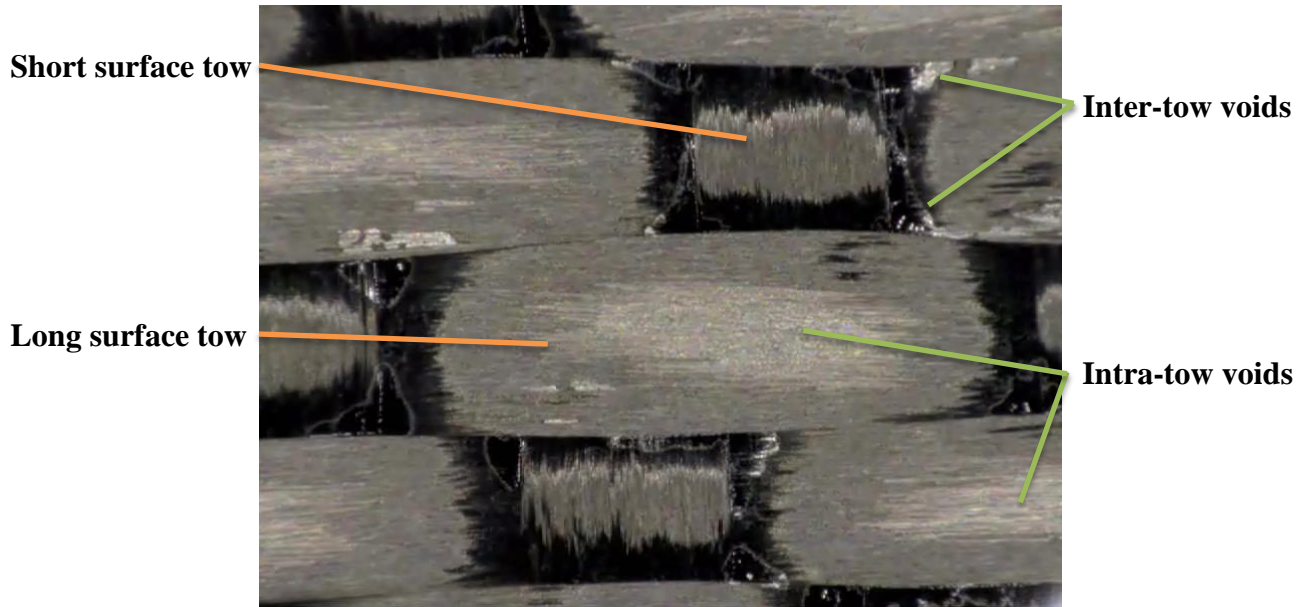


Figure 4.9: In-situ laminate surface with inter- and intra-tow voids.

Figure 4.10 shows the surface evolution of a baseline laminate. Within the first 10 minutes of the temperature ramp (1.5°C/min) the resin pools wet the glass tool. Resin is seen to arrive at the surface through the pinholes and flow in the inter-tow channels, consistent with previous studies. Cender et al have reported inter-tow channels as regions of relatively high permeability ($K_{Inter-tow} \sim 10^{-11} \text{ m}^2$) compared to intra-tow channels ($K_{Intra-tow} \sim 10^{-12} \text{ m}^2$) [32]. The inter-tow channels are filled at approximately 24 minutes. After this the resin begins infiltrating the intra-tow channels. Complete infiltration occurs at approximately 66 minutes into the cure cycle which will be used as a benchmark for comparison to the

other tests. Baseline laminates show no resin voids or uninfiltred fiber tows (i.e. no surface porosity). Figure 4.11 plots the resin pressure and MRP for this system. The resin pressure is clearly sufficient to suppress both the moisture vapourization and ideal gas expansion resin void growth mechanisms. The results also suggest that all air was removed during the vacuum debulk and that there was sufficient resin pressure and low enough resin viscosity to completely fill all void spaces prior to resin gelation.

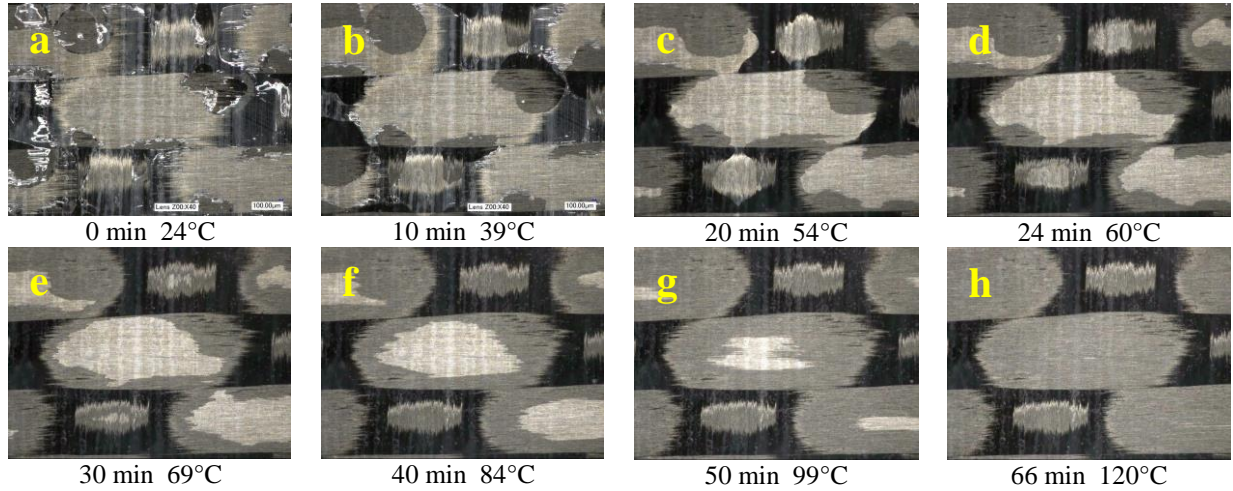


Figure 4.10: In-situ surface evolution of a baseline laminate.

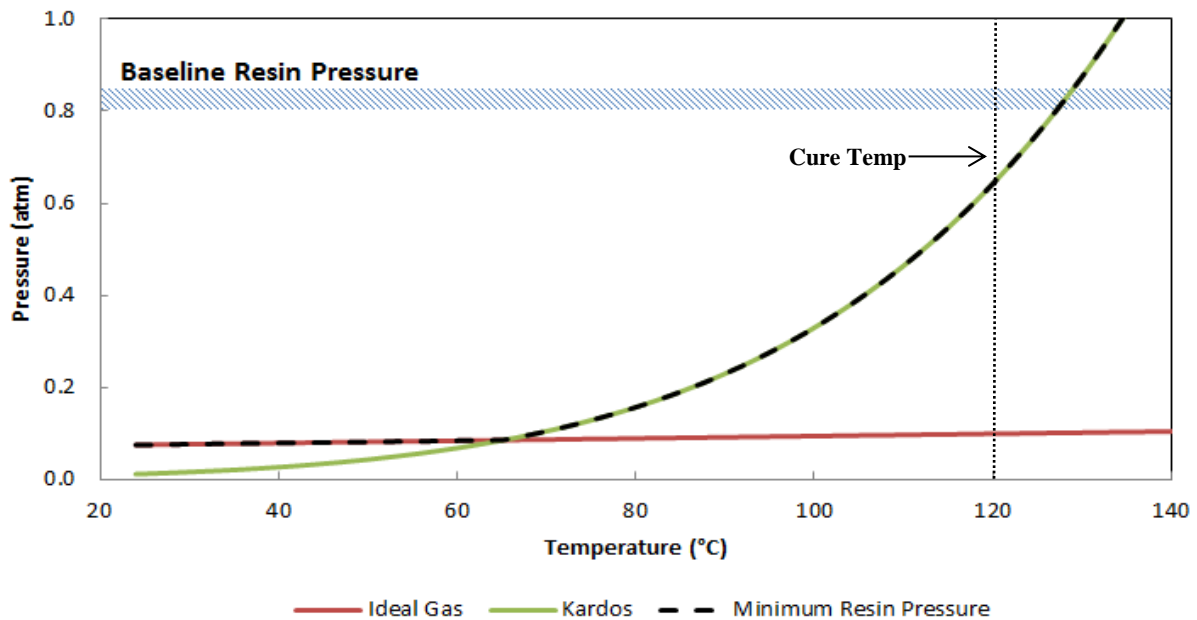


Figure 4.11: Baseline resin pressure compared to the minimum resin pressure: $RH_0 = 33\%$, $\phi_0 = 0.15\%$.

4.2.3 Reduced Consolidation Pressure Laminates Results & Observations

Figure 4.12 shows bulk and surface porosity on reduced consolidation pressure laminates and the corresponding in-situ images of these laminates at the 66 minute point (time when the baseline laminate is fully infiltrated).

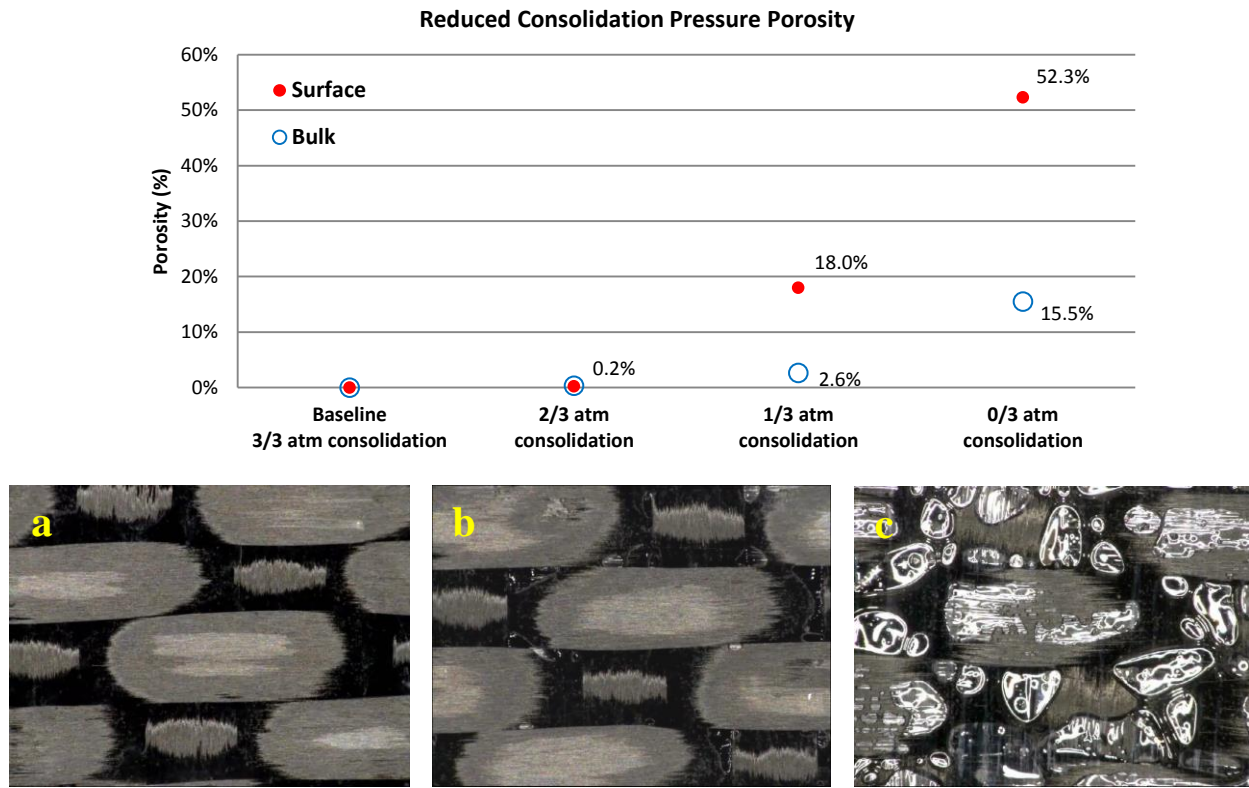


Figure 4.12: Top: Reduced consolidation pressure quantified porosity, bottom: in-situ images at 66 minutes a) 2/3 atm b) 1/3 atm c) 0/3 atm.

Laminates cured under 2/3 atm developed minimal porosity during the cure cycle. No resin void growth was observed in-situ however ex-situ surface inspection found considerable amounts of small resin voids pock marking the surface, shown in Figure 4.13. This is consistent with ideal gas expansion of resin voids under the reduced resin pressure condition; the reduced resin pressure allowed resin voids to expand but was still higher than the critical resin pressure as set by a 2% porosity cut-off. Figure 4.14 plots the resin pressure and MRP for the reduced consolidation pressure tests. The resin pressure for the 2/3 atm consolidation pressure test marginally satisfies the Kardos criterion and is well above the ideal gas porosity 2% limit. The surface fibers tows are completely infiltrated. Reduced resin pressure can be confirmed by comparing the degree of infiltration at the 66 min mark (Figure 4.12b) to the baseline

(Figure 4.10h); the 2/3 atm consolidation pressure laminate is less infiltrated than the baseline for the same amount of time due to the reduced driving force for resin Darcy flow.

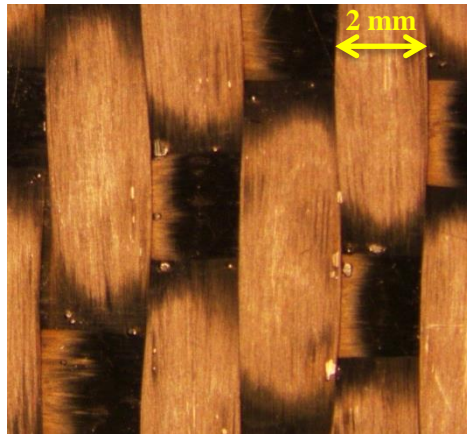


Figure 4.13: Surface porosity on a 2/3 atm consolidation laminate.

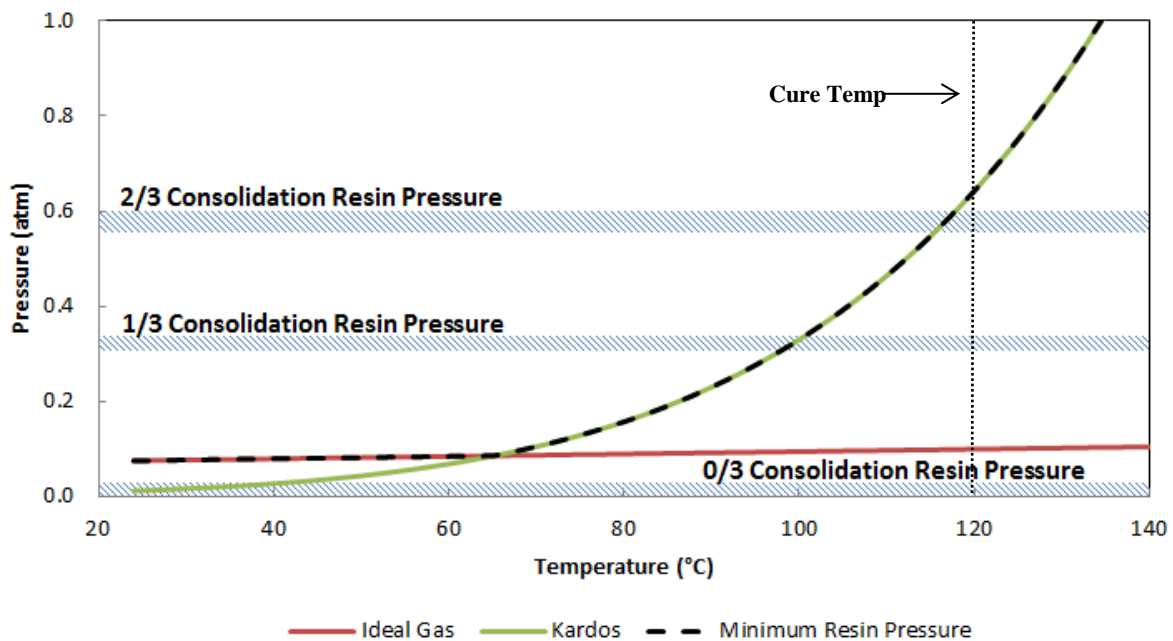


Figure 4.14: Reduced consolidation resin pressures compared to the minimum resin pressure: $RH_0 = 33\%$, $\phi_0 = 0.15\%$.

Laminates cured under 1/3 atm showed significant surface porosity and moderate bulk porosity. During the cure, resin voids are seen to appear at the pinholes and move through the resin. Some resin voids are seen to evacuate through the dry fiber tows (consistent with previous observations by Cender et al. [50]). Figure 4.15 shows a resin void arriving at a pinhole and evacuating through an EVaC. More

detail about resin void evacuation and the concept of “bubble mobility” is provided in the discussion (section 4.3.4). These resin voids are enlarged due to ideal gas expansion in the low resin pressure. Figure 4.16 shows a series of in-situ images. At approximately 40 minutes into cure the inter-tow channels are filled, resin begins to infiltrate the tows and, due to the lower permeability, resin flow is severely reduced. At this point resin voids stop moving and stagnate; the mechanism responsible for this is resin pressure homogenization in the inter-tow channels which is discussed in more detail in section 4.3.4. At approximately 100°C (~50 min) into cure the resin voids begin to slowly grow with time. Referring to Figure 4.14, this time dependent growth corresponds to the resin pressure crossing below the moisture vapourization critical resin pressure (i.e. the Kardos criterion). Porosity is consistently seen to grow from small, pre-existing resin voids and, conversely, regions without pre-existing bubbles show no bubble growth. This suggests that bubble nucleation is not a factor in surface porosity. In addition to resin void growth, resin did not fully infiltrate the long surface fiber tows and cured laminates contain surface fiber tow porosity. This is likely due to closure of the engineered vacuum channels; moisture that vapourizes into the fiber tows cannot evacuate from the laminate and will begin to resist resin infiltration. More details of this phenomenon are presented in section 4.3.3. Resin flow was much slower than for the baseline and slower than the 2/3 atm laminates confirming a further reduction in resin pressure.

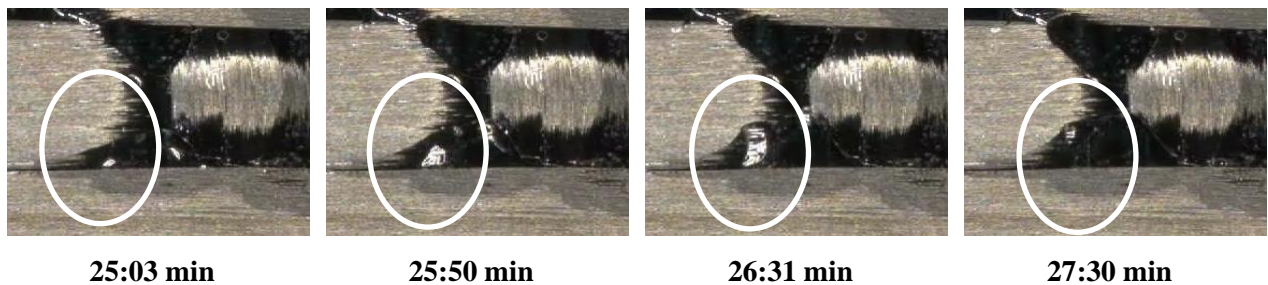


Figure 4.15: Resin void arriving at a pinhole and evacuating through an EVaC.

Laminates cured under zero consolidation pressure (0/3 atm) showed significant bulk and surface porosity. An in-situ surface image is shown in Figure 4.11c. During the temperature ramp no resin flow is seen due to the lack of consolidation pressure. At approximately 25 minutes (~62°C) into cure, the resin viscosity is low enough (~560 Pa-s) that bubble growth is observed. At first the bubbles grow slowly since the resin viscosity is still high but further into the cure cycle when the viscosity is lower the bubbles grow quite rapidly and in some cases evacuate through the fiber tows. This is due to (referring to Figure 4.13) the resin pressure being less than both the ideal gas expansion and Kardos critical pressures for all temperatures. At 75 minutes bubble growth stops, likely due to depletion of moisture in the resin. In this

test, depletion of moisture from the resin corresponds to a total volume of water vapour of approximately 44 cm^3 assuming a vapour pressure equal to its Kardos vapour pressure (the actual volume will be greater than this due to the lack of pressure) while the volume of the laminate is only 16.7 cm^3 . Volumetric expansion of even small amounts of dissolved moisture can cause catastrophic porosity.

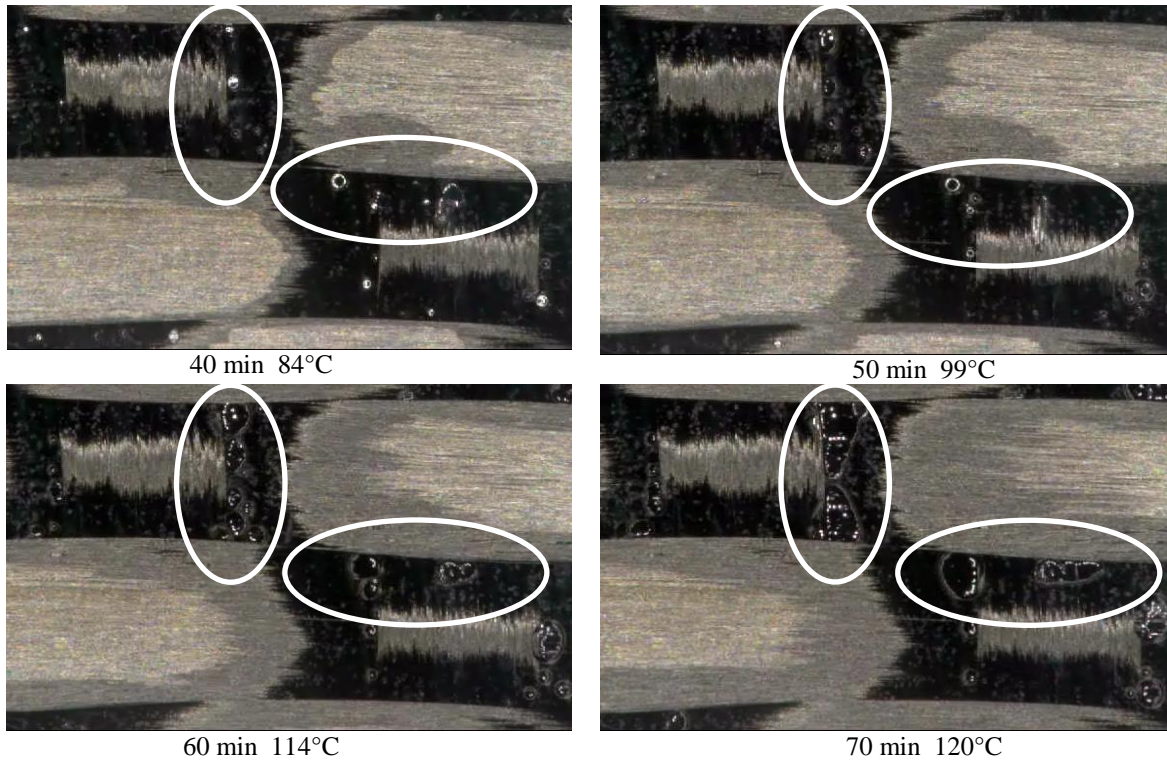


Figure 4.16: Bubble stagnation and growth in a 1/3 atm consolidation laminate.

4.2.4 Increased Moisture Content Laminates Results & Observations

Figure 4.17 shows the measured porosity for the increased moisture content tests and an in-situ image at 66 min into the cure cycle. These laminates show minor bulk porosity (consistent with Grunenfelder [16]) and very minor surface porosity. No enlarged resin voids were observed during the cure cycle consistent with the baseline laminates. Surface fiber tows were fully infiltrated for these laminates. Figure 4.18 plots the resin pressure and MRP for the increased moisture content tests. The resin pressure is well above the ideal gas expansion critical pressure explaining the lack of enlarged resin

voids. At 105-110°C the resin pressure falls below the Kardos critical pressure which is likely responsible for the measured increase in porosity.

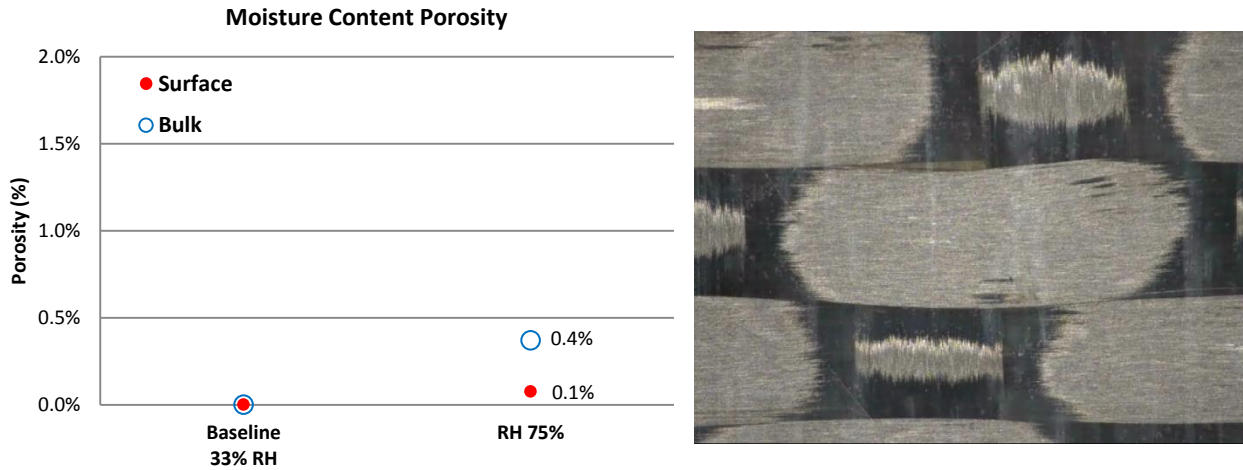


Figure 4.17: Left: Quantified bulk and surface porosity for increased moisture content tests, right: 75% RH laminate at 66 min.

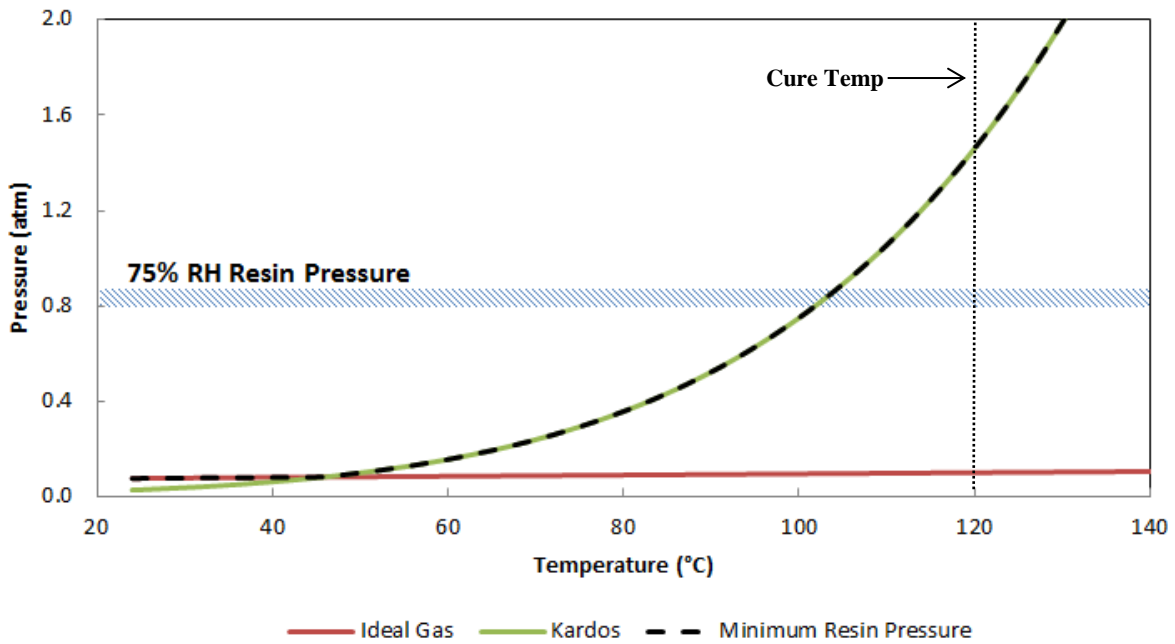


Figure 4.18: Increased moisture content resin pressure compared to the minimum resin pressure: $RH_0 = 75\%$, $\phi_0 = 0.15\%$.

4.2.5 Resin Bleed Laminates Results & Observations

Figure 4.19 shows the measured porosity for the resin bleed tests and an in-situ image at 66 min into cure of a laminate cured with 5 layers of peel ply. Laminates cured with 2 layers of peel ply lost approximately 13% resin content and showed surface behaviour similar to the baseline. The reduction in resin pressure was insufficient to cause porosity. Laminates cured with 5 layers of peel ply lost approximately 27% resin content and developed significant bulk and surface porosity. Figure 4.20 shows a series of in-situ images and a plot of the resin pressure for the first 180 minutes of the cure cycle and the MRP for the 5 peel ply bleed tests (note the horizontal axis is time). Resin pressure builds as the resin viscosity decreases during the temperature ramp. For the first 40 minutes of the cure cycle the surface evolution is identical to the baseline (i.e. no enlarged resin voids and no observed resin void growth). After 40 minutes the resin pressure begins to fall due to the resin bleeding into the peel ply and, correspondingly, resin voids are seen to slowly grow beyond this point in the cure cycle due to ideal gas expansion (Kardos criterion has not been satisfied). The resin pressure profile shows an increase to a second peak at approximately 60-70 minutes which is believed to be an artifact caused by “burping”. Burping is an over pressurization within a gas bubble due to rapid vapourization of volatile species (note the smooth to jagged transition of the pressure curve). Previous resin pressure studies on resin bleed systems have not shown any increase in resin pressure [10, 44]. Rather we expect the resin pressure to monotonically decrease through the second peak (dotted line on Figure 4.19) which corresponds well with observations; around 60-70 minutes the resin voids are seen to grow at an increased rate likely due to moisture evaporation from the resin pressure falling below the Kardos critical resin pressure. Resin pressure continues to decrease beyond this point and resin void growth continues for the duration of the video recording (90 min). The long surface fiber tows for the 5 peel ply resin bleed laminates do not fully infiltrate and in some cases were seen to act as resin void generators. Figure 4.21 shows a series of images where an uninfiltated long surface tow generates resin voids. At this point in the cure, referring the resin pressure curve on Figure 4.20, the Kardos criterion is satisfied and moisture is vapourizing into resin voids causing growth. As well, resin pressure is continuously decreasing causing ideal gas expansion of voids. Uninfiltated fiber tows are voids themselves and will grow due to moisture vapourization and ideal gas expansion. Due to the fiber tow however, intra-tow void growth is geometrically restricted and will grow along the path of least resistance, along the fibers (similar to inter-tow resin voids taking the shape of the inter-tow channels). If there is a low resistance growth path along the fibers that connects to the inter-tow channels then the intra-tow void can “tunnel” out and form a resin void. This process is seen to happen twice in Figure 4.21. Another example of this mechanism is shown in Appendix B.

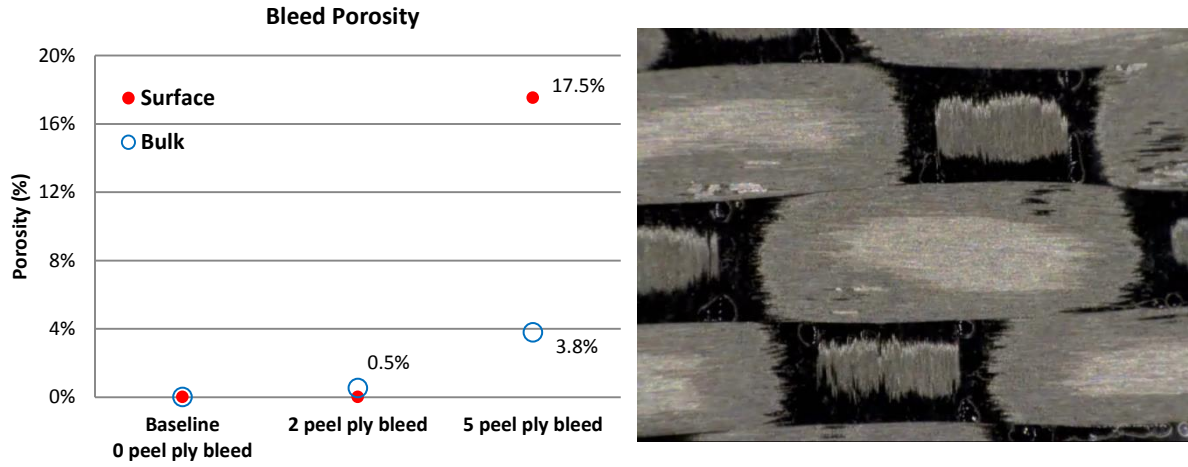


Figure 4.19: Left: Quantified bulk and surface porosity for bleed tests, right: 5 peel ply bleed laminate at 66 min.

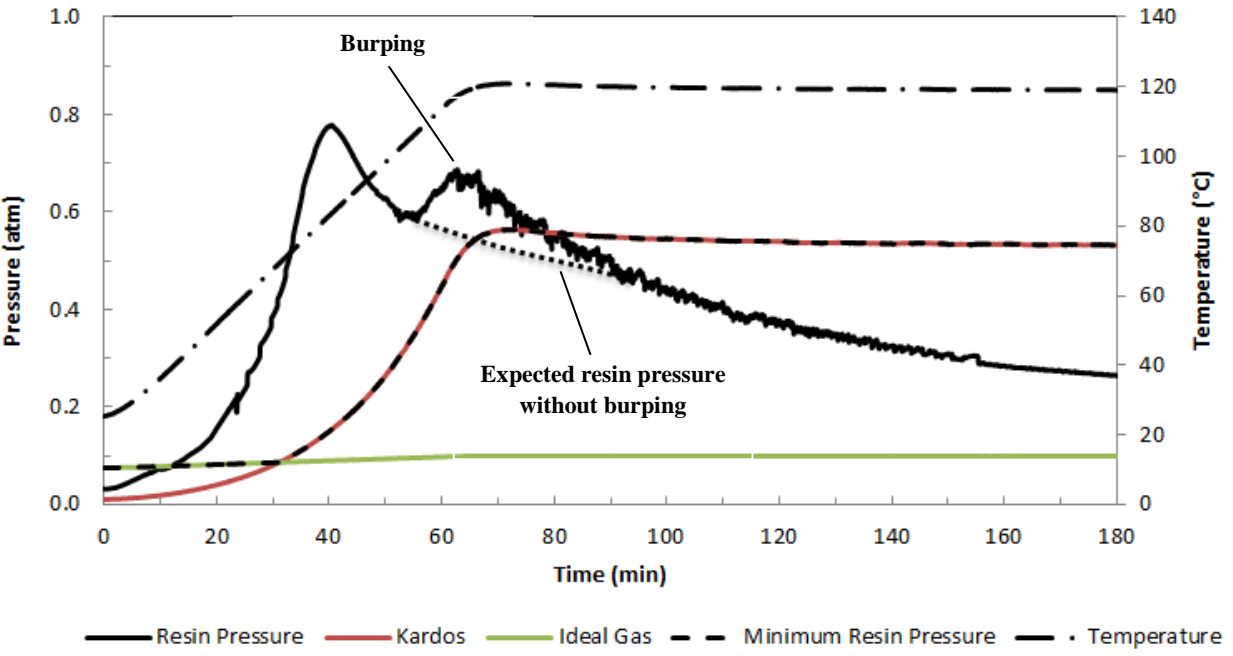
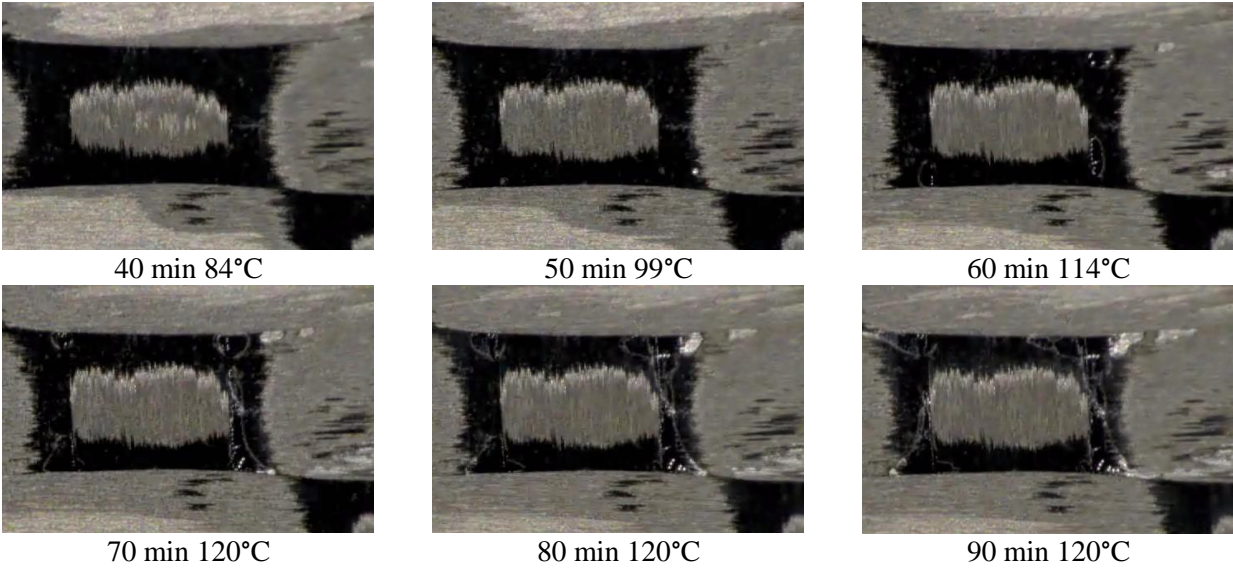


Figure 4.20: Top: Series of images showing resin void growth, Bottom: 5 peel ply resin bleed resin pressure profile and MRP: $RH_0 = 33\%$, $\phi_0 = 0.15\%$.

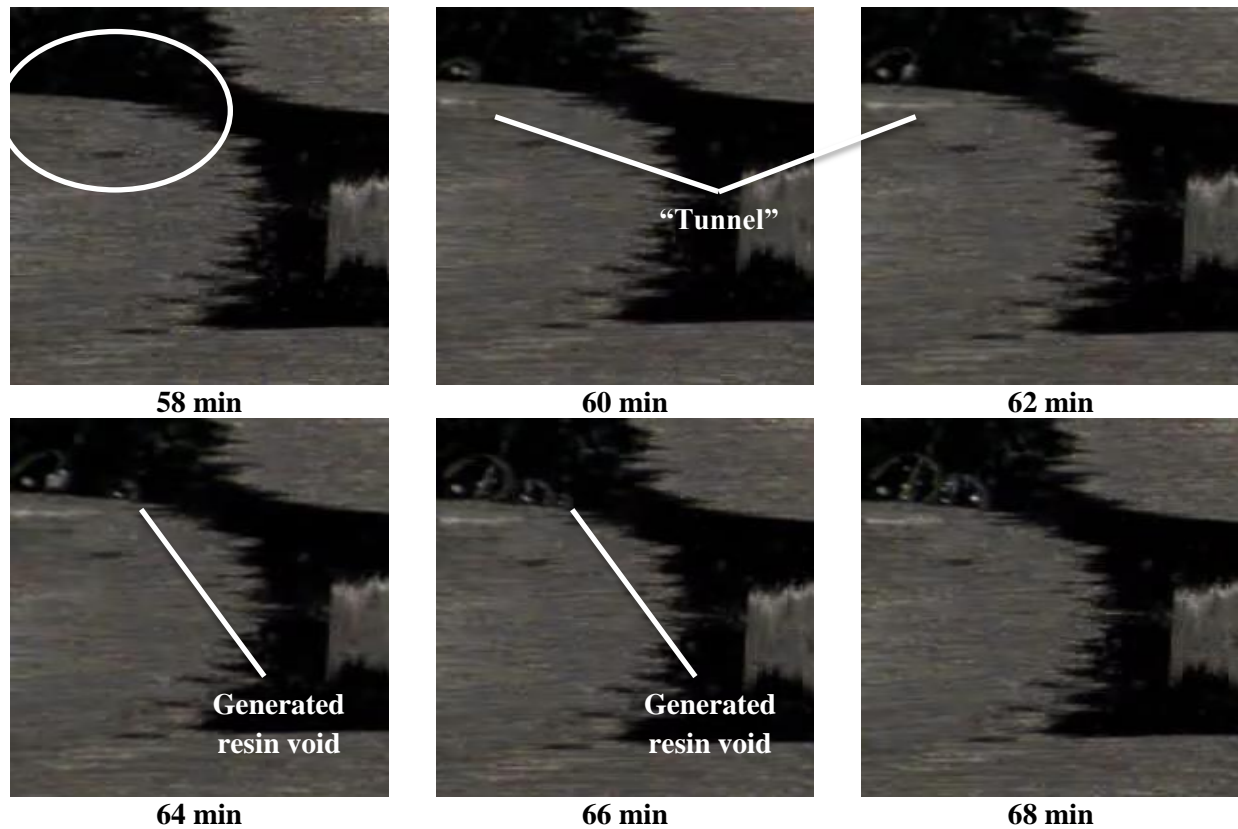


Figure 4.21: Resin void generation due to uninfiltreated surface fiber tows.

4.2.6 Increased Cure Temperature Laminates Results & Observations

Laminates subjected to the increased hold temperature cure cycle (180°C instead of 120°C) developed no bulk or surface porosity. In fact, surface evolution was identical to the baseline. Figure 4.22 plots the resin pressure and MRP for this system. Resin pressure falls below the Kardos critical resin pressure at approximately 135-140°C however no resin void growth was observed in-situ. No enlarged bubbles were observed consistent with all tests subjected to full consolidation pressure. Surface fiber tows were fully infiltrated for these laminates. It is believed that other factors are responsible for the lack of porosity despite violating the MRP for the system; some possible explanations are provided in the discussion (section 4.3.1).

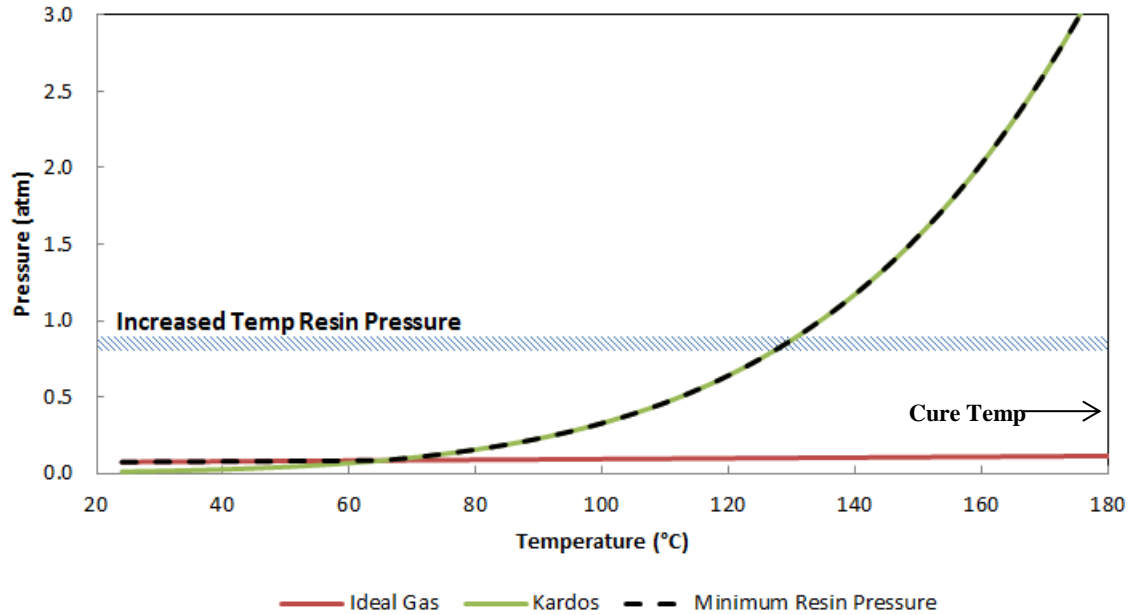


Figure 4.22: Increased cure temperature resin pressure compared to the minimum resin pressure:

$$RH_0 = 33\%, \phi_0 = 0.15\%.$$

4.3 Laminate Tests Results Discussion

4.3.1 MRP Applied to Laminates

Complete removal of the bulk void gas in a laminate does not ensure a good part. Resin voids can grow under certain conditions and cause significant porosity. The results clearly show that strong consideration must be given to the initial state of the prepreg and the resin pressure. Our simple approach at the ‘minimum required resin pressure’ was adequate in explaining the porosity results of all tests except the increased temperature laminates. In the regime of fully evacuated laminates the MRP can be used to determine the acceptable processing window. Manufacturers must be cognizant of prepreg initial conditions (e.g. RH_0 , ϕ_0), update the system specific MRP and modify the process parameters if necessary. For example, a moist prepreg (e.g. $RH_0 = 80\%$) to be used in an OOA process should either be dried before processing or cured using a different temperature cycle so as not to fall below the Kardos critical pressure. High pressure processes are not exempt from these considerations. As mentioned previously, configured structures can shield the laminate from consolidation pressure and/or create pockets for resin to bleed into compromising the local resin pressure and both reduced consolidation pressure and resin bleed test conditions showed significant porosity. The MRP can aid in the design of the

laminates geometry such that shielding and/or resin bleed will be sufficiently minimal as to not compromise the resin pressure.

The MRP investigated in this study is simplistic but effective in explaining majority of the test results. An unrealistic assumption is that the Kardos criterion assumes that bulk moisture content remains constant however it has been shown that a laminate can be dried under vacuum conditions [17, 41]. Despite this, for large enough parts this assumption is reasonably valid. In order for a water molecule to be evacuated in an air evacuated laminate it must diffuse through the resin to the resin-EVaC interface, vaporize into the EVaC and flow to the laminate edge, shown schematically in Figure 4.23. The maximum diffusion distance, Δx , is half the resin film thickness and independent of part length since resin films are assumed to have uniform thickness. The Darcy flow distance, L , is half the part length.

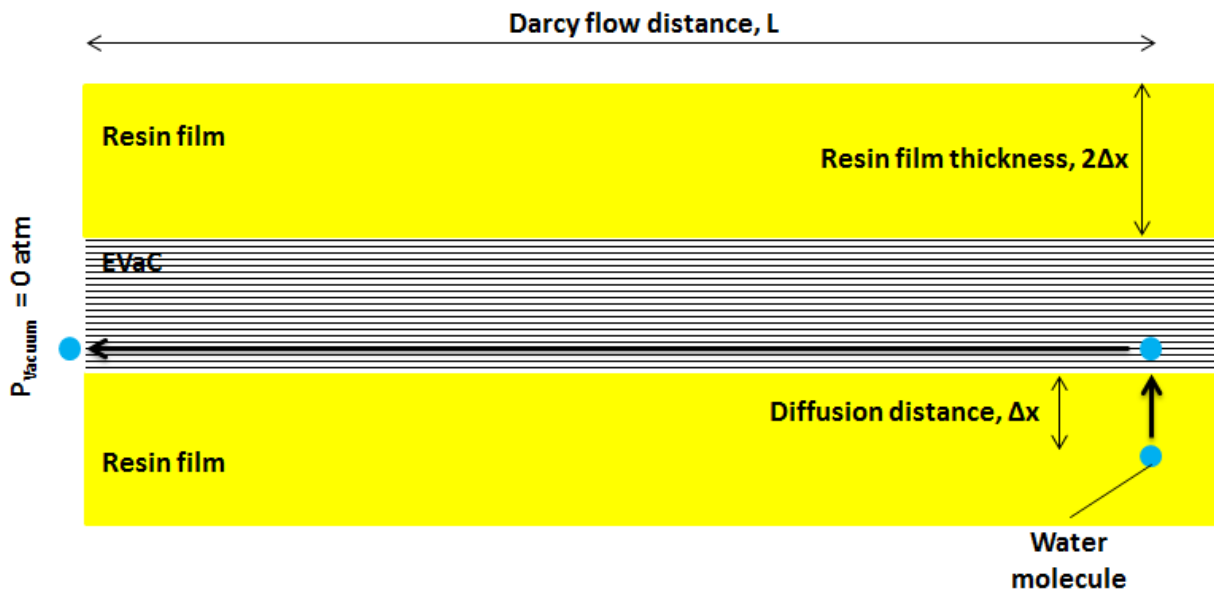


Figure 4.23: Evacuation of a moisture molecule in an air evacuated laminate.

A first order approximation of the Darcy time constant for evacuation is given by Equation 28 and a first order approximation of the time constant for diffusion through a resin film is given by Equation 29 [9].

$$t_{Darcy} \approx \frac{\phi \mu L^2}{K_{eff} \Delta P} \quad (28)$$

$$t_{Diff} \approx \frac{\rho_{H_2O} \Delta x^2}{D \Delta C} \quad (29)$$

Where μ is moisture vapour viscosity, K is fiber mat in-plane permeability, ϕ is the laminate porosity, ρ is moisture vapour density, and D is the diffusivity of moisture in epoxy resin. An effective permeability is used because of the Klinkenberg effect, at low pressure slip phenomenon occurs resulting in a higher flow velocity than predicted by Darcy's law [52]. To get to 90% of the way to equilibrium diffusion requires one time constant while Darcy flow requires six time constants worth of time. This is a result of the choice of time constants and solutions to the differential equations. For a room temperature debulk t_{Diff} is constant and independent of part length (since Δx is independent of part length) while t_{Darcy} scales with part length squared. Both values are calculated using the maximum possible driving force (shortest possible times) given by the values in Table 4.7. Figure 4.24 shows upper and lower bounds for the respective times as a function of part length. For parts larger than 0.1 m Darcy flow quickly starts becoming the time limiting step in drying a laminate. Dissolved moisture will equilibrate with the moisture vapour in the EVaCs since it takes much longer for the moisture vapour to evacuate. In this situation drying a laminate via vacuum evacuation is slow enough that resin moisture content can be taken as constant. For the current study the times to reach 90% of the way to equilibrium are comparable and some drying will have occurred, estimated to be approximately 5-7% RH.

Table 4.7: Time constant calculation parameters.

Diffusion			Darcy Flow		
D (High)	1E-09	m ² /s	Klinkenberg multiplier	10	-
D (Low)	1E-11	m ² /s	K (High)	5E-14	m ²
ρ_{H_2O}	0.804	kg/m ³	K (Low)	1E-14	m ²
ΔC	1.69	kg/m ³	ϕ	0.3	-
Δx	1E-04	m	μ	1.2E-05	Pa s
			ΔP	1054	Pa
			L	0.05	m

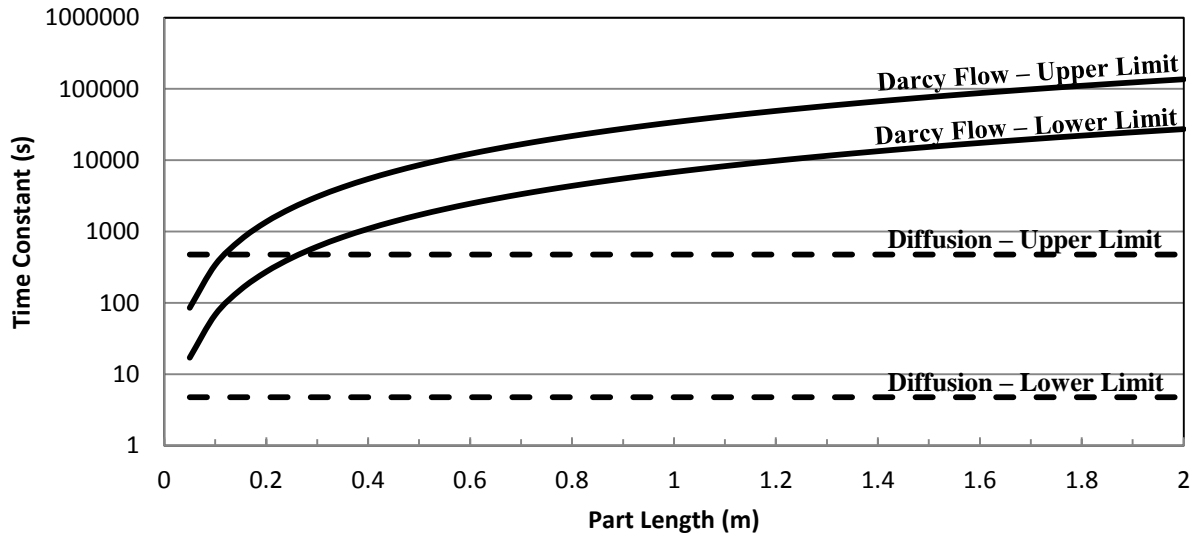


Figure 4.24: Time constants for Darcy flow and diffusion of moisture in an evacuated laminate (to reach 90% equilibrium diffusion requires one time constant, Darcy flow requires six time constants).

Another assumption is that resin void concentration is uniformly distributed throughout the laminate. However, inspection of neat resin has shown that resin void concentration can be highly localized increasing the local MRP. The MRP used in this study also fails to explain the results of the increased cure temperature tests indicating that other factors must be included for a comprehensive porosity prediction tool. Further experimentation is required to explain the results of the increased cure temperature tests however it is speculated that complete infiltration of the fiberbed and/or increasing resin viscosity due to the cure reaction at the time of satisfying the Kardos criterion may be influential factors.

4.3.2 MRP as Part of a Comprehensive Porosity Mitigation Tool

To develop a comprehensive porosity mitigation tool all voids within a laminate must be considered. In this study only resin voids have been considered as the source of porosity. However, in laminates the majority of initial porosity comes from the bulk voids (~11.75% [9]) while only a small contribution comes from the resin voids (~0.15% was measured in this study and ~0.2% has been reported by Farhang [9]). Despite this the results presented have shown that resin voids can contribute a significant amount of porosity under certain conditions. Total porosity of the part can be expressed as the summation of bulk void porosity and resin void porosity, Equation 30.

$$\phi_T = \phi_{Bulk Void} + \phi_{Resin Void} \quad (30)$$

Both ideal gas expansion and moisture vapourization contribute to resin void porosity which can be mitigated using the MRP concept. Elimination of bulk void porosity in OOA processes is done by removing the gas in the bulk voids from the laminate (debulking) and filling the empty space with resin (infiltration). Research has been done on both debulk gas extraction [17, 24, 27, 28] and fiber mat infiltration [22, 31, 32, 33]. It stands to reason that porosity can be mitigated by employing a set of minimum manufacturing guidelines:

- Minimum Debulk Time (MDT) – Minimum time under vacuum to remove gas from bulk voids
- Minimum Required Resin Pressure (MRP) – Minimum resin pressure to suppress resin void growth
- Minimum Fill Time (MFT) – Minimum time for resin to completely infiltrate the fiber mat

For simple part geometries the scientific and technological understanding is nearly mature enough to implement this type of porosity mitigation approach. However for more complex parts/geometries further research is required.

4.3.3 Uninfiltrated Fiber Tows

Uninfiltrated surface fiber tows are not resin voids however they are a relevant source of porosity and, in the scope of this project, influenced by moisture vapourization and ideal gas expansion resin void growth mechanisms. Both the 1/3 atm consolidation pressure and 5 peel ply bleed laminates contain uninfiltrated surface fiber tows. Farhang showed that laminates conditioned at higher RH take more time to fully infiltrate fiber tows compared to lower RH conditioned laminates for the same cure cycle [9]. This suggests that the fiber tows contain moisture vapour that resists resin infiltration and, accordingly, laminates conditioned at higher RH will have higher moisture vapour within the tows, shown below in Figure 4.25. During debulk pressure within the fiber tows decreases and asymptotically approaches the equilibrium vapour pressure of the moisture dissolved in the resin since the evacuation of the moisture vapour requires very long times under vacuum (discussed in section 4.3.1). Subsequent heating of the laminate increases the equilibrium vapour pressure of moisture and the pressure within the fiber tows will increase accordingly. Once the EVaCs are closed (in-plane permeability is effectively zero) uninfiltrated fiber tows become isolated voids and pressure within the fiber tows will resist resin infiltration driven by resin pressure and a capillary pressure [31]. Depending on the resin pressure two scenarios are possible:

- If $P_{Resin} + P_{Capillary} > P_{H2O}$ resin will compress the moisture vapour as it infiltrates the tow causing the moisture vapour pressure to exceed equilibrium and moisture will dissolve into the resin allowing infiltration to continue.
- If $P_{Resin} + P_{Capillary} < P_{H2O}$ resin cannot infiltrate the fiber tow due to the moisture vapour pressure pushing back and incomplete fiber tow infiltration will result. In some cases the voids in uninfiltrated fiber tows were observed to grow and generate new resin voids in the inter-tow channels.

Both the 1/3 atm consolidation pressure and 5 peel ply bleed laminates fall in the second scenario and contain uninfiltrated surface fiber tows due to significantly reduced resin pressure. Moisture vapour within the fiber tows is greater than the resin pressure and capillary force and thus infiltration of the fiber tows is not possible. Before infiltration stops completely, surface fiber tows for both of these laminates develop a stringy look due to the capillary pressure, shown in Figure 4.26. The baseline and 2/3 atm consolidation pressure laminates fall in the first scenario and all have fully infiltrated fiber tows. The increased temperature laminates fall in the first scenario up until resin fully infiltrates the fiber tows and then switches to the second scenario. However these laminates show no uninfiltrated fiber tows suggesting that this porosity mechanism is only relevant prior to complete infiltration. Lastly, the

increased moisture content laminates show no uninfiltred surface tows despite satisfying the Kardos criterion before complete infiltration, however they contain increased bulk porosity (~0.4%). Since these laminates show very little to no resin void growth an explanation is that the surface portion of the surface fiber tows infiltrated and corralled the moisture vapour into the bulk portion of the fiber tows. The surface energy of the glass tool may influence surface fiber tow infiltration in this regard. This also explains why the 2 peel ply bleed laminates manifested ~0.5% bulk porosity but no surface porosity.

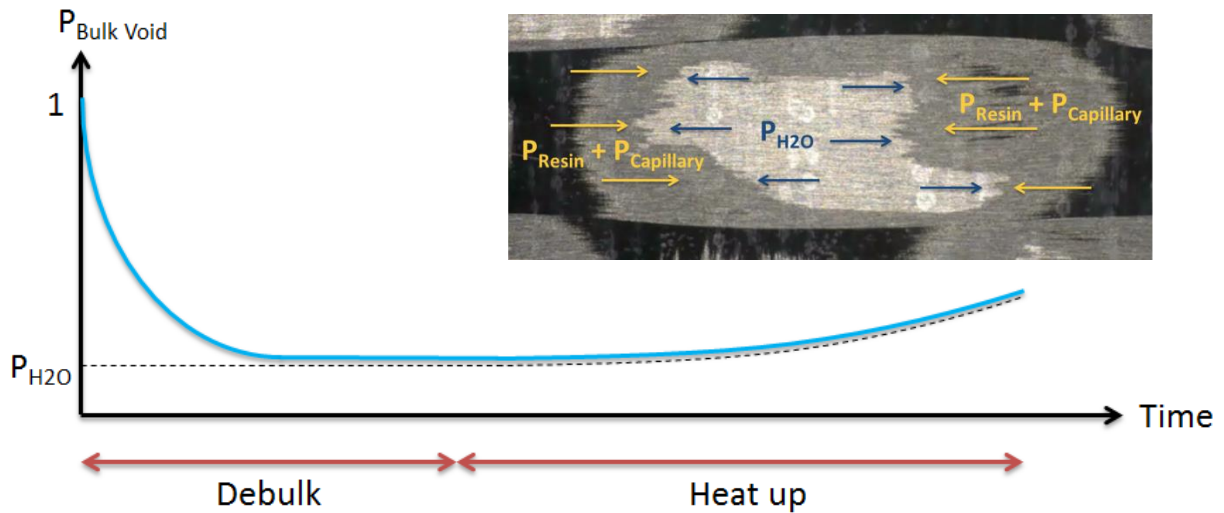


Figure 4.25: Schematic representation of fiber tow void pressure during debulk and heat up.

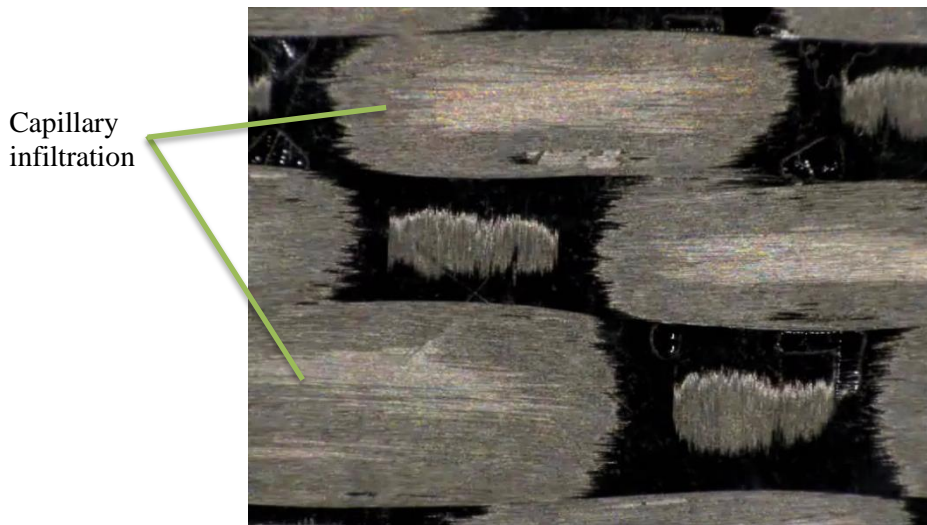


Figure 4.26: Stringy look due to capillary infiltration in a 5 peel ply bleed laminate.

4.3.4 Bubble Mobility and Evacuation

During several tests resin voids were observed to move in the resin and evacuate through an EVaC. An example of this is shown in Figure 4.15. Resin void movement through resin is currently being investigated by Advani and Gangloff [39, 40, 51]. They define bubble mobility as the ratio of bubble velocity to resin flow front velocity; bubble mobility greater than 1 is theoretically required for bubble evacuation. In their work they model resin flow as parallel channel flow with porous media boundaries (fiber tows) and two-phase resin-resin void flow using the Stokes equation combined with the level set method (the level set method tracks the resin-resin void interface with time). They assume both phases are incompressible which is valid for the resin but invalid for the resin void. This assumption is acceptable for a first order approximation and will likely be addressed in future work. From a modeling perspective they are taking the correct approach however the concept of bubble mobility can be illustrated using simpler physics.

Figure 4.27 schematically shows a resin-resin void system. Resin in the inter-tow channels will flow at a velocity, v_{Resin} , which is driven by a pressure gradient in the resin, dP_{Resin}/dx . This pressure gradient is assumed to be linear [32]. A resin void immersed in the flowing resin will be advectively transported by the resin and experience a net force towards the resin flow front. This net force arises from the pressure gradient; referring to Figure 4.27, the left side of the resin void sits in a region of higher pressure than the right side of the resin void resulting in a net force towards to resin flow front. This force will cause acceleration of the resin void towards the resin flow front giving it a higher velocity relative to the resin and therefore a bubble mobility greater than one. This is similar to an air bubble rising in water due to a gravity induced vertical pressure gradient except that the pressure gradient in this case is due to resin flow. Provided the resin is flowing under a pressure gradient and the resin viscosity is sufficiently low to minimize drag forces for resin void transport, resin voids should move faster than the resin and contact the resin flow front where they can be evacuated through an EVaC.

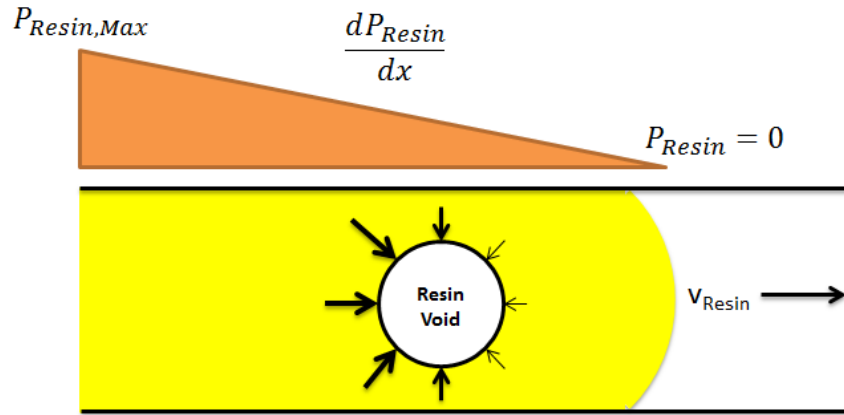


Figure 4.27: Resin void immersed in resin under a pressure gradient.

Without the pressure gradient in the resin, resin velocity will be zero and the resin void will not experience a net force, shown schematically in Figure 4.28. In this case resin voids will stop moving and stagnate. Observations have shown that the former case occurs early in the cure cycle when resin is flowing through the inter-tow channels while the latter case occurs later in the cure cycle when the resin begins to infiltrate the intra-tow channels. Figure 4.29 compares the observed bubble mobility (for illustration, bubble mobility is assigned either 1 (on) or 0 (off)) to the onset of long surface tow infiltration and Kardos criterion satisfaction in a 1/3 atm consolidation pressure laminate. At approximately 40-42 minutes into cure the inter-tow channels are filled and the intra-tow channels begin filling. Prior to this resin voids are seen to move and evacuate (and are assigned a mobility of 1) and after this resin voids are stagnant (and are assigned a mobility of 0). The Kardos criterion is satisfied after mobility becomes zero supporting the observation of resin void stagnation followed by growth. It follows then that the window for resin void evacuation is limited to inter-tow channel resin flow. A cure cycle optimized for resin void evacuation should maximize inter-tow channel filling time and bubble mobility.

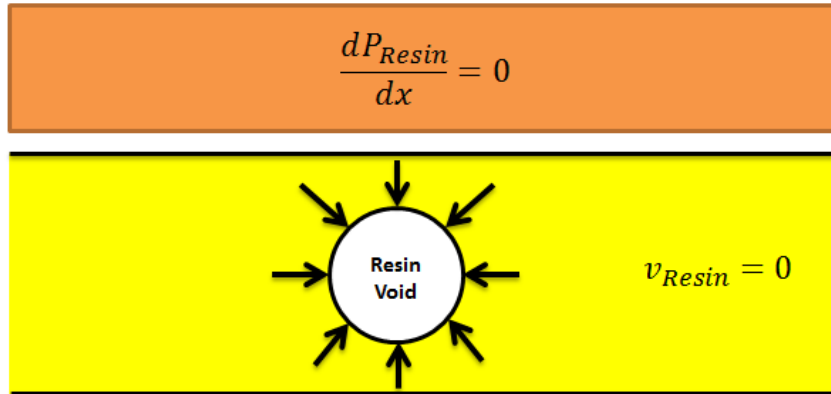


Figure 4.28: Resin void immersed in resin under constant pressure.

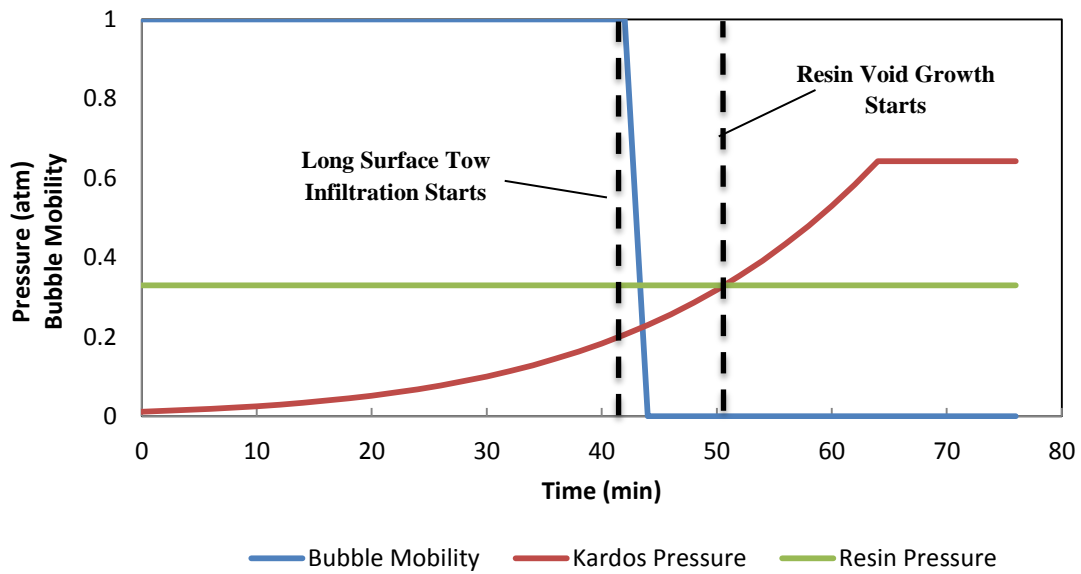


Figure 4.29: Observed bubble mobility (note that 1 = on and 0 = off) in a 1/3 atm consolidation pressure laminate compared to fiber tow infiltration and Kardos criterion satisfaction.

4.3.5 Environmental Considerations

Out-of-autoclave manufacturing is, by nature of the process, restricted to atmospheric pressure. It is commonly stated that the maximum consolidation pressure achievable in OOA processing is one atmosphere which is only true at sea level. Ridgard brought attention to this from the perspective of acceptable vacuum level based on porosity data [6]. A better approach to this issue is to use the ambient atmospheric pressure and vacuum pressure to update the resin pressure and compare to the system MRP. Atmospheric pressure decreases with elevation and if manufacturing at higher elevations the porosity free processing window dictated by the system MRP will shrink. Figure 4.30 shows the atmospheric pressure for some cities around the world; manufacturing 1 km above sea level reduces the total consolidation pressure by 10%! Mexico manufactures carbon fiber composite parts in the province of Queretaro which, on average, is 2000 m above sea level corresponding to an atmospheric pressure of just under 0.8 atm. For autoclave processes this is irrelevant for but OOA processes this is, potentially, disastrous.

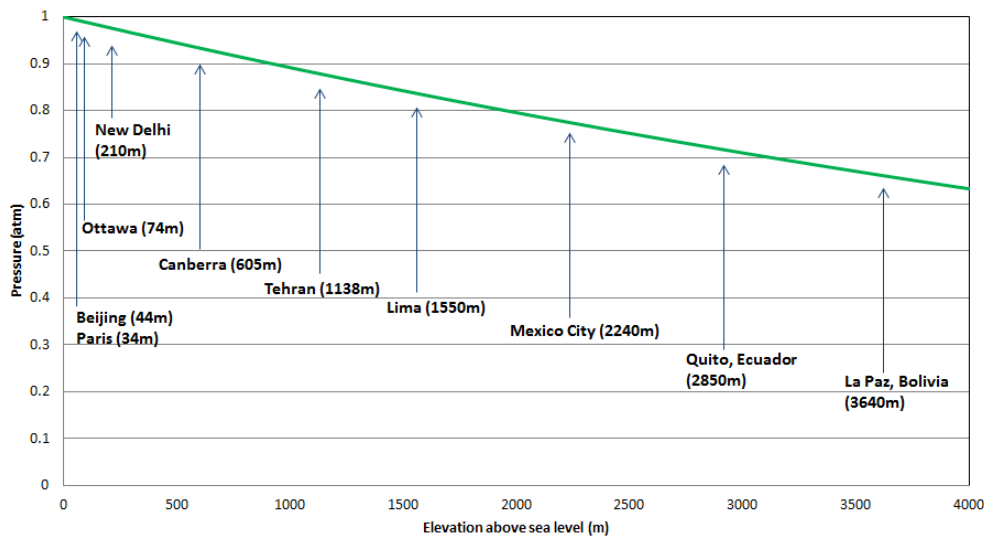


Figure 4.30: Atmospheric pressure decrease with elevation.

Another environmental consideration is ambient RH. Some manufacturing processes require the prepreg to sit exposed to the ambient environment for extended periods of time during which the prepreg will absorb moisture if the dissolved moisture is at a lower activity. For example, the yearly average RH in Indonesia and Malaysia is 85%. This can be mitigated by RH conditioning the manufacturing facility. Ambient temperature may also play a role. The solubility curve fitting constant, k_1 , in Equation 2 is a weak function of temperature. For example, if two laminates are moisture conditioned at the same RH but different temperatures, the laminate conditioned at the higher temperature will have slightly higher

moisture content. This in turn increases the moisture concentration in the resin, the potential driving force for diffusion and the amount of moisture vapourizing.

5 CONCLUSION

5.1 Conclusions of the Study

The objective of this study was to elucidate the contributions of resin voids to bulk and surface porosity and mechanisms by which resin voids can grow. Resin voids in Cytac MTM45-1 neat resin and MTM45-1 CF2426A 5HS prepreg were visually observed and recorded in-situ by use of a digital microscope and glass tool plate. Porosity was measured post-cure by means of density for bulk porosity and surface reflectivity for surface porosity. Based on the results and observations the following conclusions are made:

- 1) Neat resin contains significant quantities of resin voids ranging in initial diameter from 10 – 500 μm . Resin voids contribute approximately 0.15 – 0.2% to initial porosity on average however resin void density is spatially dependent and can be highly localized. Resin voids can grow by dissolved volatile vapourization and ideal gas expansion mechanisms. Internal resin void pressure equilibrates with the surrounding resin pressure which determines the resin void volume through the ideal gas law. Reducing resin pressure causes resin voids to grow and at pressures less than 0.2 atm resin voids grow to significant sizes due to the asymptotic relation between volume and pressure. Therefore resin pressure is a critical parameter in order to mitigate porosity by ideal gas expansion of resin voids.

Resin voids were proven to grow by vapourization of dissolved moisture. A moisture vapourization criterion developed by Kardos accurately predicted the onset of resin void growth via moisture vapourization in neat resin specimens held at 100°C and humidity conditioned at either 75% or 33% RH. Time dependent growth was only seen for $P_{Resin} < P_{Resin,Critical}$ and no growth was seen for $P_{Resin} > P_{Resin,Critical}$. Moisture was confirmed as the volatile specie causing resin void growth since desiccated neat resin subjected to the same pressure cycle as neat resin conditioned at 75% RH showed no resin void growth. Desiccated resin subjected to the 33% RH pressure cycle showed time dependent resin void growth indicating that MTM45-1 resin contains other volatile components. Resin pressure is again a critical parameter in mitigating resin void porosity. Additionally temperature and moisture content in the resin play a significant role in this mechanism.

- 2) Resin void growth was stimulated in air evacuated prepreg laminates by means of reducing the resin pressure, increasing the moisture content of the resin or increasing the cure temperature. Resin pressure was reduced by both resin bleed and reduced consolidation pressure. In-situ observations, in-situ resin pressure and post-cure porosity measurements are in good agreement with ideal gas expansion and moisture vapourization resin void growth mechanisms.

Resin pressure was seen as a critical parameter to mitigate resin void porosity. Tests in which the resin pressure was sufficiently compromised manifested the highest levels of porosity. The 1/3 atm consolidation pressure laminates showed enlarged resin voids due to ideal gas expansion and time dependent resin void growth at approximately 50 min into cure (as predicted by the Kardos criterion). The 5 peel ply bleed laminates show time dependent resin void growth both by ideal gas expansion and moisture vapourization. Both these tests have uninfiltated surface fiber tows due to resin pressure falling below the critical pressure and therefore moisture vapour resisting resin infiltration. In addition, uninfiltated surface fiber tows were seen to generate resin voids in the inter-tow channels due to moisture vapourization. Laminates cured under 0/3 atm consolidation pressure developed catastrophic porosity due to both ideal gas expansion and moisture vapourization resin void growth mechanisms. Resin void growth was observed with increasing temperature due to the decrease in resin viscosity. Tests in which the resin pressure was reduced but not compromised manifested significantly less porosity. The 2/3 atm consolidation pressure laminates show increased bulk and surface porosity relative to the porosity free baseline however much less than the 1/3 atm consolidation pressure laminates.

Moisture content was seen as a less impactful parameter. Increasing the resin moisture content by humidity conditioning laminates at 75% RH resulted in a small increase in bulk and surface porosity. This porosity increase is due to the resin pressure falling below the critical pressure predicted by the Kardos criterion since ideal gas expansion of resin voids was not stimulated (i.e. same resin pressure as the baseline) and correspondingly no enlarged resin voids were observed.

Increasing the cure temperature by ramping to 180°C resulted in no porosity development contrary to predictions. The resin pressure crossed the critical resin pressure at approximately 130°C yet no time dependent resin void growth was observed or measured. As expected, since ideal gas expansion was not stimulated, no enlarged resin voids were observed. The mechanism responsible for this result is unknown however possible reasons are presented in the discussion.

- 3) Resin voids represent a non-negligible source of porosity. In order to successfully manufacture low porosity composite parts, especially for low pressure processes such as OOA, resin voids must be taken into account in the design. The first order approximation at the minimum required resin pressure to suppress resin void growth presented was adequate in explaining all laminate results except the increased temperature test. Manufacturers must be cognizant of the prepreg initial conditions such as RH_0 and ϕ_0 as well as global parameters such as $P_{Applied}$ and T in order to successfully mitigate resin void porosity using the MRP concept.

5.2 Future Work

Based on the conclusions from this study the following recommendations for future work are proposed:

- 1) Investigate why the increased cure temperature laminates did not manifest porosity. Test the hypothesis that complete infiltration inhibits resin void growth. If true the resin void growth cut-off point is complete infiltration as opposed to resin gelation.
- 2) Investigate the interactions between resin pressure, moisture content and temperature. Each parameter was investigated separately but how do their interactions influence resin void porosity? For example, can resin void growth in a moist prepreg be mitigated by gelling at a lower temperature? What is the effect of reduced consolidation pressure in a 75% RH conditioned laminate?
- 3) Develop quantitative predictive capability for resin void porosity. The Kardos criterion indicates whether resin voids can grow by moisture vapourization but offers no indication of growth rate or final porosity.
- 4) Case study the MRP concept and integrate it into a comprehensive porosity prediction tool alongside air evacuation and resin infiltration.

5.3 Contributions

The results of this study contribute to the overall understanding of porosity by highlighting the importance of resin pressure in porosity mitigation and the potential for resin voids to grow and develop into porosity. Previously, resin voids were considered negligible since they were measured to contribute $\leq 0.2\%$ to overall porosity. This work shows that under certain conditions the resin voids can grow to non-negligible sizes and must be taken into account. In addition this work has proven that moisture vapourization indeed occurs during processing and that it can be accurately predicted by the Kardos criterion which was proposed in 1988 and never experimentally investigated. The concept of a minimum resin pressure is a key component in an overall porosity mitigation tool; while the proposed MRP may be simplistic it is a first step towards an effective tool.

REFERENCES

- [1] Campbell, F.C., *Manufacturing Processes for Advanced Composites*, 2004, Elsevier, New York.
- [2] Boeing 787, <http://www.boeing.com/commercial/787/>, Boeing, 2015. Retrieved September 10, 2015.
- [3] Airbus A350 XWB, <http://www.airbus.com/aircraftfamilies/passengeraircraft/a350xwbfamily/>, Airbus SAS, 2015. Retrieved September 10, 2015.
- [4] C Series, <http://commercialaircraft.bombardier.com/en/cseries.html>, Bombardier, 2015. Retrieved September 10, 2015.
- [5] C. Red, *"The market for OOA aero-composites (2013-2022)"*, High-Performance Composites, 2014.
- [6] Ridgard, C., Out of Autoclave Composite Technology for Aerospace, Defense and Space Structures. *Proceedings of the 2009 Society for the Advancement of Material and Process Engineering (SAMPE) conference, Baltimore, United States.*
- [7] MTM45-1 Matrix Resin Product Data Sheet, Advanced Composites Group (ACG Inc.), Vol. PDS1104/09.06/4.
- [8] Farhang, L., Fernlund, G. Void Morphology, Void Evolution and Gas Transport in Out-of-Autoclave Prepregs. *Proceedings of the 26th Annual Technical Conference of the American Society for Composites and the 2nd joint US-Canada Conference on Composites, 2011, Montreal, Canada.*
- [9] Farhang, L., *Void Evolution during Processing of Out-of-Autoclave Prepreg Laminates*, Ph.D. Thesis, 2014, University of British Columbia (UBC), Vancouver, Canada.
- [10] Campbell, F.C., Mallow, A. R., Browning, C. E., Porosity in Carbon Fiber Composites: An Overview of Causes. *Journal of Advanced Materials*, **26**, 1995, pp. 18-33.
- [11] Repecka, L., Boyd, J. Vacuum Bag Only Curable Prepregs that Produce Void Free Parts. *Proceedings of the 2002 Society for the Advancement of Material and Process Engineering (SAMPE) conference, Long Beach, United States.*
- [12] Ridgard, C. Advances in Low Temperature Curing Prepregs for Aerospace Structures. *Proceedings of the 2000 Society for the Advancement of Material and Process Engineering (SAMPE) conference, Long Beach, United States.*
- [13] Uhl, K.M., Lucht, B. Jeong, H. Hsu, D.K. Mechanical Strength Degradation of Graphite Fiber Reinforced Thermoset Composites Due to Porosity. *Review of Progress in Quantitative Nondestructive Evaluation*. **7**, 1988, pp. 1075-1082.

- [14] Costa, M.L., Almeida, S.F.M.d., Rezende, M.C. The Influence of Porosity on the Interlaminar Shear Strength of Carbon/Epoxy and Carbon/Bismaleimide Fabric Laminates. *Composites Science and Technology*, **61**, 2001, pp. 2101-2108.
- [15] Thorfinnson, B., Biermann, T.F. Degree of Impregnation of Prepregs: Effect on Porosity. *Proceedings of the 1987 Society for the Advancement of Material and Process Engineering (SAMPE) conference, Anaheim, United States.*
- [16] Grunenfelder, L.K., Nutt, S.R. Void Formation in Composite Prepregs – Effect of Dissolved Moisture. *Composites Science and Technology*, **70**, 2010, pp. 2304-2309.
- [17] Kay, J., Fernlund, G. Processing Conditions and Voids in Out-of-Autoclave Prepregs. *Proceedings of the 2012 Society for the Advancement of Material and Process Engineering (SAMPE) conference, Baltimore, United States.*
- [18] Centea, T., Hubert, P. Out-of-Autoclave Prepreg Consolidation under Deficient Pressure Conditions. *Journal of Composite Materials*, **48**, 2014, pp. 2033-2045.
- [19] Louis, B.M., Hsiao, K., Fernlund, G. Gas Permeability Measurements of Out of Autoclave Prepreg MTM45-1/CF2426A. *Proceedings of the 2010 Society for the Advancement of Material and Process Engineering (SAMPE) conference, Seattle, United States.*
- [20] Grunenfelder, L.K., Nutt, S.R. Air Removal in VBO Prepreg Laminates: Effects of Breathe-out Distance and Direction. *Proceedings of the 43rd tech conference for the Society for the Advancement of Material and Process Engineering (SAMPE), 2011, Fort Worth, United States.*
- [21] Wysocki, M., Larsson, R., Toll, S. Modelling the Consolidation of Partially Impregnated Prepregs. *Proceedings of the 17th International Conference on Composite Materials (ICCM), 2009, Edinburgh, Scotland.*
- [22] Centea, T., Hubert, P. Measuring the Impregnation of an Out of Autoclave Prepreg by micro-CT. *Composites Science and Technology*, **71**, 2011, pp. 593-599.
- [23] Darrow, D.C., Poropatic, P.A., Brayden Jr., T.H. Elimination of Mold Surface Porosity on Composite Parts. *Journal of Advanced Materials*, **27**, 1995, pp. 41-46.
- [24] Arafath, A.R.A., Fernlund, G., Poursartip, A. Gas Transport in Prepregs: Model and Permeability Experiments. *Proceedings of the 17th International Conference on Composite Materials (ICCM), 2009, Edinburgh, Scotland.*
- [25] Lane, M., Poursartip, A., Fernlund, G., Willden, K., Nelson, K. Robust Processing of Composite Structures. *Proceedings of the 2010 Society for the Advancement of Material and Process Engineering (SAMPE) conference, Seattle, United States.*

- [26] Wells, J., Kay, J., Poursartip, A., Lane, M., Fernlund, G. Surface and Bulk Porosity in Out-of-Autoclave Prepregs. *Proceedings of the 20th International Conference on Composite Materials (ICCM), 2015, Copenhagen, Denmark.*
- [27] Louis, B.M. Gas Transport in Out-of-Autoclave Prepreg Laminates. M.A.Sc. Thesis, 2010, University of British Columbia (UBC), Vancouver, Canada.
- [28] Hsiao, K. Gas Transport and Water Vapourization in Out-of-Autoclave Prepreg Laminates. M.A.Sc. Thesis, 2012, University of British Columbia (UBC), Vancouver, Canada.
- [29] Kratz, J., Hubert, P. Anisotropic Air Permeability in Out-of-Autoclave Prepregs: Effect on Honeycomb Panel Evacuation Prior to Cure. *Composites: Part A*, **49**, 2013, pp. 179-191.
- [30] Kratz, J., Centea, T., Hubert, P. Air Permeability of Out-of-Autoclave Honeycomb Structures During Processing. *Proceedings of the 26th Annual Technical Conference of the American Society for Composites and the 2nd joint US-Canada Conference on Composites, 2011, Montreal, Canada.*
- [31] Centea, T., Hubert, P. Modelling the Effect of Material Properties and Process Parameters on Tow Impregnation in Out-of-Autoclave Prepregs. *Composites: Part A*, **43**, 2012, pp. 1505-1513.
- [32] Cender, T., Simacek, P., Advani, S.G. Resin Film Impregnation in Fabric Prepregs with Dual Length Scale Permeability. *Composites: Part A*, **53**, 2013, pp. 118-128.
- [33] Thomas, S., Nutt, S.R. Temperature Dependence of Resin Flow in a Resin Film Infusion (RFI) Process by Ultrasound Imaging. *Applied Composite Materials*, **16**, 2009, pp. 183-196.
- [34] Brand, R.A., Brown, G.G., McKague, E.L. *Processing Science of Epoxy Resin Composites*. 1984, Materials Laboratory, Air Force Wright Aeronautical Laboratories.
- [35] Kardos, J.L. "Void Growth and Dissolution" in Processing of Composites, Edited by R.S. Dave and A.C. Loos, 2000, Hanser Publishers, Munich, pp. 182-206.
- [36] Scriven, L.E. On the Dynamics of Phase Growth. *Chemical Engineering Science*, **10**, 1959, pp. 1-13.
- [37] Wood, J.R., Bader, M.G. Void Control for Polymer-matrix Composites (2): Experimental Evaluation of a Diffusion Model for the Growth and Collapse of Gas Bubbles. *Composites Manufacturing*, **5**, 1994, pp. 149-158.
- [38] Ledru, Y., Bernhart, G., Piquet, R., Schmidt, F., Michel, L. Coupled Visco-mechanical and Diffusion Void Growth Modelling during Composite Curing. *Composites Science and Technology*, **70**, 2010, pp. 2139-2145.
- [39] Gangloff Jr., J.J., Daniel, C., Advani, S.G. A Model of Two-phase Resin and Void Flow during Composites Processing. *International Journal of Multiphase Flow*, **65**, 2014, pp. 51-60.

- [40] Gangloff Jr., J.J., Hwang, W.R., Advani, S.G. Characterization of Bubble Mobility in Channel Flow with Fibrous Porous Media Walls. *International Journal of Multiphase Flow*, **60**, 2014, pp. 76-86.
- [41] Hsiao, K., Kay, J., Fernlund, G. Gas Transport and Water Evaporation in Out-of-Autoclave Prepregs. *Proceedings of the 26th Annual Technical Conference of the American Society for Composites and the 2nd joint US-Canada Conference on Composites, 2011, Montreal, Canada*.
- [42] Kardos, J.L., Dave, R., Dudukovic, M.P. Voids in Composites. *Proceedings of Manufacturing International*, 1988. Vol. 4, *Manufacturing Science of Composites*, American Society of Mechanical Engineers, 1988.
- [43] Butt, H.J., Graf, K., Kappl, M. *Physics and Chemistry of Interfaces*, 2006, Wiley-VCH, Weinheim, Germany.
- [44] Lynch, K., Hubert, P., Poursartip, A. Use of a Simple, Inexpensive Pressure Sensor to Measure Hydrostatic Resin Pressure during Processing on Composite Laminates. *Polymer Composites*, **20**, 1999, pp. 581-593.
- [45] Xin, C., Gu, Y., Li, M., Li, Y., Zhang, Z. Online Monitoring and Analysis of Resin Pressure Inside Composite Laminate during Zero-bleeding Autoclave Process. *Polymer Composites*, **32**, 2011, pp. 314-323.
- [46] Gutowski, T.G., Morigaki, T., Cai, Z. The Consolidation of Laminate Composites. *Journal of Composite Materials*, **21**, 1987, pp. 172-188.
- [47] Roy, M., Kay, J., Fernlund, G., Poursartip, A. Porosity in Configured Structures, *Proceedings of the 2015 Society for the Advancement of Material and Process Engineering (SAMPE) conference, Baltimore, United States*.
- [48] MTM45-1 Matrix Resin Product Data Sheet, Advanced Composites Group (ACG Inc.), Vol. PDS1104/09.06/4.
- [49] Equilibrium Relative Humidity: Saturated Salt Solutions, Omega Engineering Inc.
- [50] Cender, T., Gangloff Jr., J.J., Simacek, P., Advani, S.G. Void Reduction during Out-of-Autoclave Thermoset Prepreg Composite Processing. *Proceedings of the 2014 Society for the Advancement of Material and Process Engineering (SAMPE) conference, Seattle, United States*.
- [51] Gangloff Jr., J.J., Hwang, W.R., Advani, S.G. The Investigation of Bubble Mobility in Channel Flow with Wavy Porous Media Walls. *International Journal of Multiphase Flow*, **70**, 2015, pp. 1-14.
- [52] Ho, C.K., Webb, S.W. *Gas Transport in Porous Media*, 2006, Springer Netherlands, Netherlands.

- [53] Srinivasan, R.S., Gerth, W.A., Powell, M.R. A Mathematical Model of Diffusion-limited Gas Bubble Dynamics in Tissue with Varying Diffusion Region Thickness. *Respiration Physiology*, **123**, 2000, pp. 153-164.
- [54] Standard Test Methods for Density of Compacted or Sintered Powder Metallurgy (PM) Products Using Archimedes' Principle, ASTM International, ASTM B962 - 15.

APPENDICES

Appendix A: Laminate Air Evacuation

Air evacuation from a laminate during debulk was modeled by Arafath et al. [24] based on the assumption that the gas flow obeys Darcy's Law. Numerical solving of the partial differential equation in one dimension for the transient flow case yields Equation 31. This equation predicts the time, t , required under debulk to reduce the mass fraction of gas, m/m_0 , in the laminate to a specified level.

$$t = \frac{\mu \phi L^2}{p_0 K} \left[-\frac{1}{0.9} \ln \left(\frac{m}{m_0} \right) \right]^{1/0.6} \quad (31)$$

Where t is time, p_0 is the initial pressure of the gas in the laminate, ϕ is porosity, L is part length, K is in-plane permeability and m/m_0 is mass fraction of gas. Using typical values for these parameters, listed in Table A.1, debulk time for assumed mass fractions was calculated and plotted in Figure A.1.

Table A.1: Values used for the parameters in Equation 31.

Parameter	Value	Unit
μ	1.85×10^{-5}	Pa s
ϕ	0.3	-
p_0	101325	Pa
K	3.5×10^{-14}	m ²
L	0.05	m

Based on Figure A.1, the mass fraction of gas within the laminate reaches 1% after only 2 minutes of debulk. Debulk times were approximately 5-10 min prior to starting the tests. Therefore it is safe to assume that the laminates used in this study were devoid of air.

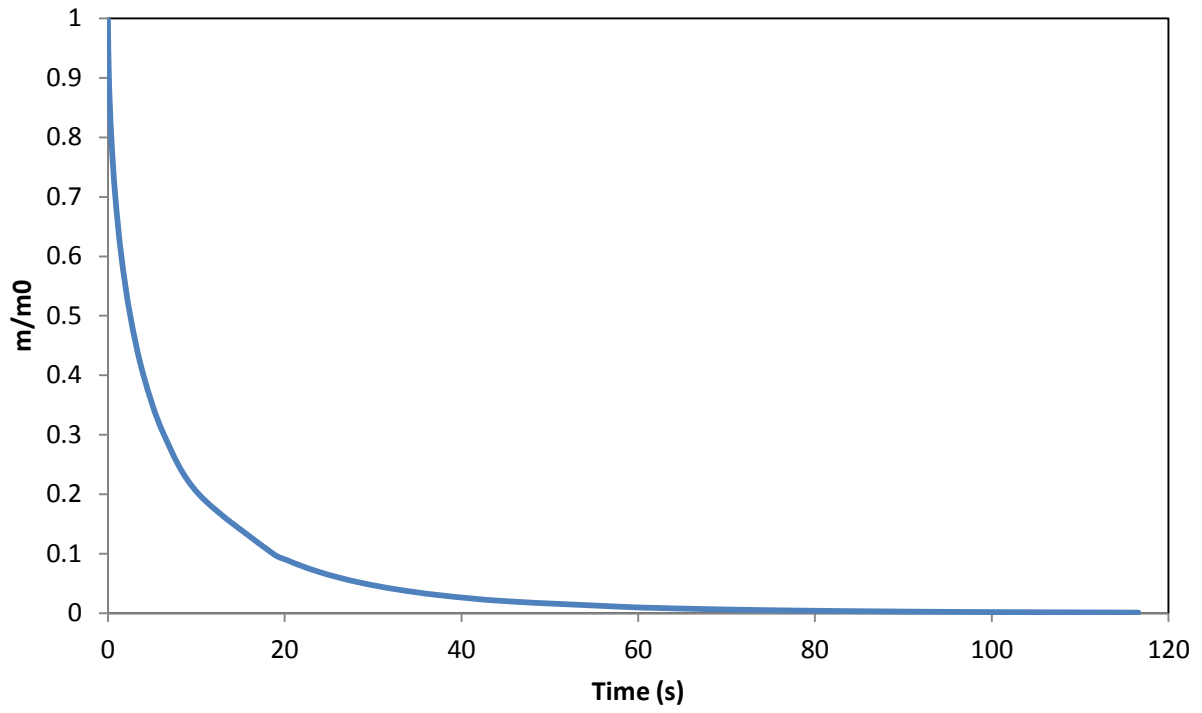


Figure A.1: Relative mass of air in the laminate during debulk.

Appendix B: Resin Void Generation by an Uninfiltrated Fiber Tow

Figure B.1 is a series of in-situ laminate surface images showing an uninfiltrated fiber tow growing by “tunneling” to the inter-tow channels where it contributes to resin void growth in the inter-tow channels.

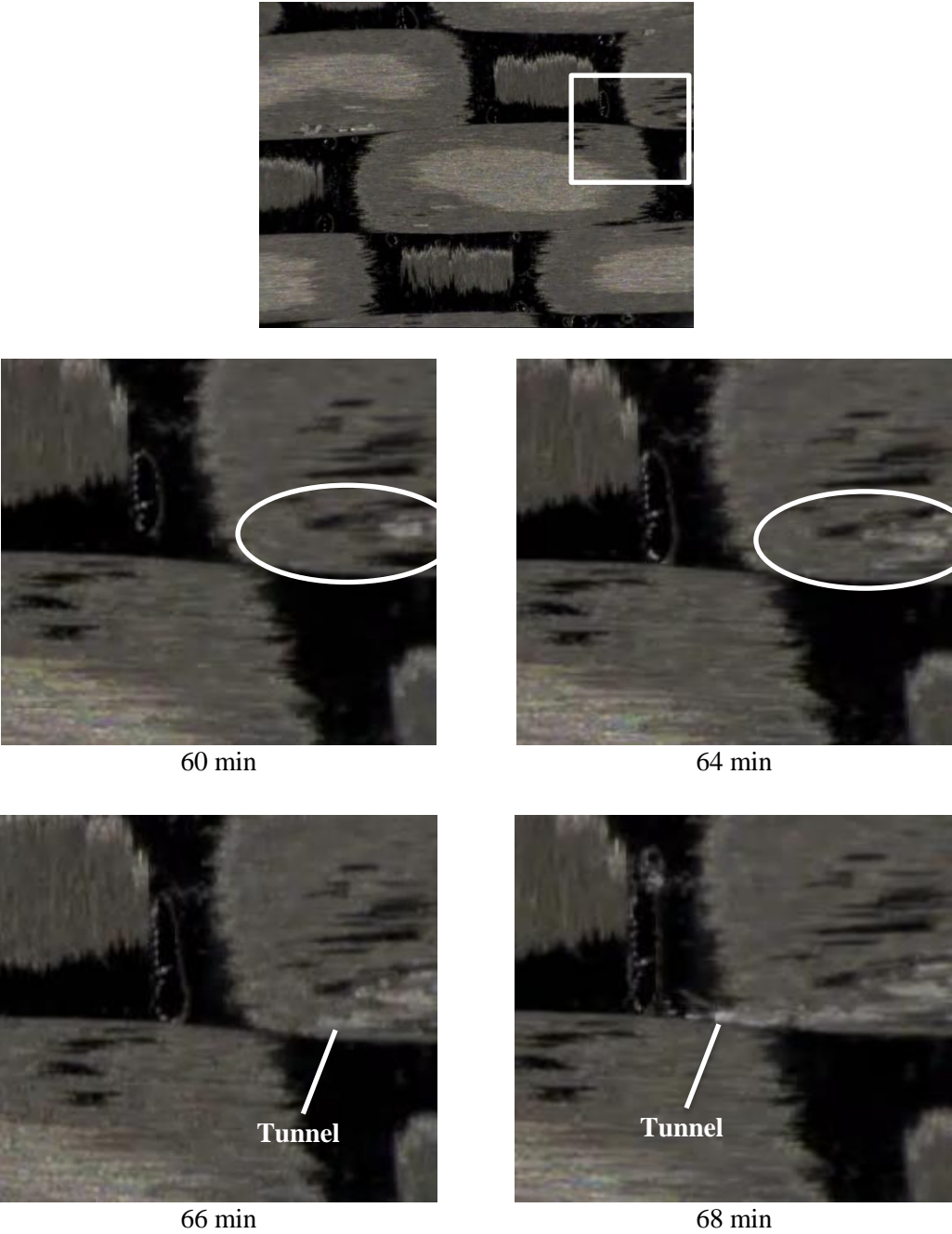


Figure B.1: Resin void generation due to uninfiltrated surface fiber tows.

Appendix C: 75% RH Kardos Criterion Test with Incorrect Boundary Pressures

Figure C.1 shows resin void growth due to moisture vapourization for neat resin conditioned at 75% RH. When this test was designed the predicted $P_{R,Critical}$ was lower than the actual value due to a calculation error. Accordingly, the high and low pressure values used for this test do not bound the critical resin pressure. In fact the critical resin pressure equals P_H . The test was redone with more suitable values for the high and low pressures. Despite this, since moisture content can only decrease during the test, the result is consistent with the results shown in section 3.2.

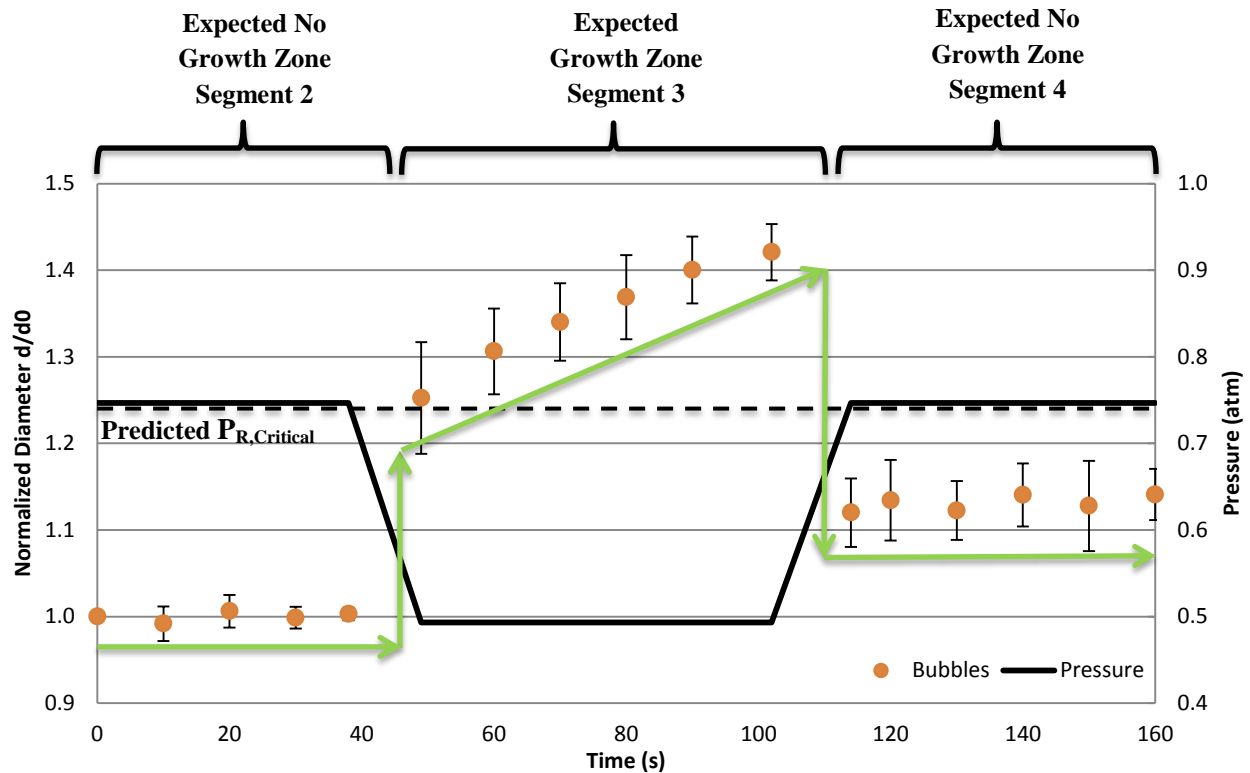


Figure C.1: Average normalized void diameters for 75% RH neat resin tests with high and low pressure values chosen due to a calculation error for $P_{R,Critical}$.

Appendix D: Measuring Bulk Porosity by Density and Thickness

Density of an object can be determined using Archimedes' principle. The Archimedes' principle states that an object wholly or partially immersed in a fluid will be buoyed upwards by a force equal to the weight of the displaced fluid. Density can therefore be calculated by knowing the weight of the object in air and in water and the density of the water, Equation 32.

$$\frac{\rho_{Object}}{\rho_{H2O}} = \frac{W_{Object,Air}}{W_{Object,Air} - W_{Object,Immersed}} \quad (32)$$

Where ρ_{Object} is the density of the object of interest, ρ_{H2O} is the density of water, $w_{Object,Air}$ is the weight of the object in air and $w_{Object,Immersed}$ is the weight of the object immersed in water. Weight of laminates in both air and water was measured using a precision electronic balance.

Bulk porosity for a porous laminate can be calculated knowing the density of the porous laminate and the density of a porosity free laminate by Equation 33.

$$\phi = 1 - \frac{\rho_{Porous}}{\rho_{Porosity Free}} \quad (33)$$

Where ϕ is porosity, ρ_{Porous} is the density of the porous laminate, $\rho_{Porosity Free}$ is the density of a porosity free laminate. Porosity will only reduce the laminate density (to a minimum of zero) therefore this equation is bound between 0 and 1.

Bulk porosity may also be measured using the thickness of a porous laminate and the thickness of a porosity free laminate, Equation 34.

$$\phi = 1 - \frac{t_{Porosity Free}}{t_{Porous}} \quad (34)$$

Where ϕ is porosity, t_{Porous} is the thickness of the porous laminate, $t_{Porosity Free}$ is the thickness of a porosity free laminate. Porosity increases the thickness of a laminate therefore this equation is bound between 0 and 1.